Heteromeric TRPV4-C1-P2 and TRPV4-P2 Channels: Assembly and Function

DU, Juan

A Thesis submitted in Partial Fulfillment of
the Requirements for the Degree of
Doctor of Philosophy
in
Physiology

The Chinese University of Hong Kong
August 2011

ProQuest LLC.
789 East Eisenhower Parkway
P.O. Box 1346
Ann Arbor, MI 48106 - 1346

Thesis/Assessment Committee

Professor YUNG Wing-Ho (Chair)

Professor YAO Xiaoqiang (Thesis Supervisor)

Professor LAM Fu-Yuen (Committee Member)

Professor LI Ronald A（External Examiner）

Declaration of Originality

The work contained in this thesis is original research carried out by the author in the School of Biomedical Sciences, Faculty of Medicine, The Chinese University of Hong Kong, starting from August 2008 to May 2011. No part of the work described in this thesis has already been or is being submitted to any other degree, diploma or other qualification at this or any other institutions.

Abstract of the thesis entitled:

Heteromeric TRPV4-C1-P2 and TRPV4-P2 channels: assembly and function

Submitted by Du Juan

for the degree of Doctor of Philosophy

at The Chinese University of Hong Kong in July 2011

TRP channels are a superfamily of cation channels that can be divided into seven subfamilies and include 28 members. These channels function as cellular sensors to perceive and respond to a variety of environmental stimuli, such as pressure, fluid flow, temperature and pain. Functional TRP channels are tetrameric complexes consisting of four pore-forming subunits. Channels can comprise identical subunits, forming homomeric channels, or can be assembled from two or three different TRP channel subunits, forming heteromeric channels. Heteromeric channels often have properties that are distinct from those of homomeric channels. Heteromeric assembly is an effective way of diversifying the biophysical properties and function of the TRP channels. Up to the present, studies from our group and others have only shown that TRPV4, -C1 and -P2 are capable of forming cross-subfamily heteromeric channels including heteromeric TRPV4-C1, TRPC1-P2 and TRPV4-P2. In the present study, I hypothesize the possible existence of heteromeric TRPV4-C1-P2 channels that are composed of the subunits from three different TRP subfamilies. I further tested functional role of such heteromeric channels in response to fluid flow in HEK293 overexpression system and native vascular endothelial cells.

Two-step co-immunoprecipitation (co-IP), chemical cross-linking experiments and FRET detection were used to demonstrate the presence of TRPV4-C1-P2 heteromers in HEK293 cells overexpressing TRPV4, C1, and P2, and in the primary mesenteric artery endothelial cells. I found that flow was able to induce $[Ca^{2+}]_i$ rises and whole-cell cation currents in HEK293 cells that were co-expressed with TRPV4, -C1 and -P2. Compared to the HEK293 cells that were expressed with TRPV4 alone, TRPV4-C1-P2-co-expressing HEK293 cells displayed a much prolonged $[Ca^{2+}]_i$ transient and cation current in response to flow. Dominant-negative construct against each of these three TRP isoforms abolished the flow-induced $[Ca^{2+}]_i$ rises and whole-cell cation currents in these cells, suggesting that all three isoforms are required for flow response. My data support the existence of heteromeric TRPV4-C1-P2 channels that are sensitive to flow stimulation. In rat MAECs (mesenteric artery endothelial cells), flow-induced $[Ca^{2+}]_i$ rises and cation currents were also strongly suppressed by dominant-negative construct against TRPV4, -C1, or -P2, suggesting the existence of heteromeric TRPV4-C1-P2 channels in native endothelial cells. Taken together, my results identified the first heteromeric TRP channels that are composed of subunits from three different subfamilies, and uncovered the functional role of this heteromeric TRPV4-C1-P2 channel in flow response.

I also studied the flow response in renal epithelial cells. I found that in renal epithelial cells, because of lack of TRPC1 expression, it is heteromeric TRPV4-P2 rather than TRPV4-C1-P2 that mediates flow-induced Ca^{2+} influx. The role of heteromeric TRPV4-P2 channel complex in flow response was studied using M1-cortical collecting duct (CCD) cells and HEK293 cells co-expressing TRPV4 and -P2. Co-IP experiments and double immunostaining showed that TRPV4 and TRPP2 physically interact with each other to form a

heteromeric channel in the M1 CCD cells and in HEK293 cells over-expressing TRPV4 and -P2. I also studied the regulation of flow-induced calcium influx by cGMP and protein kinase G (PKG). The results showed that activation of PKG by cGMP inhibited flow-induced calcium influx and whole-cell currents in HEK293 cells co-expressing TRPV4 and -P2. The inhibitory effect of cGMP was abolished in the presence of PKG inhibitor KT5823. Point mutations at two consensus PKG phosphorylation sites markedly reduced the inhibitory effect of cGMP. In M1 CCD cells, flow-induced calcium influx was also inhibited by 8-Br-cGMP, the effect of which was reversed by KT5823. The cGMP inhibition was absent in M1 CCD cells that were pretreated with fusion peptides TAT-TRPP2^{S827} + TAT-TRPP2^{T719}, which compete for endogenous PKG phosphorylation sites on TRPP2. In conclusion, I demonstrated that TRPV4 physically associated with TRPP2 in M1 CCD cells and HEK293 cells over-expression system. This association prolongs the flow-induced Ca^{2+} influx and enables this influx to be negatively regulated by PKG in M1 CCD cells and HEK293 cells co-expressing TRPV4 and -P2.

論文摘要

暫態受體電位通道 （TRP 通道）是一個成員眾多的陽離子通道家族，可以分成 7 個亞家族, 共有 28 個成員。這些通道可以作為細胞的感受器感覺各種環境刺激，如壓力、液體的流動、溫度和疼痛等，並且可以對這些刺激作出反應。有功能的暫態受體電位通道是一個四聚體，由四個亞基組成孔結構。這四個亞基可以是相同的，也可以是來自兩個、甚至三個不同亞家族的成員。這些異聚體通道的特性常常不同於同聚體的通道。這種異聚體的組合可以更高效的調節細胞功能、改變通道的亞細胞的分佈及通道的生物特性。

在我目前的研究中，兩步法免疫共沉澱、化學交連實驗和共振能量轉移實驗證實了 TRPV4-C1-P2 異聚體在過表達 HEK293 細胞和原代培養的腸系膜動脈內皮細胞的存在。液體流動會刺激 TRPV4, TRPC1, TRPP2 共同表達的 HEK293 細胞產生鈣的內流和陽離子電流。但與 TRPV4 單獨表達的 HEK293 細胞相比較，TRPV4-C1-P2 共表達細胞的鈣內流和陽離子電流的時間曲線不同，是持續存在，而不是一過性的。這三種不同的 TRP 通道蛋白的顯性負性結構均可消除液體流動引起的胞內鈣濃度升高和全細胞陽離子電流，表明這三種 TRP 通道蛋白對於液體流動反應都是必需的。這些資料表明 TRPV4-C1-P2 可以形成異聚體通道複合物，這一通道複合物對於液體流動刺激是敏感的。在大鼠的腸系膜動脈內皮細胞，TRPV4, TRPC1, TRPP2 顯性負性結構也可顯著降低液體流動引起的胞內鈣離子濃度升高和陽離子電流，表明在固有的內皮細胞也存在 TRPV4-C1-P2 通道異聚體。總之，我的研究結果揭示了第一個由三個不同亞家族成員組成的 TRPV4-C1-P2 通道異聚體的存在，同時也揭示了這一通道異聚體在液體流動反應中的功能作用。

在腎上皮細胞， 因為缺少 TRPC1 的表達，所以是 TRPV4-P2 而不是 TRPV4-C1-P2 異聚體通道參與液體流動引起的鈣內流。所以在另外一個研究中，我也探討了腎集合管內皮 M1 細胞 CCD 和共表達 TRPV4-P2 的

HEK293 細胞中，TRPV4-P2 通道複合物在液體流動引起的細胞內鈣濃度增加中的作用。TRPV4 和 TRPP2 都表達于腎上皮細胞膜和纖毛，可能參與纖毛的機械感受功能和介導腎上皮細胞的鈣內流和鈣信號。有報導 TRPP2 可以與 TRPV4 結合形成機械和溫度敏感的分子感受器。在我目前的實驗中，免疫共沉澱和免疫染色實驗證實了 TRPV4 與 TRPP2 的物理結合，這種結合既存在於 TRPV4 和-P2 過表達的 HEK293 細胞，也存在於 M1-CCD 細胞。在共表達 TRPV4-P2 的 PHEK 細胞，通過啟動蛋白激酶 G 可抑制液體流動引起的鈣內流和全細胞電流，cGMP 的這種抑制作用可因 KT5823 (GMP 的抑制劑)的存在而消除。點突變 TRPP2 的 PKG 磷酸化位點也可顯著降低 cGMP 的抑制作用。在 M1 細胞，液體流動引起的鈣內流可被 8-Br-cGMP (GMP 的激動劑) 抑制，KT5823 可消除這種抑制作用。用 PKG 磷酸化位點的融合肽 TAT-TRPP2^{S827} + TAT-TRPP2^{T719} 預處理 M1-CCD 細胞，cGMP 的抑制作用則消失。總之，我證實了在 M1 細胞和共表達了 TRPV4-P2 的 HEK293 細胞，TRPP2 可與 TRPV4 結合，從而延長 TRPV4 介導的液體流動引起的鈣內流的時間。另外，PKG 對這一過程具有負反饋調節作用。

Acknowledgements

My deepest gratitude goes first and foremost to Professor Xiaoqiang Yao, my supervisor, for his constant encouragement and guidance. Professor Yao walked me through every stage of these three years, opened the interesting research door before my eyes; leaded me to enter physiological science world; gave me very much valuable advice and thoughtful guidance on my research work; carefully and in detail revised my scientific paper and this thesis.

I would like to express my genuine gratitude to Professor Yu Huang for his help and support during my PhD study. I also thank the labmates in Professor Yu Huang's lab for their help.

I would like to thank Dr Xin Ma for his patient and meticulous teaching techniques and doing some experiments together with me. He also has given me some valuable advises and always encourage me to confront troubles in experiments.

I would like to thank Dr Bing Shen for his help in my experiments and in my life in Hong Kong.

I would like to thank Miss Judy Wong for quick mutation and ligation experiments, ordering and everything that she did for me. She always showed delight in my success and encouraged me when I was depressed. I wish to send my heartfelt gratitude to her.

I want to thank Dr Rong Ma. He has taught me a lot and made me having good background to start my PhD study. He has given me some precious advices in research work. He also gave me TRPP2 dead mutation gene D511V.

I also thank Dr. B. Nilius (KU Leuven, Belgium) for TRPV4 and $TRPV4^{M680D}$ constructs, Dr. G. Germino (John Hopkins, USA) for TRPP2 construct, and Dr. IS. Ambudkar (NIH, USA) for $TRPC1^{\Delta 567\text{-}793}$ and TRPC1multi-pore constructs.

I wish to thank that my labmates Miss Yan Ma, Miss Yan Qi, Miss Lei Sun, Mr Ching On Wong, Miss Eva, and Miss Xiaochen Ru for their help in my study and research work.

I would like to extend my grateful thanks to all my colleagues and staff in SBS for their help and care and acknowledge the financial support from the Chinese University of Hong Kong and RGC granting me the postgraduate studentship and research, which has allowed me to study here in Hong Kong and finish this work.

Last but not least, I would like to give my special thanks to my family, they always give me the greatest support. In particular my daughter, she has grown up from a three month baby to a little girl after three years of my PhD study. She enjoyed the time so much with mommy, but I always left her with her grandfather and grandmother. She gives me peace in heart and power to keep moving forward.

Abbreviations

ACh	acetylcholine
ARD	Ankyrin receptor domain
ANK	ankyrin
ATP	adenosine 5'-triphosphate
AT1R	angiotension II type 1 receptor
8-Br-cGMP	8-Bromoguanosine 3',5'-phosphoric acid
BSA	bovine serum albumin
Ca^{2+}	calcium ion
$[Ca^{2+}]_i$	intracellular calcium
CCD	cortical collecting duct
CHO-k1	Chinese hamster ovary K1
cGMP	cyclic GMP
DAG	diacylglycerol
DMSO	dimethyl sulfoxide
DSS	disuccinimidylsuberate
DTSSP	3,3´-Dithiobis[sulfosuccinimidylpropionate]
EDHF	endothelium-derived hyperpolarizing factor
EDTA	ethylenediaminetetraacetic acid, disodium salt
EGF	epidermal growth factor
EGTA	ethylene glycol-bis(*L*-aminoethyl ether)-N,N,N',N',-tetraacetic acid
eNOS	endothelial nitric oxide
FBS	fetal bovine serum
GFP	green fluorescent protein
GPCR	G protein-coupled receptor
IP3	inositol 1,4,5-trisphosphate
MAEC	Mesenteric artery endothelial cell
MSCC	The mechanosensitive cation channel
NO	nitric oxide
NSCC	nonselective cationic channel current
PCR	polymerase chain reaction

PGI_2	prostaglandin I_2
pH	plechstrin homology
PI3K	phosphoinositide 3-kinases
PIP2	phosphatidylinositol-4,5-bisphosphate
PIP3	phosphatidylinositol 3,4,5-trisphosphate
PKG	protein kinase G
PLC	phospholipase C
PT	proximal tubule
RNAi	RNA interference
SAC	Stretch-activated cation channel
SDS	sodium dodecy sulphate
siRNA	short interfering RNA
SOC	store-operated channels
TBA	tetrabutylammonium chloride
TEMED	N,N,N',N'-tetramethyl-ethylenediamine
TG	thapsigargin
TRP	transient receptor potential
TRPC	canonical transient receptor potential
TRPP	transient receptor potential polycystin
TRPV	transient receptor potential vanilloid
Tween-20	polyoxyethylenesorbitan monolaurate
VSMCs	vascular smooth muscle cells

Table of content

List of figures

1. Chapter 1: Introduction

1. 1 Interaction of TRP channels

Based on amino acide sequence homology, TRP channels can be classified into seven subfamilies: TRPC (TRP canonical), TRPM (TRP melastatin), TRPV (TRP vanilloid), TRPA (TRP ankyrin), TRPP (TRP polycystin), TRPML (TRP mucoliptin), TRPN (TRP NOMPC (no mechanoreceptor potential C)). Except for TRPN, all of the subfamilies can be found in mammals. Functional TRP channels are tetrameric complexes consisting of four pore-forming subunits (Hoenderop et al, 2003). Each subunit contains six transmembrane regions (S1–S6) and a re-entrant loop between transmembrane segments S5 and S6 that constitute the ion conducting pore (Lepage et al, 2007). Channels can comprise identical subunits, forming homomeric channels, or can result from the assembly of two or three different TRP channel proteins to form heteromultimeric channels. These heteromultimeric channels have properties that are distinct from those of homomeric channels. Because multiple TRP subunits are available for co-assembly, combinations of ultimately-formed tetrameric channels are numerous.

1.1. 1 Heteromeric assembly of TRP channel subunits in same subfamily

1.1.1. 1 Heteromeric assembly of classical TRP channels (TRPC)

TRPC channel family can be divided into two major subgroups: TRPC1, -C4, and -C5 and TRPC3, -C6, and -C7, excluding TRPC2 which is a non functional pseudogene in humans (Wes et al, 1995). TRPC channels can form functional homo- and heterotetramers within two defined subgroups (TRPC1/4/5 and TRPC3/6/7) (Hofmann T et al, 2002; Goel M et al, 2002). Co-immunoprecipitations (co-IP) showed that TRPC1, -4, and -5 could interact with each other, while TRPC3, -6, and -7 also could interact among themselves (Goel et al. 2002; Liu et al. 2005; Schilling and Goel 2004; Strübing et al. 2001). In addition, TRPC1 may act as a linker. When TRPC1 is present, TRPC4/5 may heteromultimerize with TRPC3/6/7 (Strübing et al, 2003).

1.1.1.1.1 TRPC1/TRPC5; TRPC1/TRPC4

Biochemical and functional interactions between TRPC1 and TRPC5 were shown in hippocampal neurons (Goel et al. 2002; Strübing et al. 2001). The biophysical properties of recombinant TRPC1/TRPC5 channels were surprisingly different from those of TRPC5 homomer (Strübing et al. 2001). Homomeric TRPC5 was doubly-rectifying and had a conductance of 38 pS, TRPC1/TRPC5 was outwardly rectified and displayed an 8-fold smaller conductance (5 pS). TRPC1/TRPC5 heteromers were activated by G_q-coupled receptors but not by depletion of intracellular Ca^{2+} stores, which were in contrast to the more common view of the TRP family as comprising store-operated channels.

TRPC1 is expressed in many brain regions, including hippocampus and cortex. TRPC5 is evidently present in hippocampus but not in cortex, while its close

homolog TRPC4 is found in cortex (Philipp et al, 1998; Mori et al, 1998). TRPC1 and TRPC4 may form a novel cation channel in mammalian brain and generate whole-cell currents that are difference from that of heteromeric TRPC1/TRPC5 channels (Strübing et al, 2001).

1.1.1.1.2 TRPC1/TRPC3; TRPC3/TRPC4

TRPC units only can form heterodimers with phylogenetically close relatives: TRPC1/TRPC4/TRPC5 or TRPC3/TRPC6/TRPC7 (Hofmann et al, 2002). However, some group reported that distant TRPC members could form heteromeric channels. TRPC3 can assemble with TRPC1 in salivary gland cell lines (Lintschinge et al, 2000; Liu et al, 2005) and TRPC4 in endothelial cells (Poteser et al, 2006).

Some groups reported that TRPC1 and TRPC3 formed heteromeric complex in embryonic rat brain (Strübing et al. 2001), in native smooth muscle cells (Chen et al, 2009), salivary gland cell line (Liu et al. 2005), and over-expressing system (Lintschinger et al, 2000). Functional experiments in TRPC1 and TRPC3 co-expressing system showed that TRPC1-TRPC3 heteromulterization generated diacylglycerol-sensitive Ca^{2+}-regulated cation currents different from the currents produced by TRPC1 or TRPC3 homomers (Lintschinger et al, 2000). In native smooth muscle cells, TRPC1/TRPC3 heteromers can be activated by UTP stimulation and significantly inhibited by exogenous nitric oxide or a cell permeable analog of cGMP (Chen et al, 2009). The inhibition of TRPC1/TRPC3 channels contributes to NO-mediated vascular vessel relaxation in carotid artery (Chen et al, 2009). In human

parotid gland ductal cells, TRPC1 and TRPC3 form a novel thapsigargin- and OAG-sensitive, store-operated non-selective cation channel (Liu et al, 2005).

Co-immunoprecipitation and FRET experiments confirm that TRPC3 and TRPC4 form heteromeric channel in over-expressing system and in porcine aortic endothelial cells (PAECs) (Hofmann et al, 2002; Schilling et al, 2004; Poteser et al, 2006). Co-expression of TRPC3 and TRPC4 gives rise to a cation channel activity of unique properties. The observed 44 pS cation conductance is clearly different from the so far described TRPC3 (68 pS) or TRPC4 (hTRPC4α: 30.3 + 0.6 pS and hTRPC4β: 29.7 + 1.0 pS) unitary conductance generated by overexpression of individual channel proteins (Poteser et al, 2006). Co-expression of TRPC3 and TRPC4 also generates a channel that displays distinct regulatory properties. Expression of dominant negative TRPC4 proteins suppresses TRPC3-related channel activity in HEK293 over-expression system and in native endothelial cells. In addition, blocking TRPC4 inhibits TRPC3-related currents in HEK293 over-expressing system and the redox-sensitive cation conductance in PAECs (Poteser et al, 2006).

1.1.1.1.3 TRPC6/TRPC7

TRPC6 and TRPC7 are able to assemble to form heteromultimeric channels in vascular smooth muscle cells, where they play an important role in vasopressin-induced cation current (Goel et al, 2002; Maruyama et al, 2006).

1.1.1.1.4 TRPC2/TRPC6

In primary erythroid cells and over-expressing system, TRPC2 and TRPC6 interact to modulate calcium influx stimulated by erythropoietin (Chu et al, 2004). This result is difference with Hofmann's report that TRPC2 has not been found to interact with any other TRPCs (Hofmann et al, 2002). This is not completely unexpected because of the relatively close phylogenetic relationship of TRPC2 and TRPC6 (Hofmann et al, 2002).

1.1.1.1.5 TRPC1/TRPC3/TRPC5; TRPC3/TRPC6/TRPC7

Native TRPC1/TRPC4/TRPC5 and TRPC3/TRPC6/TRPC7 heteromers were found in rat cortex and cerebellum, respectively (Goel et al, 2002). An even more promiscuous association between TRPC1, TRPC3, and TRPC5 has been found in the embryonic but not in adult brain (Strübing et al, 2003).

1.1.1.2 Vanilloid receptor-related TRP Channel (TRPV)

The vanilloid receptor family consists of six mammalian members TRPV1-TRPV6. Homo-oligomeric TRPV1-TRPV4 channels form poorly selective cation channels that are thermosensitive, but have different temperature activation profiles (Caterina et al, 1997; Caterina et al, 1999; Smith et al, 2002; Watanabe et al, 2002). TRPV isoforms demonstrate osmosensitivity and mechanosensitivity, may play important roles as osmoreceptors and in sensing mechanical stimulation. Within TRPV subfamily, osmosensitivity and mechanosensitivity have been mainly attributed to TRPV1, TRPV2, and TRPV4 (Ciura and Bourque, 2006; Naeini et al, 2006 ; Muraki et al, 2003; Liedtke and Friedman, 2003; Strotmann et al, 2000; Birder et al, 2002; Caterina et al, 2000; Christoph et al, 2008; Mishra and Hoon, 2010; Fernandes et al, 2008). In addition, TRPV1 is regulated by protons and various lipid

mediators including chilli pepper constituent capsaicin (Caterina et al, 1997). TRPV4 is activated by 4-phorbol esters or hypotonic extracellular solutions (Watanabe et al, 2002; Strotmann et al, 2000). TRPV5 and TRPV6 are phylogenetically closely related Ca^{2+}-selective channels expressed in epithelia of intestine and kidney and exhibit a constitutive activity. They are transcriptionally regulated by 1,25-dihydroxycholecalciferol.

TRPV1 and TRPV2, TRPV1 and TRPV3, TRPV5 and TRPV6 may form heteromeric complex. It is surprising that no evidence show an efficient heteromeric assembly of TRPV4 with any other TRPV channel subunit. However, TRPV4 may form functional complex with TRPC1 or TRPP2.

1.1.1.2.1 TRPV1-TRPV2

TRPV1 and TRPV2 are mostly expressed in different tissues or cell types (Caterina et al, 1997; Caterina et al, 1999; Birder et al, 2002; Rutter et al, 2005). There are reports of co-association of TRPV1 and TRPV2 in co-expressing HEK cells and F-11 dorsal root ganglion hybridoma cells (Rutter et al, 2005). However, subcellular distribution of heteromer is different in two cell lines. In neuronal F-11 cell line, TRPV1 and TRPV2 colocalize on the cell surface, whereas in HEK 293 cells, both TRPV1 and TRPV2 were distributed diffusely in intracellular structures. In addition to the over-expressing system, TRPV1 and TRPV2 are colocalizated in a subset of cells in dorsal root ganglion (DRG) sections and the co-IP of TRPV1/TRPV2 heteromers is found in rat DRG lysates.

1.1.1.2.3 TRPV1-TRPV3

TRPV1 and TRPV3 are thermosensitive, nonselective cation channels that are co-expressed in dorsal root ganglion neurons (Smith et al, 2002; Peier et al, 2002). TRPV1 is activated by noxious heat and capsaicin. TRPV3 is a heat-sensitive but capsaicin-insensitive channel. When heterologously expressed, TRPV3 is able to associate with TRPV1 and may modulate its responses. If TRPV1 and TRPV3 are co-expressed in a heterologous expression system, a positive co-IP and a synergistic functional response to capsaicin stimulation are documented (Smith et al, 2002). A co-localization or a significant interaction between rodent TRPV1 and TRPV3 isotypes was also found (Hellwing et al, 2005). However, FRET data for TRPV1/TRPV3 was unable to demonstrate an efficient heteromultimerization occurring between TRPV1 and TRPV3 (Hellwig et al, 2005). These finding indicate that the interaction between TRPV1 and TRPV3 is in minor amount, but still clearly preferred in some studies (Hellwing et al, 2005; Smith et al, 2002). Overall it remains unclear, whether TRPV1 and TRPV3 subunits are endogenously co-expressed in native cell types and whether they can co-assemble into heterooligomeric pore complexes *in vivo*.

1.1.1.2.4 TRPV5-TRPV6

TRPV5 and TRPV6 are highly Ca^{2+} selective and are involved in Ca^{2+} re-absorption in small intestine, kidneys and placenta, and play a key role in calcium homeostasis (Hoenderop et al, 2002; Hoenderop et al, 2003; Nijenhuis et al, 2003; Vennekens et al, 2000). RT-PCR and northern blot analysis revealed the co-expression of TRPV5 and TRPV6 in the small intestine, kidney, pancreas, testis and prostate (Muller et al, 2000; Peng et al, 2000; Hoenderop et al, 2001). Biochemical approaches including co-

immunoprecipitaion, chemical crosslinking and density gradient centrifugation as well as functional and biophysical assays proved that TRPV5 and TRPV6 subunits assemble into the same pore complex and combine with each other to form heteromultimeric channels (Hoenderop et al, 2003). TRPV5/TRPV6 heteromers display novel properties that are different from homotetrameric TRPV5 or TRPV6 channels (Hoenderop et al, 2003). Electrophysiological analyses of concatemeric polypeptides revealed that all heterotetrameric TRPV5/TRPV6 channels are functional and different in transport kinetics (Hoenderop et al, 2003). Increase in the TRPV6 to TRPV5 channel subunits ratio in the heterotetrameric channel affects the kinetics of Ca^{2+}-dependent inactivation and causes a decrease in its affinity to Ruthnium Red block (Hoenderop et al, 2003). TRPV5 and TRPV6 co-localize in various epithelial tissues and their expression levels influence intestinal and renal Ca^{2+} absorption. During aging, renal and intestinal Ca^{2+} re-absorption through TRPV5 and TRPV6 declines due to expression decrease (van Abel et al, 2006).

1.1.1.3 TRPP subfamilies

TRPP1 (polycysin-1, PC1 or PKD1) is encoded by PKD1. This protein is a large integral membrane glycoprotein and possesses a large extracellular domain: 11 predicted transmembrane-spanning segments and short intracellular carboxyl terminal domain (Delmas, 2004; Wilson, 2004; Zhou, 2009; Harris and Torres, 2009). The large extracellular region contains several protein motifs that are involve in protein-protein interactions, protein-sugar interactions, or linking of TRPP1 to one or several putative ligands. The cytosolic carboxy terminal domain includes a coiled-coil domain that is implicated in protein-protein interactions. Several TRPP1-like proteins have

been identified, including PKDREJ, PKD1L1, PKD1L2 and PKD1L3 (Delmas, 2005).

TRPP2 (polcystin-2, PC2 or PKD2) is encoded by PKD2. TRPP2 shows moderate similarity to the last six transmembrane segments of TRPP1. This protein includes two cytosolic extremities with two EF-hands, two coiled-coil domains, and an endoplasmic reticulum (ER) retention signal in its C-terminal domain (Delmas, 2004; Wilson, 2004; Zhou, 2009; Harris and Torres, 2009). Other members of TRPP subfamily include PKD2L1 and PKD2l2, which share structural homology with TRPP2 (Delmas, 2005).

TRPP1 and TRPP2 interact with each other via their carboxy terminal coiled-coil domains (Delmas, 2004; Wilson, 2004; Zhou, 2009; Harris and Torres, 2009). TRPP1 is localized at plasma membrane, whereas TRPP2 is localized at both plasma membrane and ER. The association of TRPP1 and TRPP2 induces the translocation of TRPP2 to the plasma membrane where it serves as a calcium permeable nonselective cation channel (Montell, 2005). TRPP1 and TRPP2 colocalize at the membrane of the primary cilia of renal epithelial cells and endothelial cells where they are proposed to transduce luminal shear stress into a calcium signal (Nauli et al, 2003; Nauli et al, 2008). With its large extracellular amino-terminal domain, TRPP1 has been suggested to be a mechanical sensor regulating the opening of the associated calcium-permeable channel TRPP2 (Nauli et al, 2003). Loss of this mechanosensory function (i.e., flow sensing) is thought to result in altered cellular signaling subsequently leading to cyst formation (Nauli and Zhou, 2004). TRPP2 also interacts with multiple partners, including the TRP channel subunits TRPC1 and TRPV4 (Kottgen et al, 2008; Tsiokas et al, 1999; Bai et al, 2008)

1.1.1.4 Melastatin-related TRP channels (TRPM)

The TRPM (transient receptor potential melastatin) subfamily includes eight TRP channel subunits (TRPM1–TRPM8) that display structural relationship with the putative tumor suppressor melastatin first identified in melanoma cells (Clapham, 2003; Fleig and Penner, 2004). Based on the similarity in primary sequence, the eight TRPM proteins fall into four distinct groups: TRPM6/7, TRPM1/3, TRPM4/5, TRPM2/8. TRPM possess a membrane topology similar to that of the well-studied voltage-gated potassium channel subunits. They are integral membrane proteins, and each subunit comprises six membrane-spanning segments with a pore-forming loop region between the fifth and sixth segments, and intracellular N- and C-termini. The N-terminus contains four regions that show sequence similarity but have no defined functions. The C-terminus exhibits common and subunit-specific structural features. All TRPM subunits contain a TRP motif and a coiled-coil domain, some have unique enzymatic domains in the distal tail (Perraud et al, 2001). TRPM subunits form cationic channels (Ca^{2+}-permeable except TRPM4 and TRPM5) that activated by numerous physiochemical stimuli and are important in a variety of physiological functions in both excitable and non-excitable cells (Clapham, 2003; Fleig and Penner, 2004).

All the TRPM subunits can form functional homomeric channels (Perraud et al, 2001; Nadler et al, 2001; Runnels et al, 2001; Xu et al, 2001, Grimm et al, 2003; Lee et al, 2003; Launay et al, 2002; Pérez et al, 2002; Chubanov et al, 2004, Voets et al, 2004; McKemy et al, 2002; Peier et al, 2002; Li et al, 2006). However only TRPM6 specifically interacts with its closest homolog, the Mg^{2+}-permeable cation channel TRPM7, resulting in the assembly of

functional TRPM6/TRPM7 complexes in the cell surface (Chubanov et al, 2004). Co-expression of the TRPM6 and TRPM7 subunits results in a heteromeric TRPM6/TRPM7 channel that exhibits several functional properties distinct from the homomeric TRPM6 and TRPM7 channels, such as the sensitivity to pH, modulation by 2-aminoethoxydiphenyl borate and single-channel conductance (Chubanov et al, 2004; Li et al, 2006). Compared with expressing TRPM7 alone, co-expression of TRPM6 with TRPM7 results in a marked enhancement of manganese entry (Chubanov et al, 2004). TRPM7 could modulate the subcellular distribution of TRPM6. Expressing of TRPM6 alone was not detectable on the cell surface, whereas co-expression of TRPM6 with TRPM7 resulted in trafficking of TRPM6 to the plasma membrane (Chubanov et al, 2004). However, the targeting-deficiency of human TRPM6 could not be confirmed by other studies in which heterologous expression of TRPM6 efficiently reconstituted a Mg^{2+} entry pathway without equivalent amounts of TRPM7 being co-expressed (Voets et al, 2004). The loss of heteromeric assembly of S141L-mutated TRPM6 with TRPM7 leads to a disruption of TRPM7-assisted surface targeting of TRPM6 (Chubanov et al, 2004). The homozygous S141L missense mutation in TRPM6, like other defects in TRPM6, is associated with autosomal recessive hypomagnesemia with secondary hypocalcemia (HSH) (Schlingmann et al, 2002). Thus these findings provide a biological explanation for the human disease.

1.1.2 Inter subgroup interaction

In addition to intra-subfamily coassembly, cross-subfamily assembly of TRP subunits could also happen. TRPP2 interacts with members of two other TRP subfamilies, TRPC1 (Kobori, et al, 2009; Zhang, et al, 2009; Bai et al, 2008; Tsiokas et al, 1999) and TRPV4 (Stewart et al, 2010; Köttgen et al, 2008).

TRPC1 and TRPV4 may also interact to form a difference channel mediating flow-induced Ca^{2+} influx in vascular endothelial cells (Ma et al, 2010a, b). Functional studies indicate that heteromultimeric channels may display properties different from those of homomultimeric channels (Hofmann et al, 2002; Strübing et al, 2001; Köttgen et al, 2008). Heteromeric coassembly greatly diversifies the structure and function of TRP channels, and allows TRP channels to control and/or regulate many distinct cellular processes.

1.1.2.1 TRPC1 and TRPP2

TRPC1/TRPP2 complex represents the first example of intergroup subunit interaction. Co-IP experiments showed that TRPP2 interacts with TRPC1 through two distinct domains (Tsiokas et al, 1999). Atomic force microscopy found a decoration pattern indicating a TRPC1:TRPP2 subunit stoichiometry of 2:2 (Kobori et al, 2009). The C-terminal domain of TRPP2 is sufficient but not necessary for the TRPC1-TRPP2 association. A more N-terminal region, which is part of the TM domain and includes S2-S5 plus a putative pore helical region between S5-S6, is also able to mediate an interaction independently of the C-terminal region. The specific and direct interaction region of TRPC1 with TRPP2 is S639-S750. Moreover, it is found that L884H mutation abolishes the TRPP1-TRPP2 interaction, whereas the D886A mutation abolishes the TRPC1-TRPP2 interaction. These results demonstrated that TRPP2 interacts with TRPC1 by specific residues in the C-terminal cytoplasmic region of TRPP2.

Co-IP using kidney membrane fraction and double immunofluorescent staining experiments showed that TRPP2 is colocalized with TRPC1 in

primary cilia of LLC-PK1 (pig kidney epithelial cells) and mlMCD3 cells (Bai et al, 2008). Biochemical, gain-of-function and loss-of-function experiments using single-channel and whole–cell analysis in LLC-PK1 and mlMCD3 cells showed that TRPP2 and TRPC1 assemble into a new GPCR-activated channel with biophysical properties distinct from that of individual channels (Bai et al, 2008). The single-channel conductance of TRPP2/TRPC1 hetero-complex was lower than TRPP2 homomers but higher than that of TRPC1 homomers (Bai et al, 2008; Zhang, et al, 2009). Imaged channel structure in AFM studies showed that the calculated volume of TRPP2 is much larger than that of the homomeric TRPC1. The larger intramolecular space in TRPP2 in comparison with TRPC1 may help to explain the larger pore conductance of TRPP2 than TRPC1 (Zhang et al, 2009). This phenomenon affects the electrophysiological and regulatory properties of TRPP2/TRPC1 heteromeric complex, and makes the properties of TRPP2/TRPC1 different from TRPP2 or TRPC1 homomers.

1.1.2.2 TRPC1 and TRPV4

Co-IP, double immunostaining and FRET experiments demonstrated that TRPC1 and TRPV4 interact physically (Ma et al, 2010a). The properties of TRPC1-TRPP2 complex are distinct from TRPC1 or TPRV4 homers. Functionally, the association of TRPC1 with TRPV4 prolongs the flow-induced $[Ca^{2+}]_i$ transient and 4α-PDD–stimulated whole-cell current, and it also enables this $[Ca^{2+}]_i$ transient to be negatively modulated by protein kinase G (PKG) (Ma et al, 2010a). This TRPV4-C1 complex plays a key role in flow-induced endothelial Ca^{2+} influx. In another study, TIRFM, cell surface biotinylation, and functional data demonstrated that Ca^{2+} store depletion enhances the vesicular trafficking, resulting in insertion of more TRPV4-C1 heteromeric channels into the plasma membrane (Ma et al, 2010b). Studies

also found that TRPV4 and TRPC1 are co-localized with caveolin-1 in the caveolar compartment. Caveolae in endothelial cells have been implicated as plasma membrane microdomains that sense or transduce hemodynamic changes into biochemical signals that regulate vascular function (Ma et al, 2010b). These findings suggest a functional role of caveolar localization of TRPV4 and TRPC1 in flow sensing of endothelial cells.

1.1.2.3 TRPP2 and TRPV4

TRPP2 and TRPV4 physically and functionally interact. FRET and co-IP results showed that TRPP2 and TRPV4 form heteromultimers and colocalize in the primary cilia of MDCK cells. Atomic force microscopy study found a decoration pattern indicating a TRPP2:TRPV4 subunit stoichiometry of 2:2 (Stewart et al, 2010).

TRPP2 utilizes TRPV4 to form a mechano- and thermosensitive molecular sensor in the cilium (Köttgen et al, 2008). Electrophysiological analysis showed that cell swelling may induce a current in TRPV4-expressing oocytes, but not in those expressing TRPP2. Co-expression of TRPP2 and TRPV4 significantly magnified the swelling-activated current in Xenopus oocytes, but steady-state currents were unchanged. The swelling-induced conductance also increased about two fold in TRPV4-P2 co-expressing cells when compared to TRPV4-expressing cells. An increase in extracellular Ca^{2+} concentration caused a significant increase in whole cell currents in TRPV4-expressing oocytes. Co-expressing TRPP2 with TRPV4 in oocytes dramatically increased this effect. These data demonstrated that TRPP2 alters the functional properties of TRPV4. Co-expression of TRPV4 significantly increases the

TRPP2 surface expression, however TRPP2 reduces the surface expression of TRPV4. Thus the increases in swelling–induced conductance are not the result of increased TRPV4 surface expression but rather caused by an altered channel property through formation of TRPV4-P2 heteromers. Taken together, these data suggest that TRPV4 and TRPP2 not only interact physically but also functionally. The whole cell current of TRPV4 at warm temperatures (39°C) was doubled in the presence of TRPP2, which suggests that the TRPV4-TRPP2 channel complex exerts a thermosensory function (Köttgen et al, 2008).

1.1.2.4 TRPA1 and TRPV1

Co-IP analysis revealed direct interactions between TRPA1 and TRPV1 in an expression system as well as in sensory neurons. Fluorescence-based fluorescence resonance energy transfer experiments indicated that a TRPA1-TRPV1 complex can be formed on the plasma membrane. Single channel properties of TRPA1 are regulated by TRPV1 independently of intracellular Ca^{2+}. These data suggest that TRPV1 and TRPA1 form a complex and that TRPV1 influences intrinsic characteristics of TRPA1 channel (Staruschenko et al, 2010).

1.1.3 Assembly domains in TRP channels

TRP channels are complexes consisting of four pore-forming subunits (Hoenderop et al., 2003; Kedei et al, 2001). The N- and C-terminal domains are thought to be intracellular, where they may engage in subunit-subunit interactions, associate with other cellular proteins, and interact with cytoplasmic factors. Although TRP channels appear to share a common

transmembrane scaffold, individual family members display varied mechanisms of activation and ion selectivity (Clapham et al, 2001). This molecular variation is particularly manifested within the cytoplasmic domains.

1.1.3.1 Ankyrin repeat domain

Ankyrin repeat domain is one of the most common protein-protein interaction motifs. Its structure includes a 33-amino-acid sequence representing a highly conserved helix-turn-helix structure. There are six ankyrin repeats that seem to be conserved in all TRPV channels. Different TRP subtypes have intracellular ankyrin repeats. TRPC, TRPV, TRPN and TRPA channels contain an ankyrin repeat domain in their N-termini that are thought to play key roles in protein–protein interactions. The ankyrin repeats in N-terminus are essential for the tetramerization of TRPV4, TRPV5 ad TRPV6 (Arniges et al, 2006; Erler et al, 2004).

1.1.3.2 Coiled-coil domain

Some members of the TRPC, TRPM, and TRPV subfamilies have been suggested to contain cytoplasmic coiled-coil domains (Jenke et al, 2003; Montell, 2005). Coiled-coils are the most common and best understood protein-protein interaction domain (Lupas and Gruber, 2005; Woolfson, 2005). Some TRP interactions are mediated not only by ankyrin repeat domain but also by coiled-coil motif, such as tetramerization of TRPC4 and TRPC6. Evidence suggested that TRPC1 channels assemble into homomers through their N-terminal coiled-coil domains. In addition, the first ankyrin repeat of TRPC1 is involved in the interaction with N-terminus of TRPC3 (Lepage et al, 2006). Deletion or single point mutations within coiled-coil domain of

TRPM8 and TRPV1 abolish the function of respective channels (Tsuruda et al, 2006; García-Sanz et al, 2004).

1.1.3.3 Transmembrane domains

In addition to cytosolic interactions, additional determinants of TRP subunit interactions are presumably located in the transmembrane parts of the proteins. The transmembrane domains of *Drosophila* TRP and TRPL may co-IP with full-length TRP, indicating that these transmembrane domains may be involved in subunit assembly.

1.1.4 Physiological function of TRP channels assembling

A feature share by many members of the TRP superfamily of proteins is that closely related TRP channels are often capable of forming heteromultimers. Heteromeric assembly is an effective mode for modulating the function, subcellular localization, and biophysical properties of the interacting channels. Firstly, heteromultimerization provides a mechanism for regulating the channel conductance as the biophysical properties of the heteromultimers are distinct from those of the homomultimers (Xu, et al, 1997; Xu, et al, 2000). For example, the interaction between TRPC1 and TRPC5 lead to the generation of novel channels with biophysical properties distinct from those of TRPC1 to TRPC5 homomutimers (Strübing, et al, 2001). Secondly, heteromultimeric interactions among group 2 TRPs can also affect subcellular distributions of the channels. For example, interaction of TRPP1 and TRPP2 drives the translocation of TRPP2 from intracellular compartments to the plasma membrane (Montell, 2005).

1.2 TRP channels and Mechanosensation

All TRP channels are cation permeable, and most are not selective for monovalent versus divalent ions. Exceptions include TRPV5 and TRPV6, which display significant specificity for Ca^{2+} ions (Van de Graaf, et al, 2007; Theun de Groot1, et al, 2008), and TRPM4 and TRPM5, which are highly selective for monovalent cations and inpermeable to Ca^{2+} (Hofmann et al, 2003; Launay et al, 2002; Liu et al, 2003; Prawitt et al, 2003). TRP channels were first described in a Drosophila mutant that had an impaired visual transduction response (Cosens and Manning, 1969). In addition to their responses to light, TRP channels are activated by a variety of stimuli, including mechanical, chemical, temperature, osmolarity, intracellular Ca^{2+}, fatty acids and receptor-dependent vasoconstrictor agonist etc (Damann, et al, 2008).

Mechanically sensitive ion channels are very important in variety of key physiological functions ranging from touch sensitivity to arterial pressure regulation. Several TRP channels are sensitive to various forms of mechanical stress.

1.2.1 TRPC

1.2.1.1 TRPC1

The mechanosensitive cation channel (MSCC), also referred to as a stretch-activated cation channel (SAC), transduces membrane stretch into cation (Na^+, K^+, Ca^{2+} and Mg^{2+}) influx, and is implicated in cell-volume regulation, cell

motion, muscle dystrophy and cardiac arrhythmias. Based on detergent solubilization of frog oocyte membrane proteins, followed by liposome reconstitution and evaluation by patch-clamp, Maroto et al (2005) found that TRPC1 forms a mechanosensitive cationic channel. Heterologous expression of the human TRPC1 resulted in a tenfold increase in MSCC patch density, whereas injection of a TRPC1-siRNA abolished endogenous MSCC activity. Xenopus MSCC is directly gated by negative pressure applied in the patch pipette (Hamill and Martinac, 2001). It was thus concluded that TRPC1 is a component of the vertebrate MSCC, which is gated by tension developed in the lipid bilayer, as it is the case in various prokaryotic mechanosensitive channels. Transfection of human TRPC1 into CHO-K1 cells also significantly increases the expression of MSCC by functional assay. However, some reports have failed to confirm the mechanosensitivity of TRPC1 either in transfected cells or in native arterial myocytes (Dietrich et al, 2007; Gottlieb et al, 2008). Gottlieb et al (2008) found that the MSCC activity was not significantly different between non-transfected and TRPC1-transfected CHO-K cells. Further, in isolated cerebral artery, no difference was detected in mechanically activated cation current and pressure-induced vasoconstriction between wild-type and TRPC1-deficient mice (Dietrich et al, 2007). One explanation is that the methods to activate channel are difference in different studies. Some used osomotic swelling or cell inflation, while the others used most classical way of applying a negative pressure through the patch petite while recording channel activity in the cell-attached or inside-out configuration (Dietrich et al, 2007; Pedersen et al, 2007).

In addition, TRPC1 is over-expressed in transverse aortic constriction-induced hypertrophy (Ohba et al, 2007). Cardiomyocytes isolated from $TRPC^{-/-}$ mice failed to show an increase in the markers of cardiac remodeling in response to

cyclic stretch (Seth et al, 2009). TRPC1 activation by stretch via the angiotention II type 1 receptor (AT1R) is responsible for calcium entry which takes part in cardiac hypertrophic signaling (Seth et al, 2009).

More recently, our group (Ma et al 2010a) showed that TRPC1 forms a functional complex with TRPV4 in co-expressing HEK cells and native endothelial cells. In native endothelial cells, TRPV4-C1 complex is the main molecular entity that is responsible for flow-induced Ca^{2+} influx and subsequent vascular dilation. Moreover, protein kinase G negatively regulates TRPC1-TRPV4 complex through its action on TRPC1 subunit. These results showed that TRPC1 may not be a direct effector for flow response, instead it takes part in the flow response through its interaction with TRPV4.

1.2.1.2 TRPC5

TRPC5 is highly expressed in tissues that are subjected to strong hydrostatic forces, such as heart, vascular, renal podocities and gastric smooth muscle (Earley et al, 2004; Kraft and Harteneck, 2005; Dietrich et al, 2006; Inoue et al, 2006). The hypoosmotic stimulation and pressure induced membrane stretch activate TRPC5 channels resulting in a large calcium influx, which can be blocked by GsMTx-4, an inhibitor of stretch and mechanically activated ion channels (Suchyana et al, 2000; Park et al, 2008). The TRPC5 current activated by hypoosmotic stimulation is dependent on extracellular Ca^{2+} and is prevented by intracellular Ca^{2+} buffering. These data indicated that Ca^{2+} elevation and basal Ca^{2+} levels are necessary to sustain the activation of TRPC5 channel. TRPC5 channels can be turned on by activating receptors that

are coupled to PLC. However, direct hypoosmotic activation of TRPC5 is independent of phospholipase C function (Schaefer et al, 2000; Putney, 2004).

TRPC5 is highly expressed in the frontal cortex, hypothalamus, hippocampus, visceral sensory neurons and trigeminal sensory neurons (Philipp et al, 1998; Ricco et al, 2002, Greka et al, 2003; Glazebrook et al, 2005; Fowler et al, 2007; Gomis et al, 2008). Neurons expressing TRPC5 in the trigeminal ganglion were mainly of small diameter, most of which in sensory ganglia are nociceptive and respond to noxious mechanical forces. Osmo-mechanical characteristics of TRPC5 channels together with its expression in sensory neurons suggest its conjectural function in mechnosensory transduction. It is known that TRPC channels can form some functional heteromeric complex (Strubing et al, 2001; Hofmann et al, 2002), TRPC5 may assemble to form heteromeric complex with other TRPCs to exert mechanosensitive role.

1.2.1.3 TRPC6

TRPC6 is a calcium-permeable non-selective cation channel which is widely expressed in a variety of tissues including cardiovascular system (Dietrich and Gudermann, 2007). TRPC6 could be a sensor of mechanically and osmotically induced membrane stretch. TRPC6 is inhibited by the spider toxin GsMTx-4, a blocker of SACs (Spassova et al, 2006; Bode et al, 2001; Suchyna et al, 2002), and is also directly activated by diacylglycerol (DAG) (Hofmann et al, 1999). Unfortunately, similar to TRPC1, subsequent studies failed to confirm the direct mechanosensitivity of TRPC6 cells (Mederos et al, 2008; Inoue et al, 2009). TRPC6 was shown to become mechanosensitive when co-expressed with the angiotentin II type 1 receptor (AT1R), even in the absence of the

ligand Angiotensin II (Ang II) (Mederos et al, 2008). The TRPC6 activation by stretch or swelling is blocked by PLC inhibition or by GDPβs, which impairs G protein activation (Mederos et al, 2008; Park et al, 2003). In the absence of AT1R overexpression, TRPC6 can not be activated by membrane stretch (Spassova et al, 2006), suggesting that endogenous G protein coupled receptors (GPCRs) do not underlie stretch-induced TRPC6 activation (Mederos et al, 2008; Inoue et al, 2009). Unfortunately, similar to TRPC1, some studies failed to confirm the direct mechanosensitivity of TRPC6 cells (Mederos et al, 2008; Inoue et al, 2009). Taken together, the present evidences suggest that TRPC6 may not be intrinsically mechanosensitive, and that its activation by stretch is dependent on ligand-induced receptor activation.

Knocking-down of TRPC6 was found to strongly reduce pressure-induced myocyte depolarization, myogenic response and swelling-induced current (Welsh et al, 2002). In ventricular cardiac cells, TRPC6 localized in T tubules is involved in the stretch-sensitive depolarizing current (Dyachenko et al, 2009). Recent evidence demonstrates that TRPC6 and TRPC3 expression are increased in hypertrophic and failing hearts, and are involved in the increase of intracellular calcium during cardiac hypertrophy (Kuwahara et al, 2006; Bush et al, 2006; Nakayama et al, 2006; Onohara et al, 2006; Seth et al, 2009).

1.2.2 TRPV

1.2.2.1 TRPV1

TRPV1, acting as a low pressure baroreceptor, is expressed in various renal tissues and is especially abundant in renal pelvis, where most sensory nerve

fibers originate (Feng et al, 2008). TRPV1 regulates neuropeptide release from primary renal afferent C-fivers in response to mechanostimulation.

1.2.2.2 TRPV2

TRPV2 is mainly expressed in medium and large sensory neurons, brain and spinal cord, also in vascular and cardiomyocytes (Caterina et al, 1999; Bender et al, 2005; Kanzaki et al, 1999; Muraki et al, 2003). TRPV2 is a major component of native Ca^{2+}-permeable cation channels, which is respond to membrane stretch in mouse aortic myocytes. In Chinese Hamster Ovary K1 (CHO-K1) cells transfected with mouse TRPV2, Single channel recording showed that membrane stretch through the patch pipette and cell swelling caused by hypotonic solution are capable of activating nonselective cationic channel current (NSCC), inducing Ca^{2+} influx, but not in control CHO-K1 cells (Muraki et al, 2003). In mouse aortic myocytes, cell swelling caused by hypotonic solution activates a NSCC and elevates $[Ca^{2+}]_i$. These responses were effectively inhibited by ruthenium red, a general TRPV blocker. However 4α-PDD, a potent activator of TRPV4, was not effective in aortic myocytes. TRPV2 antisense oligonucleotides was found to suppress hypotonicity-induced activation of cation channel current (Muraki et al, 2003). The cyclic stretch may translocate TRPV2 to the plasma membrane (Iwata et al, 2003). Taken together, these results suggest that TRPV2 functions as an important mechanosensitive channel.

1.2.2.3 TRPV4 and its complex

1.2.2.3.1 TRPV4

TRPV4 is activated by mechanical stimuli, such as hypotonic cell swelling (Liedtke et al, 2000; Strotmann et al, 2000), pressure (Suzuki et al, 2003), membrane stretch (Thodeti et al, 2009), and shear stress (Gao et al, 2003).

Mechanical forces caused by fluid flow and hydrodynamic pressure provide the key signals that regulate glomerulotubular balance in the proximal tubule and ion transport in the distal nephron including the cortical collecting duct (CCD). In mouse kidney M1-1 (CCD) cells and TRPV4-HEK cells, hypotonicity- and flow-induced activation of calcium influx could be largely abolished by suppressing TRPV4 using siRNA or TRPV general channel blocker ruthenium red (Caterina and Julius , 2001; Cebrian et al, 2004; Chen et al, 2001). In CCD, the activation of the TRPV4 channels induced by flow allows calcium influx, which results in the activation of the maxi-K^+ channels and leads to the secretion of K^+ into the luminal fluid (Taniguchi et al, 2007). Urinary excretion of K^+ depends on urine volume, which was explained by flow-dependent K^+ secretion from distal nephron segments, including the distal convoluted tubule, connecting tubule (CNT) and cortical collecting duct (CCD) (Malnic et al, 1989).

TRPV4 is only expressed in the kidney tubule segments that lack constitutive apical water permeability, where a transcellular osmotic gradient is expected to develop. Expression of TRPV4 is entirely absent along the early parts of the kidney tubule where passive water reabsorption takes place, otherwise, at the hairpin turn, TRPV4 expression abruptly emerges (Tian et al, 2004). The TRPV4 distribution in renal tubules implies that TRPV4 also has osmosensing function and plays a role in cell volume regulation. Under hypotonic conditions, swelling of HaCaT keratinocytes, human airway epithelia and

TRPV4-transfected CHO cells lead to an activation of TRPV4, resulting in an influx of Ca^{2+} followed by regulatory volume decrease (RVD) (Arniges et al, 2004; Becker et al, 2005). In addition, functional interaction between TRPV4 and F-actin takes part in sensing hypotonicity and the onset of RVD (Becker et al, 2009).

In vascular endothelial cells, shear stress generated by blood flow is a key physiological stimulus. Flow induces the release of endothelial vasodilator factors that subsequently cause relaxation of underlying smooth muscles, this phenomenon named as flow-mediated dilation (Busse and Fleming, 2003). Ca^{2+} signaling has been believed to be involved in endothelial mechanotransduction and flow-induced dilation (Davies, 1995). TRPV4, a Ca^{2+}-permeable cation channel, is expressed in vascular endothelial cells of several species and is shown to participate in the regulation of vascular tone, including flow-mediated dilation (Earley et al, 2009; Hartmannsgrube et al, 2007; Köhler et al, 2006; Loot et al, 2008; Marrelli et al, 2007; Saliez et al, 2008; Willette et al, 2008; Yao and Garland, 2005; Zhang et al, 2009). A shear stress induced TRPV4-mediated Ca^{2+} entry has been demonstrated in overexpression systems (Gao et al, 2003). In MDCK cells, TRPV4 is also shown an essential for flow-induced calcium response (Köttgen et al, 2008). Flow induced-vasodilation was greatly blocked by the TRPV inhibitor ruthenium red. Knocking down of TRPV4 results in blunted flow-induced dilation of carotid arteries (Hartmannsgruber et al, 2007; Loot et al, 2008) and small resistance arteries (Mendoza et al, 2010).

TRPV4 channel is essential for the normal detection of pressure and is also a receptor of the high-threshold mechanosensory complex (Suzuki et al, 2003).

In TRPV4 knockout mice, detection of pressure is impaired, whereas the mechanical touch and intact hot can still be detected (Suzuki et al, 2003). TRPV4 acts as the stretch-activated ion channel that required for activation of β1 integrins, which mediate capillary endothelial cell responses to mechanical forces and the interaction between cell and extracellular matrix (Thodeti et al, 2009). TRPV blocker ruthenium red and downregulation TRPV4 by siRNA inhibit strain-induced calcium influx (Thodeti et al, 2009).

1.2.2.3.2 The complex of TRPV4/TRPP2

The mechanosensitivity of TRPP2 has recently been linked to TRPV4. Köttgen and coworkers found that TRPP2, which by itself lacks mechanosensitive properties, utilizes TRPV4 to form a mechano- and thermosensitive molecular sensor in primary cilia of MDCK cells (Köttgen et al, 2008).

In renal system, mechanical forces due to fluid flow and hydrodynamic pressure provide the key signals that regulate glomerulotubular balance in the proximal tubule (PT) and ion transport in the distal nephron, including the cortical collecting duct (CCD). An increase in flow rate in the CCD dissected *in vitro* produced a 20% increase in diameter and $[Ca^{2+}]_i$ increased three folds in principal and intercalated cells. The regulation of TRPP2 in TRPV4-P2 channel complex is helpful to modulate elaborate glomerulotubular balance and ion transport in renal tubular. Accordingly, flow-mediated Ca^{2+} transient in renal epithelial cells requires the presence of functional TRPP2 and TRPV4 (Nauli et al, 2003; Köttgen et al, 2008), both of which are essential components of the ciliary mechanosensor.

1.2.3 The polycystin complex TRPP1/TRPP2

Almost all the types of epithelial cells contain a primary cilium such as the epithelial cells of kidney, vascular and immune system (Zhou et al, 2009; Fliegauf et al, 2007; Hildebrandt and Otto, 2005; Badano et al, 2006). The primary cilium of Madin-Darby canine kidney (MDCK) cells, a renal epithelial cell line derived from the canine distal tubule, bends and acts as a flow sensor in response to increased fluid flow rate (shear stress) (Praetorius and Spring, 2001; Praetorius and Spring, 2005). This response depends on the presence of the primary cilium. Removal of primary cilium by choral hydrate treatment renders the cells irresponsive to shear stress (Praetorius and Spring, 2003). Moreover, direct bending of the primary cilium in MDCK cells by micropipette induces intracellular calcium rise (Praetorius and Spring, 2001). Thus, the primary cilium is proposed to act as a mechano-sensitive antenna that is able to sense fluid flow in the kidney tubule (Nauli and Zhou, 2004; Praetorius and Spring, 2005). The TRPP1/TRPP2 complex is expressed at the plasma membrane of the primary cilium in kidney epithelial cells (Nauli et al, 2003). Renal cells isolated from transgenic mice that lack functional polycystin-1 do not show a calcium response to increased fluid flow (Nauli et al, 2003). And blocking antibodies directed against TRPP2 abolished the flow response of wild-type kidney epithelial cells (Nauli et al, 2003). The TRPP1/TRPP2 complex is thus proposed to be part of a mechano-transduction pathway that senses fluid flow.

TRPP1 and TRPP2 are also expressed in vascular smooth muscle and the endothelium of most blood vessels, including the aorta and cerebral arteries (Bichet et al, 2006; Ecder et al, 2009). Similar to renal epithelial cells, the

endothelial cells respond to shear stress (Hahn and Schwartz, 2009). Blood flow induces an increase in intracellular calcium concentration followed by the endothelial release of nitric oxide, which leads to vasodilation. The primary cilia of endothelial cells are also involved in blood flow sensing (Nauli et al, 2009). Endothelial cells isolated from *Ift88*-knockout mice that lack primary cilia failed to respond to fluid flow (Nauli et al, 2009). Both TRPP1 and TRPP2 are localized to the primary cilium of endothelial cells (Nauli et al, 2009; Aboualaiwi et al, 2009). Moreover, endothelial cells isolated from aortae of *Pkd1*-knockout mice or heterozygous *Pkd2*-knockout mice are not sensitive to fluid flow, although they are activated by acetylcholine (a natural vasodilator), demonstrating the selective impairment of flow sensing (Nauli et al, 2009, Aboualaiwi et al, 2009). Wissam et al (2009) also confirmed the interaction of TRPP1 and TRPP2 in endothelial cells by coimmunoprecipitation studies. These findings indicate that flow stimulation may activate the TRPP1/TRPP2 complex in endothelial primary cilia to promote calcium influx that in turn triggers nitric oxide release and vasodilation. The failure to release nitric oxide in response to shear stress has been proposed to be clinically relevant to the development of hypertension in patients with autosomal dominant PKD.

TRPP1 and TRPP2 are abundantly expressed in arterial myocytes that respond to pressure rather than flow (Bichet et al, 2006; Ecder and Schrier, 2009). An increase in intraluminal pressure causes the gradual depolarization of vascular smooth muscle cells (VSMCs) that is linked to the opening of non-selective stretch-activated cation channels (SACs). This process is followed by activation of voltage-gated calcium channels, which results in intracellular calcium rise and myocyte constriction (Brayden, 2008; Hill et al, 2006). In contrast to the role of the TRPP1/TRPP2 complex as a flow sensor in the

primary cilium of endothelial and epithelial cells, where inactivation of either TRPP1 or TRPP2 impairs flow sensing (Nauli et al, 2009, Nauli *et al* , 2003), TRPP2 is reported to inhibit SACs in some other cells including vascular myocytes and renal epithelial cells. Furthermore, this inhibition is reversed by co-expression with TRPP1 (Sharif Naeini *et al, 2009*). These findings suggest that the ratio of TRPP1 to TRPP2 may be important to regulate SAC opening. Moreover, deletion of *pkd1* in smooth muscle cells decreases SAC opening and arterial myogenic tone, and knocking down *pkd2* in *pkd1*- deficient arteries rescues both SAC activity and the myogenic tone (Sharif Naeini et al, 2009). TRPP2 also interacts with an actin cross-linking protein – filamin A, which is important for SAC regulation by TRPP1/TRPP2 (Sharif Naeini et al, 2009).

1.2.4 The ankyrin TRPA1 channel

TRPA1 was initially considered as a possible candidate mechanosensor and proposed to be the mechanically gated hair cell transduction channel required for the auditory response (Corey et al, 2004). TRPA1 includes a 14-16 amino terminal ankyrin repeat domain (ARD) that has been speculated to act as a gating spring in mechanosensing (Corey, 2006). $TRPA^{-/-}$ mice show behavioral deficits in response to punctate mechanical stimuli, suggesting that this channel contributes to mechanical transduction in nociceptor sensory neurons (Bautista et al, 2006; Corey, 2006; Kwan et al, 2006). However, later studies using TRPA1 knockout mice argued against the hypothesis of TRPA1 as hair cell mechanosensor. TRPA1 knockout mice display normal startle reflex to loud noise, a normal sense of balance, a normal auditory brainstem response, and normal transduction currents in vestibular hair cells (Bautista et al, 2006; Kwan et al, 2006). In addition, GsMTx-4, a toxin that inhibits

stretch-activated channels through a bilayer-dependent mechanism (Bode et al, 2001; Suchyna et al, 2004), causes potent activation of TRPA1 channels (Hill and Schaefer, 2007).

1.2.5 TRPM subfamily

In TRPM subfamily, TRPM3, TRPM4 and TRPM7 have been considered so far as mechanosensitive channels.

1.2.5.1 TRPM3

TRPM3 has at least 12 spice variants. A short human splice variant was able to be activated by hypotonic cell swelling (Grimm et al, 2003). However, the mechanism is still unclear.

1.2.5.2 TRPM4

TRPM4 is expressed widely in many tissues, including arterial smooth muscle and endothelial cells (Earley et al, 2004; Nilius and Vennekens, 2006; Vennekens R and NiliusB, 2007). TRPM4, acting as a voltage-dependent channel, can be activated by Ca^{2+} (Nilius et al, 2003; Vennekens and Nilius, 2007). Overexpression of hTRPM4B in HEK293 cells results in the appearance of cation channels that are activated by both negative pressure and Ca^{2+} and share the properties of native SACs in cerebral artery myocytes (Morita et al, 2007). Knocking-down of TRPM4 was found to reduce pressure-induced myocyte depolarization and myogenic contraction of isolated

cerebral arteries, whereas KCl-induced constriction did not differ between groups (Earley et al, 2004).

1.2.5.3 TRPM7

TRPM7 is expressed in multiple tissues including vascular smooth muscle (He et al, 2005; Runnels et al, 2001; Yao and Garland, 2005). TRPM7 forms an outward rectifier channel that permeates Na^+ and Ca^{2+} and is dependent on cytoplasmic Mg^{2+} and hydrolyzable ATP level. TRPM7 is a stretch and swelling-activated cation channel that plays an important role in volume regulation (Numata et al, 2007; Numata et al, 2007). Whole-cell patch clamp experiment showed that the activity of TRPM7 is excited by shear stress and by osmotic swelling in HEK cells expressing TRPM7 (Numata et al, 2007). In addition, membrane stretch increased single-channel activity (Numata et al, 2007). TRPM7 is translocated within cells in response to laminar flow (Oancea et al, 2006). After increasing shear stress, TRPM7 molecules are translocated to or near the plasma membrane (Oancea et al, 2006).

2. Chapter 2: Objective of the present study

In the present study, we employed several methods including co-IP, chemical cross-linking, FRET detection, double immunostaining, intracellular Ca^{2+} measurement, patch clamp, etc to firstly explore:

1) The physical interaction of TRPV4, -C2, -P2 in the primary cultured rat MAECs and HEK 293 cells co-expressing these three TRP proteins.

2) The functional role of heteromeric TRPV4-C1-P2 channels in flow-induced $[Ca^{2+}]_i$ rises and whole-cell currents.

3) The physical interaction of TRPV4, -P2 in M1 CCD cells and HEK 293 cells co-expressing TRPV4 and TRPP2.

4) The role of heteromeric TRPV4-P2 channels in flow-induced $[Ca^{2+}]_i$ rises in M1 and HEK 293 cells co-expressing TRPV4 and TRPP2, and its regulation by PKG.

3. Chapter 3: Materials and Methods

3.1 Materials

3.1.1 Chemicals and reagents

Human embryonic kidney cell line HEK293 was from ATCC, USA. Fura-2-AM and Pluronic F-127 were obtained from Molecular Probes, and Dulbecco's modified Eagle's medium (DMEM), Phosphate Buffered Saline (PBS), Opti-MEM, fetal bovine serum (FBS), Lipofectamine 2000, and protease inhibitors were from Invitrogen. Anti-TRPC1 and anti-TRPV4 antibodies were from Alomone Laboratories, anti-TRPP2 antibody (G20) was from Santa Cruz biotechnology. Nonidet P-40, sodium deoxycholate, SDS, EDTA, collagenase IA, $CaCl_2$, Hepes, BSA, ATP, BAPTA, CsCl, Cs^+-aspartate, Sucrose, glucose, Tris-HCl, trypsin and $MgCl_2$ were purchased from Sigma. Endothelial basic medium (EBM), Endothelial growing medium (EGM) and bovine brain extract (BBE) were from Lonza. DSS (disuccinimidylsuberate) and DTSSP (3,3′-dithiobis sulfosuccinimidylpropionate) was purchased from Thermo scientific.

3.1.2 Solutions

3.1.2.1 Solutions for western blotting

Protein extraction buffer (pH 7.4)

Reagents	**Concentration**
Tris-HCl (pH 7.4)	50 mM
NaCl	150 mM
NaF	50 mM
Nonidet P-40	1
Sodium Deoxycholate	0.5

Complete protease inhibitor cocktail tablets (50 ml/tablet) were freshly added before use.

6X SDS loading dye (10 µl)

Reagents	**Concentration**
Tris-HCl (pH 6.8)	100 mM
Bromophenol Blue	0.25%
SDS	4 %
Glycerol	20 %
2-mercaptoethanol	10 %

Resolving gel (7.5%)

Reagents	**Concentration**
H_2O	4.8 ml
40 % acrylamide	1.68 ml
1.5 M Tris-HCl (pH 8.8)	2.3 ml
10 % SDS	90 µl
10 % Ammonium persulfate (APS)	90 µl
TEMED	9 µl

Staking gel (4%)

Reagents	**Concentration**
H_2O	2.5 ml
40 % acrylamide	0.4 ml
0.5 M Tris-HCl (pH 6.8)	1 ml
10 % SDS	40 µl
10 % Ammonium persulfate (APS)	40 µl
TEMED	4 µl

Running buffer (pH 8.6)

Reagents	**Concentration**
Tris-base	25 mM
Glycine	192 mM

SDS	0.1 %

Transfer buffer (pH 9.2)

Reagents	**Concentration**
Tris-base	48 mM
Glycine	39 mM
SDS	0.05
Methanol	20 %

Washing buffer: Phosphate-buffer saline (PBS, pH 7.4)

Reagents	**Concentration**
NaCl	140 mM
Na_2HPO_4	10 mM
KCl	3 mM
KH_2PO_4	2 mM

Permeabilization buffer: PBS-T

0.01% Tween-20 PBS (pH 7.4)

Blocking buffer (pH 7.4)

5 % non-fat milk in PBS-T

3.1.2.2 Solutions for agarose gel eletrophoresis

1 X TAE buffer (pH 7.4)

Reagents	**Concentration**
Tris-HCl	40 mM
Sodium acetate	20 mM
EDTA	1 mM

6 X DNA sample loading buffer

Reagents	**Concentration**
Bromophenol blue	0.25%
Xylene cyanol FF	0.25%

Sucrose	40%

3.1.2.3 Solutions for cloning

Luria-Bertani Media (LB Media)

Reagents	**Concentration**
Tryptone	10 g/L
Yeast extract	5 g/L
NaCl	5 g/L

LB agar

15 g select agar in 1 L LB media.

3.1.2.4 Solutions used in Ca^{2+} imaging system

Normal physiological saline solution (NPSS, pH 7.4 with NaOH)

Reagents	**Concentration**
NaCl	140 mM
KCl	5 mM
$CaCl_2$	1 mM
HEPES	5 mM
Glucose	10 mM

Ca^{2+}-free physiological saline solution (OPSS, pH 7.4 with NaOH)

Reagents	**Concentration**
NaCl	140 mM
KCl	5 mM
HEPES	5 mM
Glucose	10 mM

3.1.3 Animals

Male Sprague-Dawley rats and C57BL mice were supplied from Laboratory Animal Services Center of the Chinese University of Hong Kong.

3.2 Methods

3.2.1 Cell culture

3.2.1.1 Preparation and culture of the primary rat mesenteric artery endothelial cells

All animal work was done in accordance with the Guide for the Care and Use of Laboratory Animals published by the US National Institutes of Health (NIH publication No.8523). The primary cultured mesenteric artery endothelial cells (MAECs) were isolated from male Sprague-Dawley rats of approximately 250-300g as described elsewhere (Ma, 010a). Before performing dissection, all instruments were sterilized by 70% ethanol. Rats were killed by CO_2 gas and also sterilized by 70% ethanol. After perfusing 100 ml physiological saline solution PBS (in mmol/L: 140 NaCl, 3 KCl, 25 Tris, pH 7.4) from rat heart, the small intestine was dissected out and all the vein branches of the mesenteric bed were rapidly excised. Then remained arterial branched were digested with 0.025% collagenase IA in endothelial basic medium (EBM) for 45 min at 37°C. After centrifugation at 1600×*g* for 5 min, the pelleted cells were resuspended in endothelial growing medium (EGM) supplemented with 1% bovine brain extract (BBE), and plated in a flask. Nonadherent cells were removed 1 hr later. To avoid possible effects of culture conditions on endothelial cell properties, only cells of the first two passages that were maintained in culture condition for less than 1 week were used for experiments.

The identity of the primary cultured rat MAECs were examined by immunostains using an antibody against von Willebrand factor and the results showed that 98% of cells were of endothelial origin (Kwan et al, 2000).

3.2.1.2 HEK293 cells

HEK293 cells were cultured in DMEM supplemented with 10% FBS, 100 μg/ml penicillin and 100 U/ml streptomycin. All cells were grown at 37°C in a 5% CO_2 humidified incubator.

3.2.1.3 M1 cell line

The M1-CCD cell line (CRL-2038; American Type Culture Collection, Manassas, VA) is derived from renal CCD microdissected from a mouse transgenic for the early region of SV40 virus [strain Tg(SV40E) Bri7] (Stoos BA, et al, 1991). M1-CCD cells were routinely grown in 75-cm^2 polystyrene culture flasks containing 1:1 DMEM and Ham's F-12 medium (DMEM/F-12) with fetal bovine serum (10%), supplemented with L-glutamine (2 mM), penicillin (100 U/ml), streptomycin (100 μg/ml), and dexamethasone (5 μM).

3.2.2 Molecular biology studies

3.2.2.1 Clones and transfection

Mouse TRPV4 gene (NM_022017) and $TRPV4^{M680D}$ were gifts from Dr. Bernd Nilius, Belgium. Human TRPC1 cDNA (NM_003304) was obtained by RT-PCR from human coronary endothelial cells CC2585 (BioWhittaker).

Human TRPP2 was a gift of Dr. Gregory Germino, John Hopkins University, USA. $TRPC1^{\Delta 567\text{-}793}$ and $TRPC1^{pore\text{-}mut}$ were gifts from Dr. Indus Ambudkar, NIH, USA. $TRPP2^{D511V}$ was a gift from Dr. Rong Ma, University of North Texas, USA. $TRPP2^{R636G}$ point mutation was generated by QuickChange Site-directed Mutagenesis Kit (Stratagene). Mutagenic oligonucleotide was GTATCTTCACCCAGTTCGGCATCATTTTGGGTGAT for R636G. Mutagenic oligonucleotides were CAA ACT AAA ACT GAA AAG AAA CGC TGT AGA TGC CAT CTC AGA GAG for T719A, CCA GAG CC GGA GGG GAG CCA TCT CCA GTG GGG for S827A. All clones were auto-sequenced by ABI310 autosequencer to verify the authenticity of the genes. For subcellular co-localization and FRET, TRPV4-C1 concatemer was tagged with CFP at its C-terminus, and TRPP2 was tagged with YFP at its C-terminus (Fig.3-1).

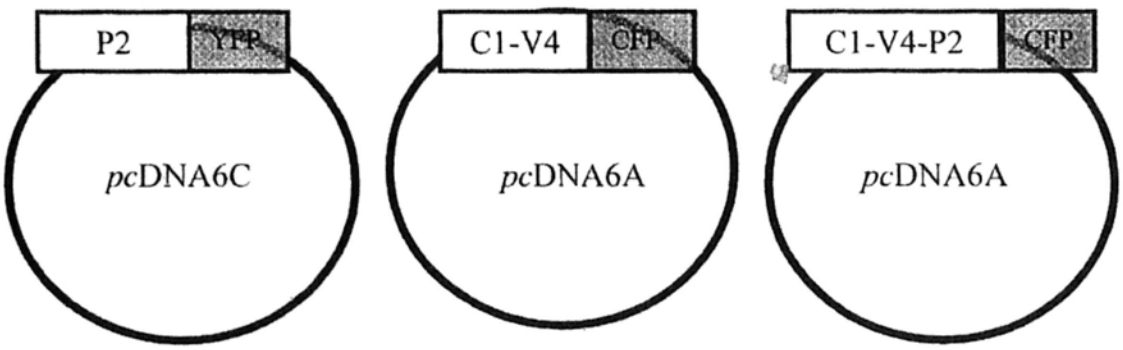

Figure 3-1. The construction of CFP or YFP –tagged TRP proteins

HEK293 cells were transfected with various constructs using Lipofectamine 2000 as described elsewhere (Ma et al, 2010). Transfection was done with 4 μg plasmid DNA of each construct and 6 μl Lipofectamine 2000 in 200 μl of Opti-MEM reduced serum medium in six-well plates. Primary cultured MAECs were transfected with various constructs by electroporation using Nucleofector II following the procedure in manufacturer's instruction manual.

About 80% of HEK293 cells and about 70% of the primary cultured rat MAECs were successfully transfected by respective protocols as indicated by control transfection using a GFP-expressing pCAGGS vector. All genes except PKG1α were transiently transfected into targeted cells. Functional studies were performed 2-3 days post transfection.

3.2.2.2 TAT-mediated protein transduction into M1 cells.

Small peptides that containing TRPP2 PKG phsphorylation sites ($TRPP2^{S827}$, SRRRGSIS; $TRPP2^{T719}$, KLKRNTVD) were conjugated to an NH_2-terminal 11-amino acid HIV Tat protein transduction domain (YGRKKRRQRRR) at Alpha Diagnostic International (USA) (Schwarze SR, et al, 1999). M1 cells were pretreated with TAT-$TRPP2^{S827}$ (100 nM) plus TAT-$TRPP2^{T719}$ (100 nM) at room temperature for at least 10 min before whole cell current recording or calcium measure.

3.2.2.3 Double immunostaining

Double immunofluorescence assay was performed.

3.2.2.3.1 Double immunostaining for chapter 4

Double immunofluorescence assay was performed. Briefly, MAEC cells were seeded on glass coverslips. The cells were rinsed with PBS three times, then fixed with 3.7% formaldehyde and permeabilized with 0.2% Triton X-100. Nonspecific immunostaining was blocked by incubating the cells with 2% BSA in PBS. The cells were then incubated with TRPV4 or TRPC1 antibody

(rabbit polyclonal antibody, Alomone Labs) or TRPP2 (G20, goat polyclonal antibody, Santa Cruz Biotechnology) antibodies for 1 h at RT. After three washes with PBS, the cells were incubated with acetylated-alpha-tubulin antibody (mouse monoclonal antibody, abcam company) for 1 h at RT. After three washes with PBS, the cells were incubated for 1 h with a mixture of secondary donkey anti-rabbit IgG conjugated to Alexa Fluor 488 (1:200) (for TRPV4 or TRPC1) and goat anti-mouse IgG conjugated to Alexa Fluor 535 (for acetylated- alpha-tubulin antibody); donkey anti-goat IgG conjugated to Alexa Fluor 546 (1:100) (for TRPP2) and rabbit anti-mouse IgG conjugated to Alexa Fluor 488 (for acetylated- alpha-tubulin antibody). After washing and mounting, immunofluorescence of the cells was detected using FV1000 confocal system.

3.2.2.3.2 Double immunostaining for chapter 5

Double immunofluorescence assay was performed. Briefly, M1 CCD cells or HEK293 cells co-expressing TRPV4 and -P2 were seeded on glass coverslips. The cells were rinsed with PBS three times, then fixed with 3.7% paraformaldehyde and permeabilized with 0.2% Triton X-100. Nonspecific immunostaining was blocked by incubating the cells with 2% BSA in PBS. The cells were then incubated with TRPV4 (Rabbit polyclonal antibody, Alomone Labs) or TRPP2 (G20, goat polyclonal antibody, Santa Cruz Biotechnology) antibodies for 1 h at RT. After three washes with PBS, the cells were incubated with acetylated-alpha-tubulin antibody (mouse monoclonal antibody, abcam company) for 1 h at RT. After three washes with PBS, the cells were incubated for 1 h with the following pairs of secondary antibodies. 1) donkey anti-rabbit IgG conjugated to Alexa Fluor 488 (1:100) (for TRPV4) and donkey anti-goat IgG conjugated to Alexa Fluor 546 (1:100)

(for TRPP2); 2) donkey anti-rabbit IgG conjugated to Alexa Fluor 488 (1:100) (for TRPV4) and goat anti-mouse IgG conjugated to Alexa Fluor 535 (1:100) (for acetylated- alpha-tubulin antibody); 3) donkey anti-goat IgG conjugated to Alexa Fluor 546 (1:100) (for TRPP2) and rabbit anti-mouse IgG conjugated to Alexa Fluor 488 (1:100) (for acetylated- alpha-tubulin antibody). After washing and mounting, immunofluorescence of the cells was detected using FV1000 confocal system.

3.2.2.4 Fluorescent immunohistochemistry.

All animal work was done in accordance with the Guide for the Care and Use of Laboratory Animals published by the US National Institutes of Health (NIH publication No.8523). Kidneys were removed from adult C57BL mice, and the cortex was isolated by dissection. The kidneys were fixed in 3.7% paraformaldehyde in PBS overnight at 4°C, and cryosectioned at 20-μm thickness. The sections were washed with PBS and permeabilized with 0.2% Triton X-100. Nonspecific immunostaining was blocked by incubating the cells with 2% BSA in PBS. The cells were then incubated with TRPP2 (G20, goat polyclonal antibody, Santa Cruz Biotechnology) antibodies for 1 h at RT. After three washes with PBS, the cells were incubated with TRPV4 antibody (Rabbit polyclonal antibody, Alomone Labs) for 1 h at RT. After three washes with PBS, the cells were incubated for 1 h with a mixture of secondary donkey anti-rabbit IgG conjugated to Alexa Fluor 488 (1:100) and donkey anti-goat IgG conjugated to Alexa Fluor 546 (1:100). After washing and mounting, immunofluorescence of the cells was detected using FV1000 confocal system.

3.2.2.5 Co-immunoprecipitation.

The whole cell lysates from M1 CCD cells or HEK293 cells over-expressing TRPV4 and -P2 were extracted with detergent extraction buffer, which contained 1% (vol/vol) Nonidet P-40, 150 mmol/L NaCl, 20 mmol/L Tris-HCl, pH 8.0, with addition of protease inhibitor cocktail tablets. TRPV4 or TRPP2 proteins were immunoprecipitated by incubating 800 μg of the extracted proteins with 5 μg of anti-TRPP2 (G20, Santa Cruz biotechnology) or anti-TRPV4 (Alomone Lab) antibody on a rocking platform overnight at 4°C. Protein A agarose (for TRPV4 antibody) or protein G agarose (for TRPP2 antibody) was then added and incubated for additional 3 hours at 4°C. The immunoprecipitates were washed with PBS for 3 times and then detected by anti-TRPV4 or anti-TRPP2 antibody in immunoblots.

For immunoblot experiments, all samples were fractionated by 7.5% SDS-PAGE, transferred to PVDF membranes, and probed with the indicated primary antibodies at 1:200 dilution in PBST buffer containing 0.1% Tween-20 and 5% nonfat dry milk. Immunodetection was accomplished using horseradish peroxidase-conjugated secondary antibody, followed by ECL detection system.

3.2.2.6 Two-step co-immunoprecipitation.

Two-step co-IP was performed according to the procedures described by Harada et al (2003). Briefly, the primary cultured rat MAECs or TRPV4-C1-P2 co-expressing HEK293 cells were lysed with protein lysis buffer (1% Nonidet P-40, 150 mmol/L NaCl, 20 mmol/L Tris-HCl, pH 8.0, with addition of protease inhibitor cocktail), sonicated, and centrifuged at 10,000*g* for 15 min at 4°C. The supernatant was subjected to the first immunoprecipitation by incubating with 2 μg of anti-TRPC1 antibody for 2 h at 4°C, followed by

immunoprecipitation overnight with 100 µl slurry of protein A (Amersham Biosciences, Piscataway, NJ) at 4°C. Immunocomplexes were washed three times with lysis buffer containing 150 mmol/L NaCl, and the protein complexes were then eluted with 350 µl of elution buffer containing 250 mmol/L NaCl and 200 µg/ml TRPC1 antigen peptide for 3 h at 4°C. The second immunoprecipitation was performed using 150 µl of the eluate from the first immunoprecipitation and 350 µl of lysis buffer containing 2 µg of anti-TRPP2 antibody or preimmune IgG for 3 h at 4°C. The immunoprecipitates were washed and then detected by anti-TRPV4 antibody in immunoblots.

Western immunoblotting was described previously 3.2.2.5.

3.2.2.7 Chemical linking

Chemical crosslink was performed essentially according to the procedures described by others (Corey et al, 1998; Corey et al, 2001; Yu et al, 2009). DTSSP contains an amine-reactive *N*-hydroxysulfosuccinimide (sulfo-NHS) ester that reacts with primary amines at pH 7-9 to form stable amide bonds. DSS is the non-sulfonated analog of DTSSP. DTSSP is membrane impermeable crosslinker that can be use to crosslink cell surface proteins. DSS is membrane-permeable. Immediately before use, DTSSP was dissolved in water, and DSS was dissolved in DMSO at 10-25 mmol/L. Cross-linker DTSSP (final concentration 5 mmol/L) was added to the cells and the reaction mixture was incubated on ice for 2 hours. The reactions were quenched by adding quenching buffer to final concentration of 50 mmol/L Tris-base and incubated at room temperature for 30 minutes. The samples were run on non-reducing SDS-PAGE with non-reducing SDS sample buffer (4.0g sucrose, 2

ml H_2O, 0.8g SDS, 1 mol/L Tris-HCl, pH 6.8, with 0.001% bromophenol blue).

3.2.2.8 Fluorescence Resonance Energy Transfer (FRET) detection

CFP-tagged TRPV4-C1 concatemer and YFP-tagged TRPP2 were co-transfected into HEK293 cells. FRET signals were detected as described elsewhere (Ma et al, 2010). Briefly, an inverted microscope equipped with three-cube FRET filters and CCD camera was used to measure FRET. Three-cube FRET filter cubes were listed as follows (excitation; dichroic; emission): YFP (S500/20 nm; Q515lp; S535/30 nm); FRET (S430/25 nm; 455dclp; S535/30 nm); and CFP (S430/25 nm; 455dclp; S470/30 nm). Average background signal was subtracted. FRET ratio (FR) was calculated by the following equation:

$$FR = F_{AD} / F_A = [S_{FRET}(DA) - R_{D1} * S_{CFP}(DA)] / R_{A1} * [S_{YFP}(DA) - R_{D2} * S_{CFP}(DA)]$$

where F_{AD} represents the total YFP emission with 430/25-nm excitation, and F_A represents the direct YFP emission with 500/20-nm excitation. In S_{CUBE}(SPECIMEN), CUBE indicates the filter cube (CFP, YFP, or FRET), and SPECIMEN indicates whether the cell is expressing donor (D, CFP), acceptor (A, YFP), or both (DA). $R_{D1} = S_{FRET}(D)/S_{CFP}(D)$, $R_{D2} = S_{YFP}(D)/S_{CFP}(D)$, and $R_{A1} = S_{FRET}(A)/S_{YFP}(A)$ are predetermined constants that require measurement of the bleed-through of the emission of only CFP- or YFP-tagged molecules into the FRET channel and the emission of only CFP-tagged molecules into the YFP channel.

3.2.3 Physiological studies

3.2.3.1 Fluorescence measurement of intracellular Ca^{2+} concentration.

Cell preparation and Ca^{2+} measurements were performed as described (Ma et al 2010). Cells were loaded with 10 μmol/L Fura-2/AM and 0.02% pluronic F-127 for 1 hour in dark at 37°C in a normal physiological solution (NPSS) containing in mmol/L, 140 NaCl, 1 KCl, 1 $CaCl_2$, 1 $MgCl_2$, 10 glucose, 5 Hepes, pH 7.4. Flow was initiated by pumping NPSS containing 1% BSA to a specially-designed parallel plate flow chamber resemble the one described by Kanai et al (Kanai et al, 1995), in which the cells were adhered to the bottom. Shear stress was ~5 dyne/cm^2. The fluorescent signal was measured using a fluorescence imaging system (Olympus). 10-20 cells were analyzed in each experiment. Changes in $[Ca^{2+}]_i$ were displayed as a change in Fura-2 ratio (F_{340}/F_{380}).

3.2.3.2 Whole cell patch clamp.

Cells cultured on coverslips which were mounted in a special flow chamber (Warner Instrument Corp) (Barakat et al, 1999). Whole cell current was measured with an EPC-9 patch clamp amplifier as described elsewhere (Ma xin et al, 2010). Steady laminar flow was administered via a syringe pump (Cole Parmer). To make the experimental conditions consistent, we maintained flow rate at (2 ml/min) and also kept the distance between flow inlet and cells under study constant. The corresponding shear stress to which the cells in the Warner chamber were exposed in this system is not precisely known; however, assuming a linear velocity variation in the direction orthogonal to flow, the shear stress is estimated to be in the range of 0.5 to 1 dyne/cm^2 (Barakat et al, 1999). For most whole-cell recording, the pipette solution contained in mmol/L: 20 CsCl, 100 Cs^+-aspartate, 1 $MgCl_2$, 4 ATP,

0.08 $CaCl_2$, 10 BAPTA, 10 Hepes, pH 7.2. Free Ca^{2+} in pipette solution was 1 nM (Votes T et al, 2002), which prevent the activation of Ca^{2+}-sensitive Cl^- channel and allow the recording of TRPV4-related channels (Votes T et al, 2002; Kwan HY et al, 2000). Bath solution contained in mmol/L: 150 NaCl, 6 CsCl, 1$MgCl_2$, 1.5 $CaCl_2$, 10 glucose, 10 Hepes, pH 7.4. For whole-cell recording in the cells that were transfected with TRPP1 and TRPP2 or TRPP1 and $TRPP2^{R636G}$, the pipette solution contained in mmol/L: 15 CsCl, 135 Cs-Aspartate, 10 HEPES, 10 glucose, pH 7.4 (adjusted with CsOH). The free Ca^{2+} concentration in pipette solution was fixed to 100 nM by adding 0.2 mmol/L EGTA and 0.12 mmol/L $CaCl_2$. The bath solution contained in mmol/L: 140 NaCl, 2.5 $CaCl_2$, 10 HEPES, 10 glucose, pH 7.4 (adjusted with NaOH). Cells were clamped at 0 mV. Whole cell current density (pA/pF) was recorded in response to successive voltage pulses of +80 mV and -80 mV for 100 ms duration. These whole cell current values were then plotted vs. time. The recordings were made before and after flow. All currents were sampled at 50 kHz and filtered at 5 kHz, and the data were analyzed with Pulse Fit. All patch-clamp recordings were performed at room temperature.

3.2.4 Statistics

Student's t-test was used for statistical comparison, with probability $p<0.05$ as a significant difference. For comparison of multiple groups, One-way ANOVA with Newman-keuls was used.

4. Chapter 4: Heteromeric coassembly of TRPV4, TRPC1 and TRPP2 to form a flow-sensitive channel

4.1 Abstract

TRP channels function as cellular sensors to perceive and respond to a variety of environmental stimuli including temperature, pain, pressure and fluid flow. These channels can be divided into seven subfamilies, including TRPV, TRPC, TRPP, and four others. Functional TRP channels are tetrameric complexes consisting of four pore-forming subunits, which could be identical (homotetrameric channels) or different (heterotetrameric channels). In this chapter, I found that TRPV4, -C1, and -P2 associate together to form a physical complex. In function study, this TRPV4-C1-P2 complex mediates flow-induced Ca^{2+} influx in HEK293 cells over-expressing TRPV4, -C1, and -P2 and in rat MAECs. Pore-dead mutant of each of these three TRP isoforms abolished or markedly reduced the flow-induced cation currents and Ca^{2+} rises, suggesting all three TRPs contribute to the ion permeation pore of the channels. Taken together, I identified the first heteromeric TRP channels composed of subunits from three different TRP subfamilies, namely heteromeric TRPV4-C1-P2 channels. Functionally, heteromeric TRPV4-C1-P2 are the main channels that mediate flow-induced Ca^{2+} rises in native vascular endothelial cells, thus plays a key role in the control of vascular tone and blood pressure.

4.2 Introduction

TRP channels are a superfamily of cation channels that can be divided into seven subfamilies, which include TRPC, TRPV, TRPP, and four others. The channels function as cellular sensors to perceive and respond to a variety of environmental stimuli (Damann et al, 2008). Functional TRP channels are tetrameric complexes consisting of four pore-forming subunits (Hoenderop *et al*, 2003). Each subunit is thought to contain six transmembrane regions (S1–S6) and a re-entrant loop between transmembrane segments S5 and S6 that constitutes the ion conducting pore (Lepage *et al*, 2007). Four pore-forming subunits could be identical (homotetrameric) or different (heterotetrameric) (Hofmann *et al*, 2002; Strübing *et al*, 2001). Heteromeric assembly usually occurs between the members within the same TRP subfamily (intra-subfamily) (Hofmann *et al*, 2002). For TRPC subfamily, its seven members can be further divided into two subgroups, TRPC1/4/5 as one subgroup and TRPC3/6/7 as the other. All members within one subgroup, for example TRPC3/6/C7, can co-assemble with each other to form a channel (Hofmann *et al*, 2002). In addition, TRPC1 may act as a linker. When TRPC1 is present, TRPC4/5 may heteromultimerize with TRPC3/6/7 (Strübing *et al*, 2003). For TRPV subfamily, the predominant type of assembly is homomeric assembly, but heteromeric assembly may occur between TRPV5 and -V6 (Hoenderop *et al*, 2003; Hellwig *et al*, 2005).

In addition to intra-subfamily coassembly, cross-subfamily assembly of TRP subunits could also happen. Three such examples have been reported, including TRPC1 with -P2 (Tsiokas *et al*, 1999; Bai *et al*, 2008; Zhang *et al*, 2009), TRPV4 with -P2 (Köttgen *et al*, 2008; Stewart *et al*, 2010), and TRPC1 with -V4 (Ma *et al*, 2010). Functional studies indicate that heteromultimeric channels may display properties different from those of homomultimeric channels (Hofmann *et al*, 2002; Strübing *et al*, 2001; Köttgen *et al*, 2008).

Heteromeric coassembly greatly diversifies the structure and function of TRP channels, and allows TRP channels to control and/or regulate many distinct cellular processes.

In the circulation system, shear stress generated from hemodynamic blood flow is an important physiological stimulus to induce vascular relaxation (Busse and Fleming, 2003). One of the key early signals in flow responses is flow-induced $[Ca^{2+}]_i$ rise in vascular endothelial cells. Previous studies from Ma et al (2010a) and others have demonstrated the involvement of TRPV4 (Hartmannsgruber *et al*, 2007; Köhler *et al*, 2006), TRPP2 (AbouAlaiwi *et al*, 2009), and heteromeric TRPV4-C1 channels (Ma *et al*, 2010a) in flow-induced Ca^{2+} influx in vascular endothelial cells.

Up to the present, only three TRP isoforms, i.e. TRPV4, -C1 and -P2, have been shown to be capable of initiating cross-subfamily assembly. Interestingly, all three isoforms have been suggested to be involved in flow-induced Ca^{2+} influx in vascular endothelial cells. In this chapter, we hypothesize that TRPV4, -C1 and -P2 can co-assemble together to form heteromeric TRPV4-C1-P2 channels. We further hypothesize that the channels mediate flow-induced Ca^{2+} influx in vascular endothelial cells. A variety of different biochemical and electrophysiological methods were used to test the hypotheses.

4. 3. Experimental procedures

Detailed experimental procedures are described in Chapter 3.

4.4 Results

4.4.1 Physical Association of TRPV4, TRPC1 and TRPP2.

Two-step co-IP was used to examine the physical association of TRPV4, -C1 and -P2 when all three were co-expressed in HEK293 cells. A schematic diagram of two-step co-immunoprecipitation is shown in Figure 4-1. In experiments, TRPV4 was detected in the immunoprecipitates pulled-down by the anti-TRPC1 followed by anti-TRPP2 antibody, but not in the control immunoprecipitates pulled-down by preimmune IgG (Figure 4-2A). These data suggest the existence of TRPV4-C1-P2 complex in HEK293 cells that were transfected with TRPV4, -C1 and -P2. Similar study demonstrated that the presence of such complex in the primary cultured rat MAECs (Figure 4-2*B*). All three antibodies used in the experiments were previously found to be highly specific to their targets by us and others (Bai *et al*, 2008; Ma *et al*, 2010a; Maroto *et al*, 2005; Yang *et al*, 2006).

Chemical cross-linking was then performed to verify the existence of TRPV4-C1-P2 complex in HEK293 cells that were expressed with TRPV4, C1 and P2 (Fig 4-3A) and in the primary cultured rat MAECs (Fig 4-3B). I used a highly reactive, amine-specific, *N*-hydroxysuccinimide (NHS) ester DTSSP as the cross-linker (Corey *et al*, 1998, 2001). After extensive cross-linking by treating the cell lysates with 5 mmol/L DTSSP for 2 hr, the main cross-linked product was found to have molecular mass of ~450 Kd, which corresponds to the predicted molecular size of tetrameric TRP channels (Figure 4-3). This band was recognized by either anti-TRPC1, anti-TRPV4, or anti-TRPP2 antibody, suggesting the presence of tetrameric TRP complex containing TRPV4, TRPC1 and TRPP2 (Figure 4-3). Another major band of ~half molecular size was also detected (Figure 4-3). This band likely represents a partial cross-linked product consisting of TRP dimers. Similar

results were obtained in experiments using DSS as another crosslinker. Note that the chemical cross-linking procedures as those shown in Figure 4-3 almost always result in diffused bands on the gel because of a large number of heterogeneously monolinked and cross-linked intermediate products are formed (Corey *et al*, 1998, 2001; Leitner *et al*, 2010). Therefore, it is expected that the bands on gel in Figure 4-3 would be more diffused than those of typical immunoblots.

Previously, Ma et al have shown that TRPV4 and TRPC1 can heteromerize to form heteromeric TRPV4-C1 channels when they are co-expressed in HEK293 cells (Ma *et al*, 2010a and b). Here, I tagged TRPP2 and TRPV4-C1 concatamers with YFP and CFP, respectively, and detected their interaction by FRET. Strong FRET signal was detected in HEK293 cells co-expressing CFP-tagged TRPV4-C1 concatamers and YFP-tagged TRPP2 (Figure 4-4), confirming direct interaction of TRPP2 with TRPV4-C1 heteromers. To further explore the subunit composition of TRPV4-C1-P2 channels, CFP-tagged TRPP2-V4-C1 contacamers were constructed. Co-expressing CFP-tagged TRPP2-V4-C1 concatamers either with YFP-tagged TRPV4 or with YFP-tagged TRPC1 or with YFP-tagged TRPP2 all resulted in strong FRET signals (Figure 4-4), suggesting that subunit stoichiometries of 2V4:1C1:1P2, 1V4:2C1:1P2, and 1V4:1C1:2P2 were all possible. No FRET signal was detected in the negative control, in which the cells were co-transfected with CFP-tagged TRPV4 and YFP-tagged GIRK4 (Figure 4-4). GIRK4 is an inwardly rectifying K^+ channel bearing no similarity to TRP, serving as membrane protein control.

4.4.2 Role of overexpressed heteromeric TRPV4-C1-P2 channels in flow-induced cation currents in HEK293 cells.

I utilized a number of mutant TRP constructs including $TRPC1^{multi\text{-}pore}$, $TRPC1^{\Delta 567\text{-}793}$, $TRPV4^{M680D}$, $TRPP2^{R636G}$, and $TRPP2^{D551V}$ to study the involvement of specific TRP isoforms in flow responses. $TRPC1^{\Delta 567\text{-}793}$ is truncation mutation with deletion from TRPC1 pore region to its C-terminus (Liu *et al*, 2003). $TRPC1^{multi\text{-}pore}$ and $TRPV4^{M680D}$ carry point mutation at the pore region of TRPC1 and TRPV4, respectively (Liu *et al*, 2003; Voets *et al*, 2002). $TRPP2^{D551V}$ carries a point mutation at the third transmembrane span of TRPP2 (Reynolds, 1999; Ma *et al*, 2005). It has previously been shown that these constructs can produce mutated TRP subunits that are capable of co-assembling with wild-type TRP subunits, resulting in the formation of malfunctioned channels. Therefore, these mutants can serve as dominant-negative constructs that can disrupt the function of endogenous TRP isoforms (Liu *et al*, 2003; Voets *et al*, 2002; Reynolds, 1999; Ma *et al*, 2005). A TRPP2 mutant $TRPP2^{R636G}$ was also constructed. $TRPP2^{R636G}$ carries a point mutation in the pore region of TRPP2. The mutant disrupted the function of wild-type TRPP2 (Figure 4-5*A, B*), thus it was used as a pore-dead dominant-negative construct in later experiments.

In experiments, application of flow elicited a whole-cell cation current in HEK293 cells co-expressing TRPV4, -C1 and -P2, but not in the cells that were transfected with empty vector (Figure 4-6*A*). Increased flow rate resulted in graded increase in currents (Figure 4-6*B*). Current-voltage curve displayed a a relatively linear relationship (Figure 4-6*C*). When any one of these three TRPs was replaced with their mutant counterpart (for example TRPV4 replaced with $TRPV4^{M680D}$), the flow-induced cation current was abolished (Figure 4-6*D*).

I also studied the flow-induced cation current in cells that were transfected with only one TRP (TRPC1, TRPV4, or TRPP2) (Figure 4-7*A-C*) or co-expressed with two TRPs (TRPV4 plus -C1, or TRPC1 plus -P2, or

TRPV4 plus -P2) (Figure 4-7*D*). Among them, only three combinations, homomeric TRPV4, heteromeric TRPV4-P2 and heteromeric TRPV4-C1, displayed a flow-induced cation current (Figure 4-7*A-D*). In agreement with other reports (Bai *et al*, 2008; Köttgen *et al*, 2008; Ma *et al*, 2010), the I-V relationships of channels formed by all these combinations were all relatively linear (Figure 4-8).

4.4.3 Role of overexpressed heteromeric TRPV4-C1-P2 channels in flow-induced Ca^{2+} influx in HEK293 cells.

Flow initiated a $[Ca^{2+}]_i$ rise in HEK293 cells in which TRPV4, -C1 and -P2 were co-expressed (Figure 4-9*A*), but not in the cells that were transfected with empty vector (Figure 4-9*A*). This $[Ca^{2+}]_i$ rise could be attributed to Ca^{2+} influx, because it was absent when cells were bathed in a Ca^{2+}-free solution (Figure 4-10A). Increased flow shear force resulted in graded increase in $[Ca^{2+}]_i$ response (Figure 4-9*B*). When any one of these three TRPs was replaced with their mutant counterpart (for example TRPV4 replaced with $TRPV4^{M680D}$), flow-induced $[Ca^{2+}]_i$ response became very small (Figure 4-9*C,D*). A tiny residual fluorescence change, which could be observed in vector-transfected HEK293 cells as well as TRP over-expressing HEK cells, might be caused by slight cell movements during flow disturbance, not an indication of $[Ca^{2+}]_i$ change. This was arbitrarily labeled as "Base line" in Figure 4-9*D*. However, for the cells transfected with $TRPC1^{multi\text{-}pore}$ or $TRPC1^{\Delta 567\text{-}793}$ (Figure 4-9*D*), the residual $[Ca^{2+}]_i$ responses were larger than that of vector-transfected HEK cells and accounted for ~30% of flow responses in HEK cells that were co-expressed with TRPV4, -C1 and -P2 (Figure 4-9*D*).

Flow-induced $[Ca^{2+}]_i$ rises were also studied in cells that were transfected with only one TRP (TRPC1, TRPV4, or TRPP2) (Figure 4-11*A*, *B*) or transfected with two TRPs (TRPV4 plus -C1, or TRPC1 plus -P2, or TRPV4 plus -P2) (Figure 4-11*C*). Similar to the electrophysiological studies, only three combinations, homomeric TRPV4, heteromeric TRPV4-P2 and heteromeric TRPV4-C1, displayed flow-induced $[Ca^{2+}]_i$ rises (Figure 4-11*A-C*).

4.4.4 Role of heteromeric TRPV4-C1-P2 channels in flow-induced Ca^{2+} influx and cation current in rat MAECs.

I next explored the role of heteromeric TRPV4-C1-P2 channels in flow response in native vascular endothelial cells. The expression of TRPV4, -C1, and -P2 proteins in rat MAECs has been reported elsewhere (Ma *et al*, 2010a) and/or demonstrated here (Figure 4-12*A-C*). Flow elicited a cation current in rat MAECs (Figure 4-13*A-C*). This current displayed a relatively linear current-voltage relationship (Figure 4-13*B*). Transfection of $TRPC1^{multi\text{-}pore}$, $TRPV4^{M680D}$ or $TRPP2^{R636G}$, each abolished the flow-stimulated cation current in rat MAECs (Figure 4-13*C*). In fluorescence $[Ca^{2+}]_i$ measurement, these mutants strongly suppressed the flow-induced $[Ca^{2+}]_i$ rises in rat MAECs (Figure 4-14*A, B*). There was a tiny residual fluorescence change to flow in $TRPV4^{M680D}$-transfected cells, the amplitude of which was similar to that in vector-transfected HEK293 cells. Again, we attributed this to the artifacts caused by cell movement during flow disturbance. However, for the cells transfected with $TRPC1^{multi\text{-}pore}$ or $TRPP2^{R636G}$ (Figure 4-14*A, B*), the residual $[Ca^{2+}]_i$ responses were larger than that of vector-transfected HEK293 cells and accounted for ~22% of flow responses in native rat MAECs (Figure 4-14*B*). As controls, transfection of pore mutants did not affect the $[Ca^{2+}]_i$ responses to

ATP (Figure 4-15A). As another control, flow $[Ca^{2+}]_i$ responses were not altered by disruption of functional TRPC5, which is not involved in flow response (Figure 4-15B). This $[Ca^{2+}]_i$ rise could be attributed mainly to Ca^{2+} influx, because there are only half size of $[Ca^{2+}]_i$ rise in about 10% MAECs when cells were bathed in a Ca^{2+}-free solution (Figure 4-10).

Note that flow-induced cation currents and $[Ca^{2+}]_i$ rises in rat MAECs were transient (Figure 4-14*A*), which was different from that of TRPV4-C1-P2 co-expressing HEK293 cells (Figure 4-9*A*). The transient nature of this response has been discussed elsewhere and could be attributed to nitric oxide-cGMP-protein kinase G-mediated inhibition of TRPC1-containing channels (Yao *et al*, 2000, Ma *et al*, 2010a). HEK293 cells lack the components of nitric oxide-cGMP-protein kinase G signal cascades, and thus do not exhibit such an inhibition. The inhibitory effect of cGMP-protein kinase G on heteromeric TRPV4-C1-P2 channels was further verified. In HEK293 cells stably expressing protein kinase G 1α, flow-induced Ca^{2+} influx through TRPV4-C1-P2 channels was found to be inhibited by 8-Br-cGMP, the effect of which was reversed by KT5823 (Figure 4-15*A, B*). Similar to our previous finding in other types of endothelial cells (Yao *et al*, 2000), flow-induced $[Ca^{2+}]_i$ rise in rat MAECs was also confirmed to be sensitive to 8-Br-cGMP inhibition, the effect of which was reversed by KT5823 (Figure 4-15*C, D*). Importantly, treatment of rat MAECs with KT5823 (1 uM) increased the magnitude and markedly slowed down the falling phase of flow-induced $[Ca^{2+}]_i$ transient (Figure 15*E*). These data support that NO-cGMP-protein kinase G inhibition on heteromeric TRPV4-C1-P2 channels contributes to the transient nature of flow $[Ca^{2+}]_i$ response in native endothelial cells.

It is documented that flow could activate Cl^- channels (Barakat *et al*, 1999) and K^+ channels (Olesen *et al*, 1988) in vascular endothelial cells and HEK cells co-expressed with TRPV4, C1 and P2. The activity of these

channels is expected to alter the membrane potentials, which could then affect Ca^{2+} influx. In the present study, treatment of rat MAECs with 40 μM niflumic acid or 5 mM Cs^{+} did not have significant effect on flow-induced Ca^{2+} rise in these cells (Figure 4-16), suggesting that these channels did not significantly contribute to flow-induced Ca^{2+} responses.

4.4.5 Co-expression of TRPV4, -C1, and -P2 in the cilia of primary cultured rat MAECs

Cilia are structure that is suggested to play a key role in flow sensation (Nauli *et al*, 2003, Kottgen *et al*, 2008). The present immunostaining results show that TRPV4, TRPC1, and TRPP2 were co-expressed in the cilia of rat MAECs (Figure 4-17).

4.5 Discussion

The major findings of this chapter are as follows: 1) Two-step co-IP, chemical cross-linking and FRET detection demonstrated the presence of TRPV4-C1-P2 heteromers in HEK293 cells that were co-expressed with TRPV4, -C1 and -P2 and in primary cultured rat MAECs. 2) Fluorescent Ca^{2+} measurement and whole-cell patch clamp detected the flow-induced Ca^{2+} influx and cation currents in these triple TRP co-expressing HEK293 cells. Pore-dead mutants of each of these three TRPs (for instance, pore-dead mutant of TRPC1), when co-expressed with two other wild-type TRPs (for instance, TRPV4 and TRPP2), markedly reduced or even abolished the flow-induced $[Ca^{2+}]_i$ rises and whole-cell cation currents. 3) In rat MAECs, flow-induced $[Ca^{2+}]_i$ rises and cation currents were also strongly suppressed by these pore-dead TRP mutants. Taken together, my results identified the first TRP channels that are

composed of subunits from three different TRP subfamilies. Furthermore, I demonstrate that TRPV4-C1-P2 is the main channels that mediate flow-induced Ca^{2+} influx and cation currents in native endothelial cells. The existence of such type of heteromeric channels crossing three different TRP subfamilies greatly increases the numeric numbers of different heteromeric TRP channels that could possibly be assembled, making the structure and function of TRP channels even more diversified. It is expected that such kind of heteromeric channels can be activated by diverse stimuli/agonists, thus allows diverse signals to converge on this TRP complex to initiate distinct cellular responses.

Heteromeric assembly usually occurs between the members within the same TRP subfamily such as TRPC1 with -C5, TRPV5 with -V6, and TRPM6 with -M7 (Hoenderop *et al*, 2003; Lepage *et al*, 2007; Strübing *et al*, 2001). However, several examples of cross-subfamily heteromerization have also been reported. These include TRPC1 with -P2 (Tsiokas *et al*, 1999; Bai *et al*, 2008), TRPV4 with -P2 (Köttgen *et al*, 2008) and TRPV4 with -C1 (Ma *et al*, 2010a). Functionally, TRPV4-P2 channels have been shown to be activated by hypotonic stress and temperature (Köttgen *et al*, 2008); TRPV4-C1 channels are activated by flow shear force (Ma *et al*, 2010a), and TRPP2-C1 channels are activated by G-protein-coupled receptor agonists (Bai *et al*, 2008). In the present study, the results from three independent methods including two-step co-IP, chemical cross-linkage and FRET all demonstrated the existence of physical association between TRPV4, -C1, and -P2 in TRP-overexpressing HEK293 cells and native endothelial cells. DTSSP was used in the chemical cross-linking experiments. DTSSP is a membrane impermeant cross-linker, which can crosslink adjacent protein subunits expressed on the cell surface (Corey *et al*, 1998; Corey *et al*, 2001). The positive results from DTSSP cross-linking experiments suggest that TRPV4, -C1, and -P2 form physical complex

in the plasma membrane. Among the above three methods, FRET is the most sensitive and reliable method for monitoring the subunit assembly of channel proteins (Ma *et al*, 2010a; Zheng *et al*, 2002). FRET reports the proximity of two fluorophores. Distances closer than 10 nm between appropriate fluorophores are required to elicit FRET (Hofmann *et al*, 2002). Previously, I showed that TRPV4 and -C1 heteromerize to form heteromeric TRPV4-C1 channels (Ma *et al*, 2010a). In this chapter, I have detected a strong FRET signal between CFP-tagged TRPV4-C1 concatamers and YFP-tagged TRPP2 when they were co-expressed in HEK293 cells. These data provided compelling evidence for the direct physical association of TRPP2 and TRPV4-C1 heteromeric channels, namely a formation of a TRPV4-C1-P2 complex.

There is intense interest in searching for the molecular identity of the channels that mediate flow-induced Ca^{2+} influx. In vascular endothelial cells, it is known that flow-induced Ca^{2+} rise stimulates the release of vasodilators, such as nitric oxide, prostacyclin and endothelium-derived hyperpolarizing factors (Hartmannsgruber *et al*, 2007; Liu *et al*, 2006), which then act on the underlying smooth muscle cells to cause vascular relaxation. Several candidate channels have been proposed to mediate flow-induced Ca^{2+} influx in vascular endothelial cells. These include TRPV4 (Hartmannsgruber *et al*, 2007; Köhler *et al*, 2006), TRPP2 (AbouAlaiwi *et al*, 2009) and TRPV4-C1 heteromeric channels (*Ma et al*, 2010a). However, all these published data could be alternatively explained by involvement of TRPV4-C1-P2 complex in the flow response, because these previous studies were based on pharmacological agents and/or siRNAs that target TRPV4 and/or TRPC1 and/or TRPP2. However, it is certain that these pharmacological agents and/or siRNAs would also target heteromeric TRPV4-C1-P2 channels. Therefore, it is possible that heteromeric TRPV4-C1-P2 channels, rather than individual TRPV4 or TRPP2 channels, may play a more important role in native endothelial cells. In

experiments, I found the pore-dead mutant for each of these three TRPs ($TRPC1^{multi\text{-}pore}$, $TRPV4^{M680D}$, or $TRPP2^{R636G}$) abolished the flow-induced cation currents in HEK293 overexpression system and rat MAECS. They also abolished or suppressed (>70%) flow-induced $[Ca^{2+}]_i$ rises in these cells. Two other dominant-negative mutants of TRPs, $TRPP2^{D551V}$ and $TRPC1^{\Delta 567\text{-}793}$, had similar inhibitory effects. These data strongly suggest that, in both the HEK293 overexpression system and native endothelial cells, the predominant flow-sensitive Ca^{2+} influx channels require all three TRPs, i.e. TRPV4, -C1 and -P2. Furthermore, all three TRP isoforms, TRPV4, TRPC1 and TRPP2, contribute to the permeation pore of the channels, namely a heterotetrameric TRPV4-C1-P2 channel. This finding represents the first identified heteromeric TRP channels across three different TRP subfamilies. Previously, TRPV4 (Hartmannsgruber *et al*, 2007; Köhler *et al*, 2006), TRPP2 (AbouAlaiwi *et al*, 2009) and heteromeric TRPV4-C1 channels (Ma *et al*, 2010) have been individually suggested to be involved in flow responses in vascular endothelial cells. Our scheme unifies all existing hypotheses into a common one in which we suggest that heteromeric TRPV4-C1-P2 channels are the predominant flow-sensitive Ca^{2+} influx channels in vascular endothelial cells.

When TRPV4, -C1, -P2 are all expressed in a single cell, beside heteromeric TRPV4-C1-P2, other types of homomeric and heteromeric assembly may also occur. Some of these assembly types, such as homomeric TRPV4, heteromeric TRPV4-C1 and heteromeric TRPV4-P2, are known to be sensitive to flow (Ma *et al*, 2010; Hartmannsgruber et al, 2007; Köhler *et al*, 2006; AbouAlaiwi *et al*, 2009; also Figure 4- 7 and Figure 4- 11). The question is whether these other assembly types could also contribute to the flow responses in native endothelial cells. In this chapter, I observed that flow-induced cation currents were abolished by mutants that disrupt the function of each of these three TRPs ($TRPC1^{multi\text{-}pore}$, $TRPV4^{M680D}$,

$TRPP2^{R636G}$, $TRPP2^{D551V}$ or $TRPC1^{\Delta 567\text{-}793}$). This fits the profile of heteromeric TRPV4-C1-P2 channels, but not any other assembly types, suggesting that the contribution of other assembly types may be very small. However, in fluorescence Ca^{2+} measurement, there was still some residual Ca^{2+} response to flow (~20%) after cells were treated with $TRPC1^{multi\text{-}pore}$, $TRPC1^{\Delta 567\text{-}793}$ and $TRPP2^{R636G}$. These residual Ca^{2+} responses could be due to the contribution of other TRP assembly types towards Ca^{2+} influx or intracellular Ca^{2+} release. To break it down, for cells transfected with $TRPC1^{multi\text{-}pore}$ or $TRPC1^{\Delta 567\text{-}793}$, residual Ca^{2+} response could be due to TRPC1-independent components such as homomeric TRPV4 and/or heteromeric TRPV4-P2. For cells transfected with $TRPP2^{R636G}$, the residual component could be TRPP2-independent components such as homomeric TRPV4 and/or heteromeric TRPV4-C1. In cells transfected with $TRPC1^{multi\text{-}pore}$+$TRPP2^{R636G}$, it could be homomeric TRPV4. Therefore, it is clear that the present results could not exclude the contribution of other TRP assembly types in flow-induced Ca^{2+} influx. However, it is also clear that the contribution from other TRP assembly types, even if they existed, were relatively small and accounted for <30% of the total Ca^{2+} responses to flow. Therefore, I can conclude that the predominant flow-sensitive Ca^{2+} influx channels are heteromeric TRPV4-C1-P2 channels. Interestingly, my data also suggest that, in cells where TRPV4, -C1 and -P2 are all expressed, assembly of TRP subunits is not random. Certain types of assembly may be strongly favored whereas other types of assembly are less significant.

Cilia is structure that is suggested to play a key role in flow sensation (Nauli *et al*, 2003; Köttgen *et al*, 2008). Vascular endothelial cells also contain cilia, and furthermore, TRPP1 and TRPP2 were found to be localized in the cilia (Nauli *et al*, 2008, AbouAlaiwi *et al*, 2009). Reports also documented the localization of TRPV4 and TRPC1 in the cilia of other epithelial cell types

including renal epithelial cells and reproductive tract epithelial cells (Köttgen *et al*, 2008; Teilmann *et al*, 2005; Nauli *et al*, 2003, Bai *et al*, 2008), although no data are available for their expression in the cilia of vascular endothelial cells. In the present study, we found the expression of TRPV4, -C1, -P2 and -P1 in the cilia of rat MAECs. These data agree with the notion that localization of TRPV4, -P1 and -P2 are important for their function in flow response.

In conclusion, the data from this chapter uncovered the first heteromeric TRP channels that are composed of subunits from three different subfamilies, being heteromeric TRPV4-C1-P2 channels. Functionally, this channel is the main entity that mediates flow-induced Ca^{2+} influx and cation currents in vascular endothelial cells.

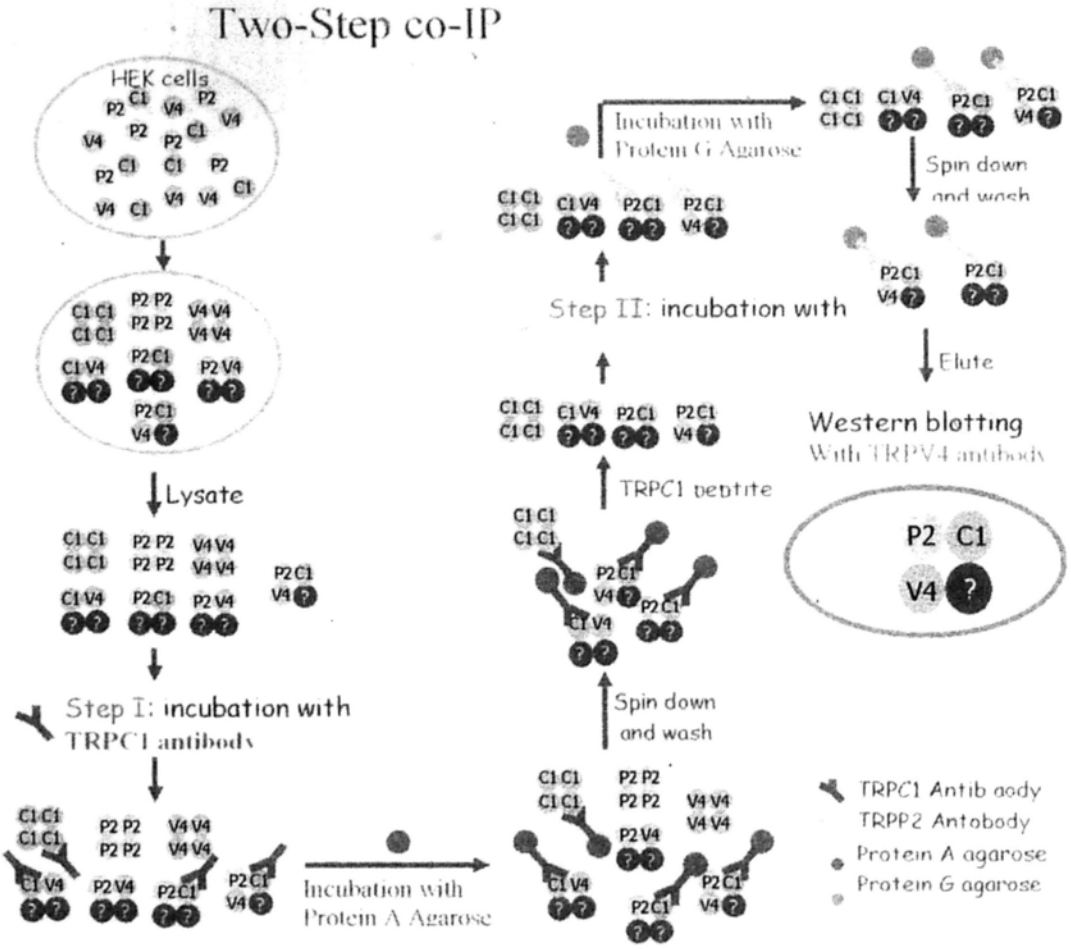

Figure 4- 1. Physical interaction of TRPV4, -C1 and -P2.

Schematic figure showing the procedure of two-step co-immunoprecipitation to generate Fig. 4-2 A, B.

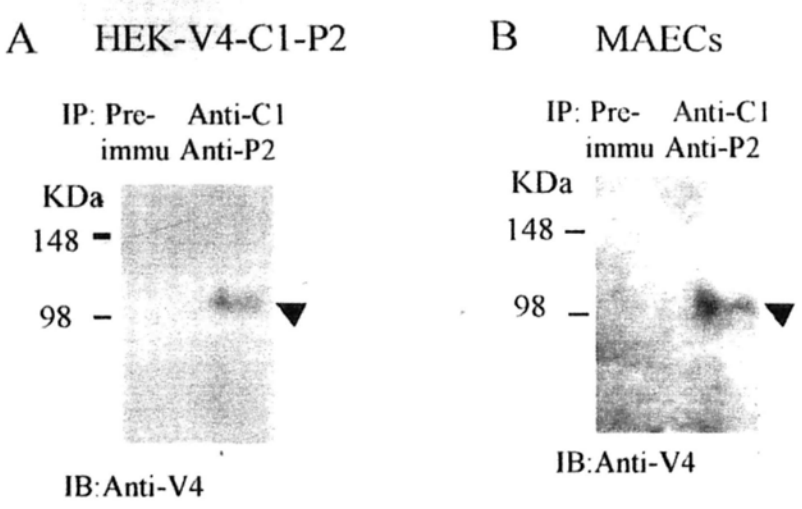

Figure 4- 2. Two step co-IP of TRPV4-C1-P2.

The first immunopricipitation was performed using anti-TRPC1 antibody, followed by elution with TRPC1 antigen peptide. The second immunprecipitation was performed with anti-TRPP2 antibody or with preimmune IgG as control. The precipitates were immunoblotted with anti-TRPV4 antibody. A, B, Representative gel pictures of two step co-immunoprecipitation in HEK293 cells co-expressing TRPV4, C1 and -P2 (HEK-V4-C1-P2) (A) and the primary cultured rat MAECs (B). IP, immunoprecipitation; IB, immunoblot; Anti-C1: anti-TRPC1 antibody; Anti-V4: anti-TRPV4 antibody; Anti-P2: anti-TRPP2 antibody.

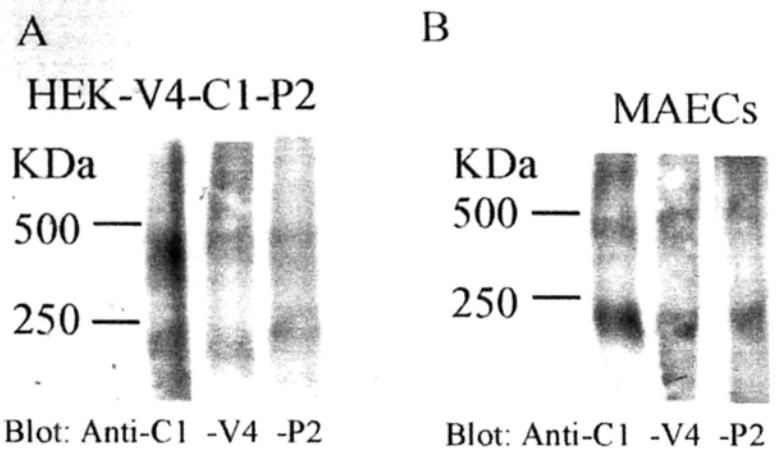

Figure 4- 3. Chemical cross-linking of TRPV4, -C1 and -P2.

Representative immunoblots of HEK293 cells that were co-expressed with TRPV4, -C1, -P2 (Left panel) and primary cultured rat MAECs (Right panel) after membrane proteins were cross-linked by 5 mM DTSSP. Lane 1-3 in C left panel and right panel, immunoblotted with anti-TRPV4, anti-TRPC1 and anti-TRPP2, respectively.

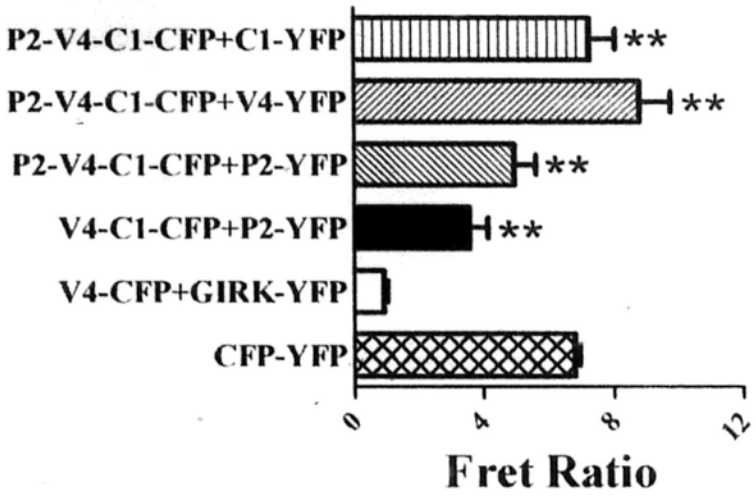

Figure 4- 4. FRET detection.

Horizontal axes indicate FRET ratio of living cells expressing the indicated constructs. When the FRET ratio is 1, there is no FRET; when the FRET ratio is greater than 1, there is FRET. Data are given as mean ± SE. GIRK4, G-protein-activated inwardly rectifying K^+ channels. ** $P<0.01$ *vs.* negative controls.

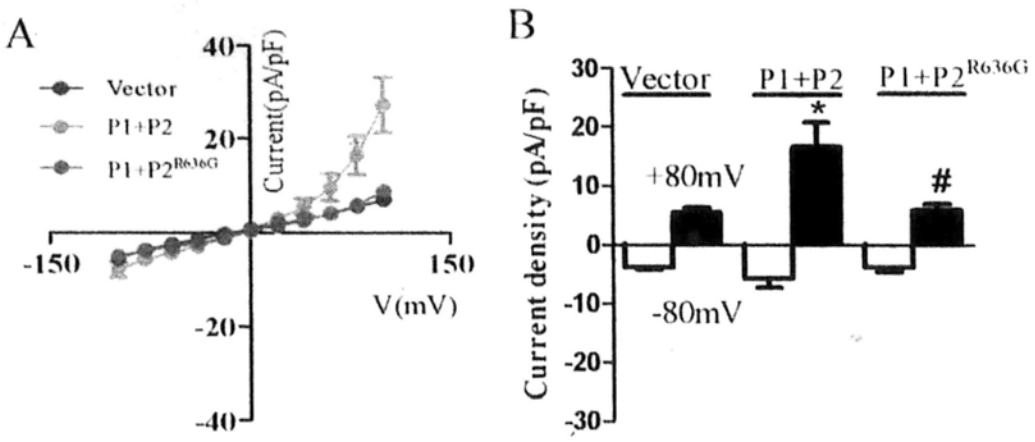

Figure 4- 5. Effect of pore mutant TRPP2^{R636G} on whole-cell current in HEK293 cells.

HEK293 cells were either transfected with TRPP1+TRPP2 (labeled as P1+ P2) or with TRPP1+TRPP2^{R636G} (labeled as P1+ P2^{R636G}) or with empty vector (labeled as Vector). A. I-V curves. B. Summary data of whole-cell currents at ±80 mV. Data are given as the mean ± SE (n = 6-8). * $P<0.05$ *vs.* Vector; # $P<0.05$ *vs.* P1+P2.

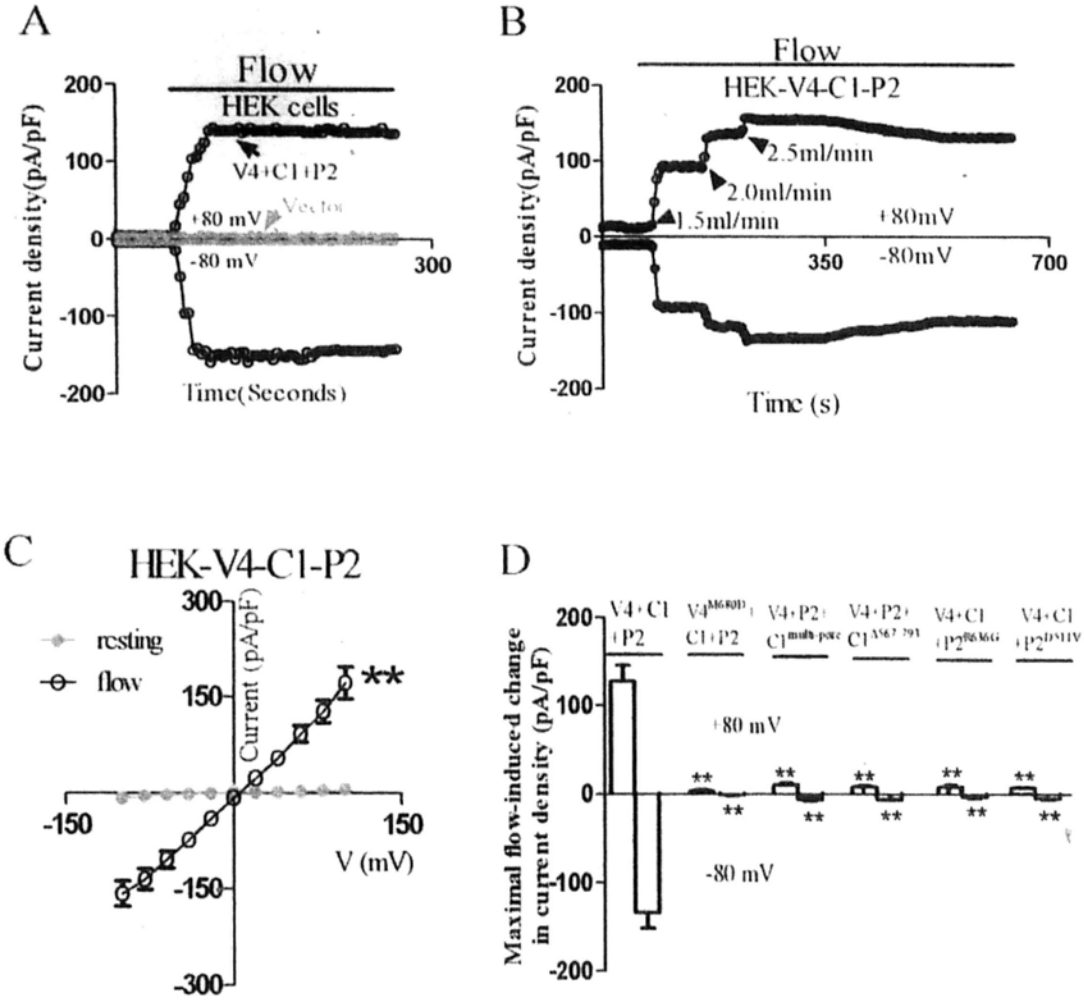

Figure 4- 6. Flow-induced whole-cell current in HEK293 cells that were co-expressed with TRPV4, -C1 and -P2.

A,B . Representative time course of flow-stimulated whole-cell current at ±80 mV in HEK293 cells co-expressing TRPV4, -C1 and -P2. C. I–V curve for cells in A before and after flow. D. Summary data of maximal amplitude of flow-induced whole-cell cation currents increase at ±80 mV. In D, control cells were co-expressed with TRPV4, -C1 and -P2 (labeled as V4+C1+P2). In others, TRPV4 was replaced with $TRPV4^{M680D}$ (labeled as $V4^{M680D}$+C1+P2); or TRPC1 was replaced with $TRPC1^{multi\text{-}pore}$ or $TRPC1^{\Delta 567\text{-}793}$ (labeled as $V4+C1^{multi\text{-}pore}$+P2 or $V4+C1^{\Delta 567\text{-}793}$+P2); or TRPP2 was replaced with $TRPP2^{R636G}$ or $TRPP2^{D511V}$ (labeled as $V4+C1+P2^{R636G}$ or $V4+C1+P2^{D511V}$). The solid bar on top of the traces indicates the period when laminar flow was applied. Data are given as the mean ± SE (n = 5-7). $^{**}P < 0.01$ *vs* before flow in C or *vs* V4+C1+P2 in D.

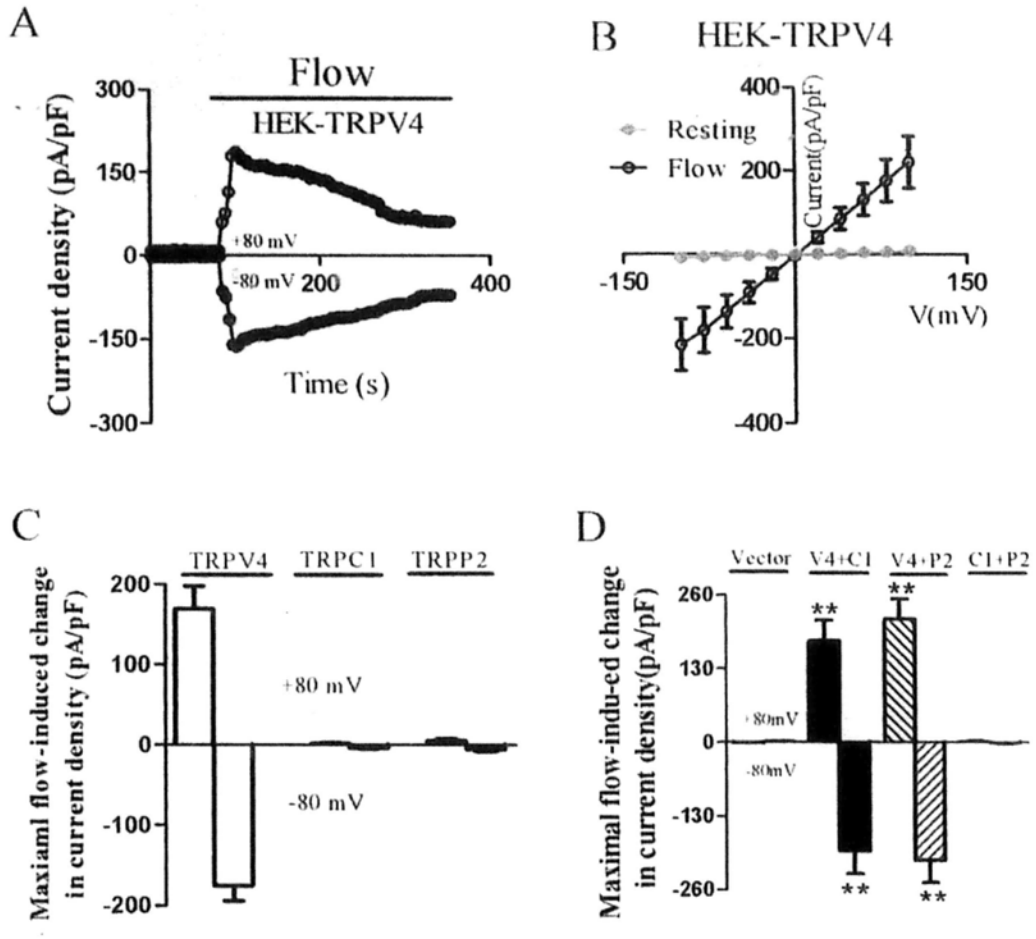

Figure 4- 7. Flow-induced whole-cell current change in HEK293 cells that were individually expressed with TRPV4, -C1 or -P2, or co-expressed with two TRPs.

A. Representative time course of flow-stimulated whole-cell current at ±80 mV in TRPV4-expressing cells. B. I–V curve of TRPV4-expressing cells before and after flow. C. Summary data of maximal amplitude of flow-induced whole-cell cation currents increase at ±80 mV in cells that were individually expressed with TRPV4, TRPC1 or TRPP2. D. Summary data of maximal amplitude of flow-induced whole-cell cation currents increase at ±80 mV in cells that were co-expressed with two TRPs. The solid bar on top of the traces indicates the period when laminar flow was applied. Data are given as the mean ± SE (n = 5-8). $^{**}P$ 0.01 *vs.* Vector.

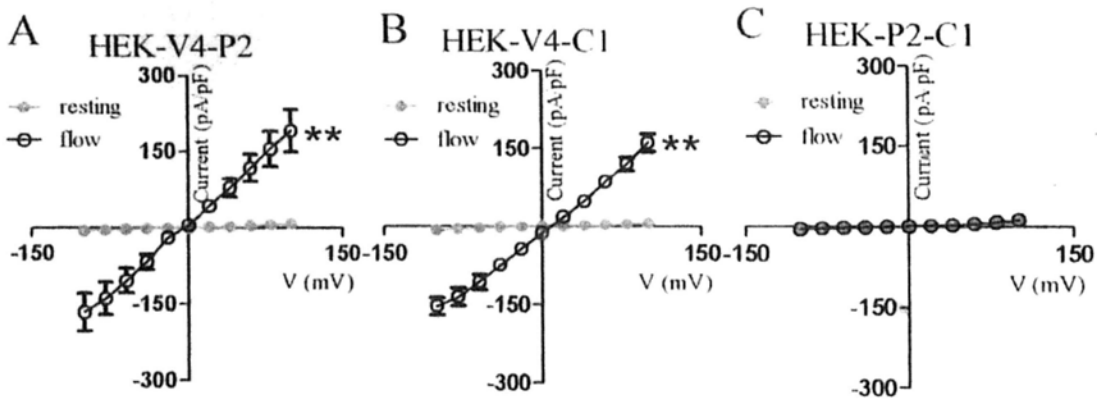

Figure 4- 8. Flow-induced whole-cell current change in HEK293 cells co-expressed with any two of TRPV4, -C1 or -P2.

A, B, C. I–V curve of HEK cells co-expressed with any two of TRPV4,-C1 and -P2 in before and after flow. Data are given as the mean ± SE (n = 6-8). $^{**}P < 0.01$ *vs.* Resting.

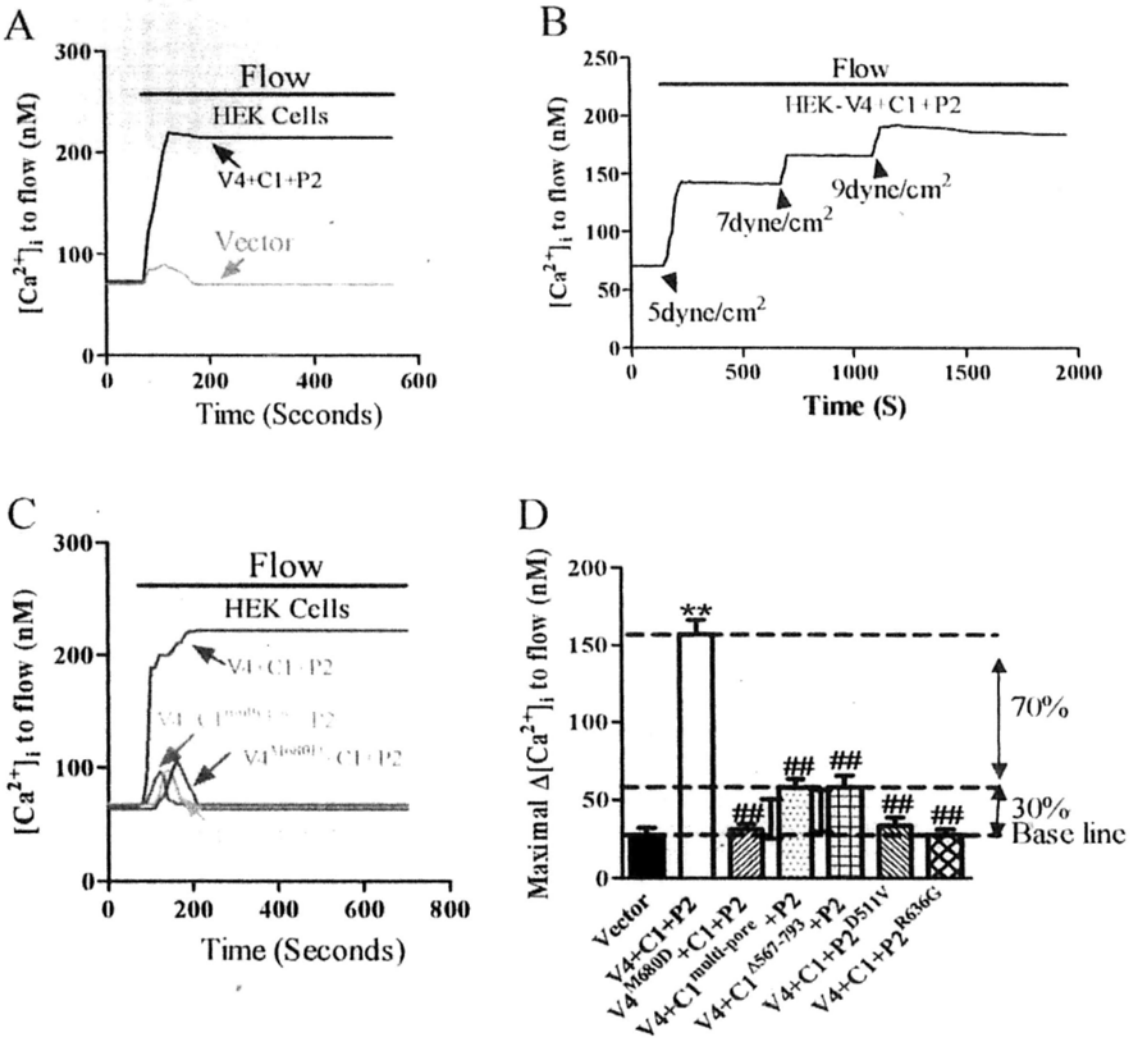

Figure 4- 9. Flow-induced $[Ca^{2+}]_i$ change in HEK293 cells that were co-expressed with TRPV4, -C1 and -P2.

A, B, C. Representative time course of flow-induced $[Ca^{2+}]_i$ increase. D, Summary showing the maximal amplitude of flow-induced $[Ca^{2+}]_i$ increase. Control cells were co-expressed with TRPV4, -C1 and -P2 (labeled as V4+C1+P2). In others, TRPV4 was replaced with $TRPV4^{M680D}$ (labeled as $V4^{M680D}$+C1+P2); or TRPC1 was replaced with $TRPC1^{multi\text{-}pore}$ or $TRPC1^{\Delta 567\text{-}793}$ (labeled as V4+$C1^{multi\text{-}pore}$+P2 or V4+$C1^{\Delta 567\text{-}793}$+P2); or TRPP2 was replaced with $TRPP2^{R636G}$ or $TRPP2^{D511V}$ (labeled as V4+C1+$P2^{R636G}$ or V4+C1+ $P2^{D511V}$); or empty vector-transfected (labeled as vector). All cells were bathed in NPSS containing 1% BSA. Solid bar on top of the traces indicates the time period when laminar flow was applied. Data are given as the mean ± SE (n=5-9 experiments, 10 to 20 cells per experiment). $^{**}P<0.01$ *vs* vector (Vec). ## $P<0.01$ *vs* V4+C1+ P2.

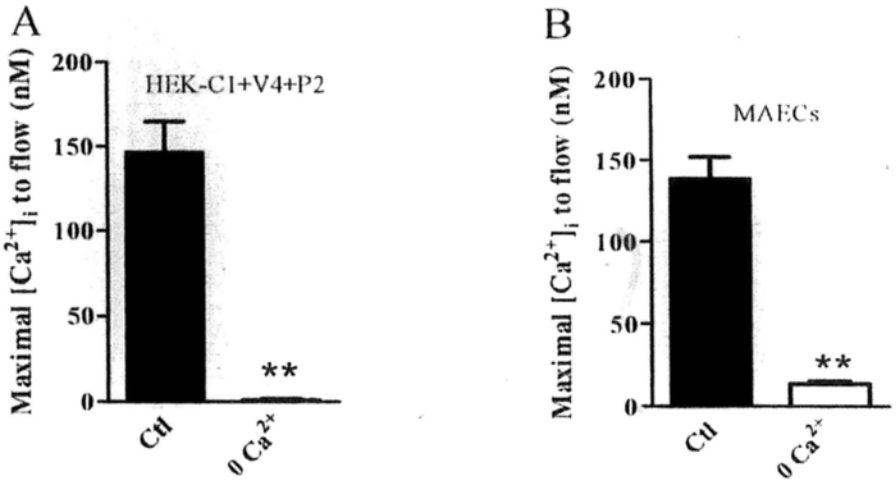

Figure 4- 10. Flow-induced $[Ca^{2+}]_i$ change in HEK cells coexpressed with TRPV4, -C1 and -P2 and primary cultured rat MAECs.

A, B. Summary showing the maximal amplitude of flow-induced $[Ca^{2+}]_i$ increase. Cells were bathed in NPSS containing 1% BSA or in 0 Ca^{2+} OPSS containing 1% BSA. Data are given as the mean±SE (n=6-8 experiments, 10 to 20 cells per experiment). $^{**}P< 0.01$ *vs.* Ctl.

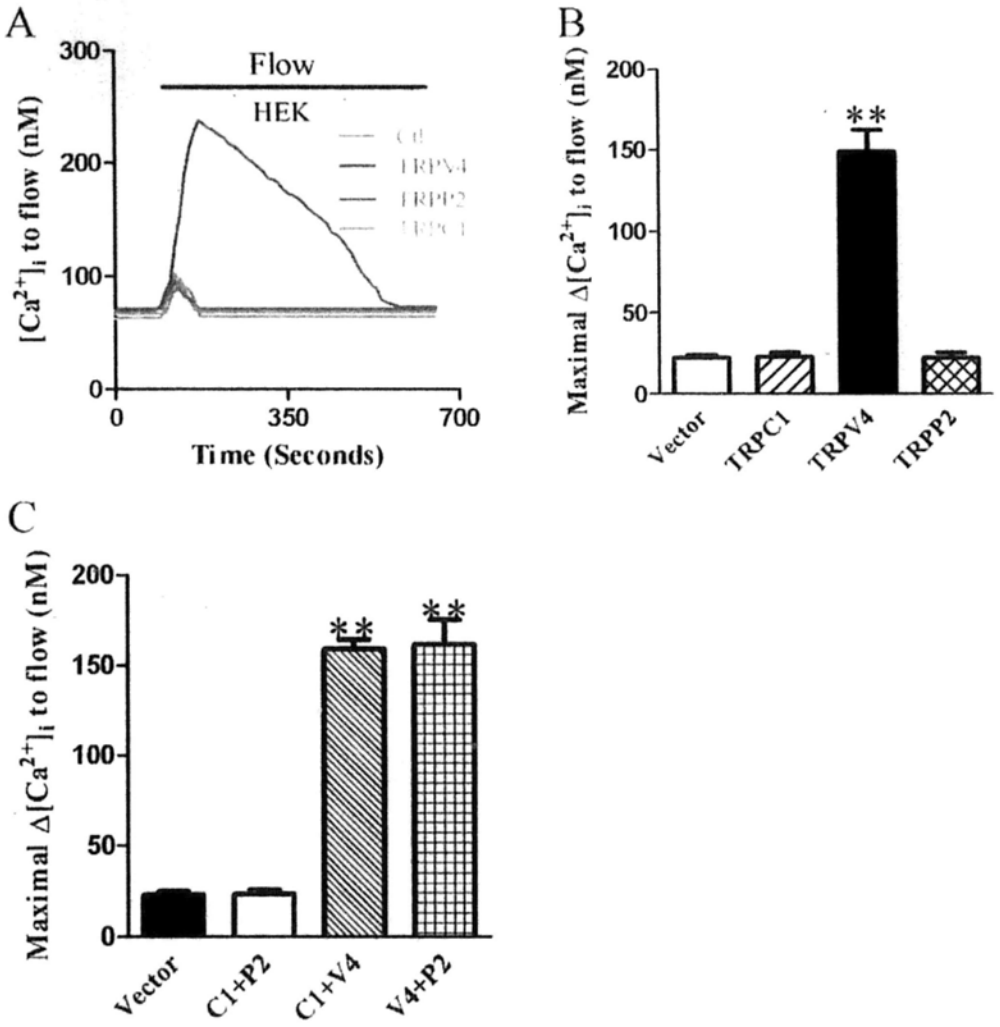

Figure 4- 11. Flow-induced $[Ca^{2+}]_i$ change in HEK293 cells that were individually expressed with TRPV4, TRPC1, or TRPP2, or co-expressed with two TRPs.

A. Representative traces showing flow-induced $[Ca^{2+}]_i$ change in HEK293 cells that were individually expressed with TRPV4, TRPC1, or TRPP2. B and C. Summary showing the maximal amplitude of flow-induced $[Ca^{2+}]_i$ increase. B. Cells were individually expressed with TRPV4, TRPC1, or TRPP2. C. Cells were co-expressed with two TRPs. All cells were bathed in NPSS containing 1% BSA. The solid bar on top of the traces indicates the period when laminar flow was applied. Data are given as the mean ± SE (n = 7-9 experiments, 10 to 20 cells per experiment). **P< 0.01 *vs.* Vector.

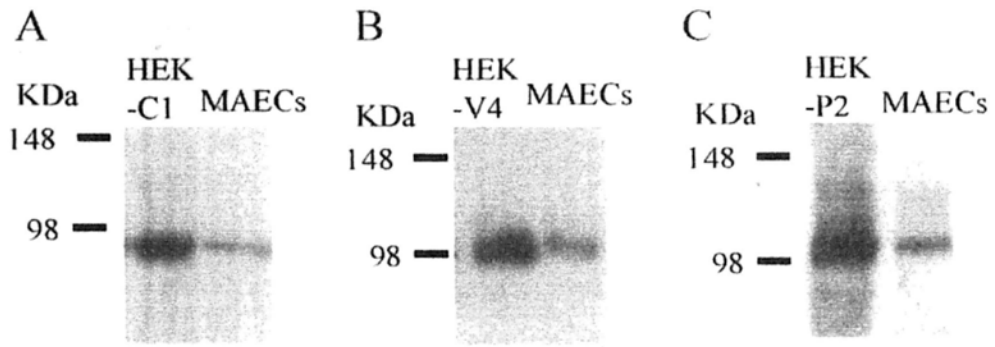

Figure 4- 12. Expression of TRPV4, -C1 and -P2 in the primary cultured rat MAECs.

Shown are representative immunoblots. The whole cell lysates from HEK293 cells (left lane) and the primary cultured MAECs (right lane) were immunoblotted with antibodies against TRPC1 (A), TRPV4 (B) and TRPP2 (C). HEK293 cells that were transfected with TRPC1 (A), TRPV4 (B) and TRPP2 (C) were used as positive controls. n = 3 for each experiment.

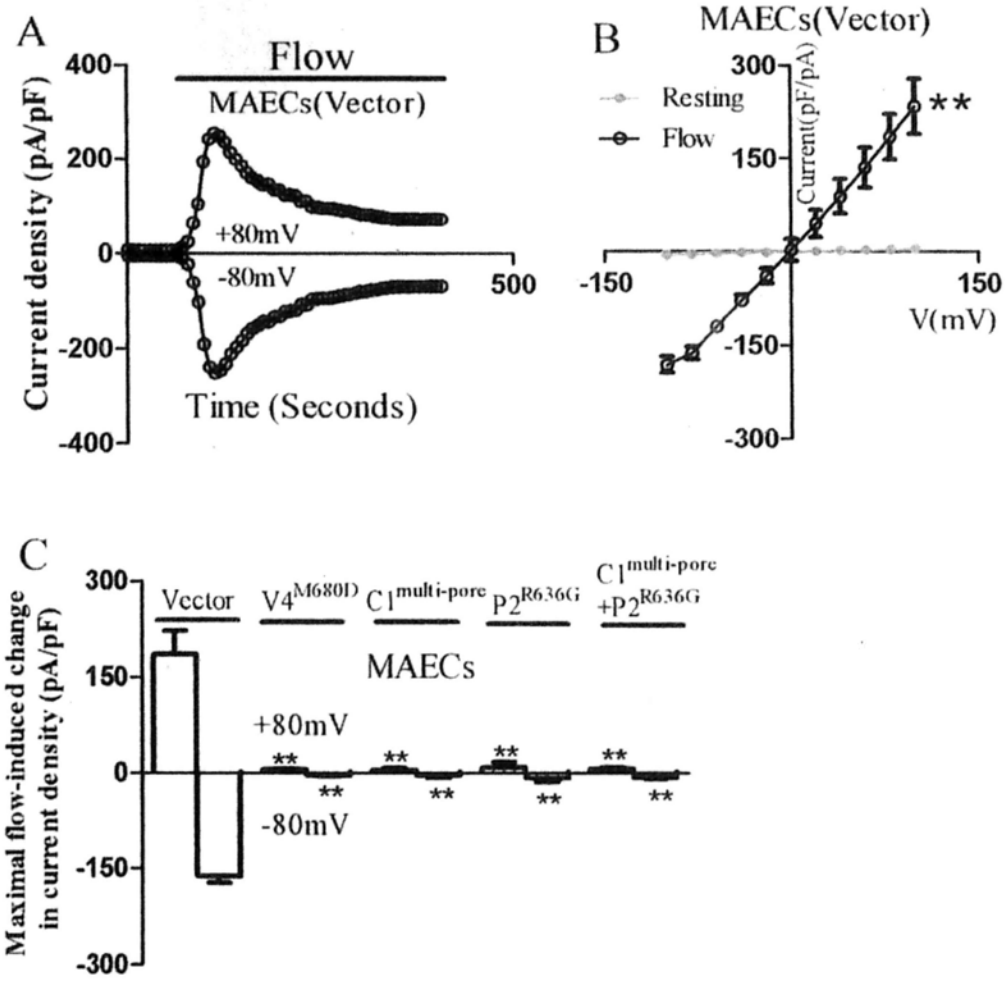

Figure 4- 13. Flow-induced whole-cell current in the primary cultured rat MAECs.

A. Representative time course of flow-stimulated whole-cell current at ±80 mV in rat MAECs. B. I–V curves of rat MAECs before and after flow. C. Summary data of maximal amplitude of flow-induced whole-cell cation currents increase at ±80 mV. In C, cells were transfected with empty vector (labeled as vector), $TRPC1^{multi\text{-}pore}$ (labeled as $C1^{multi\text{-}pore}$), $TRPV4^{M680D}$ (labeled as $V4^{M680D}$), or $TRPP2^{R636G}$ (labeled as $P2^{R636G}$). The solid bar on top of the traces indicates the period when laminar flow was applied. Data are given as the mean ± SE (n = 6-8). $^{**}P < 0.01$ *vs* before flow in B or *vs* Vector in C.

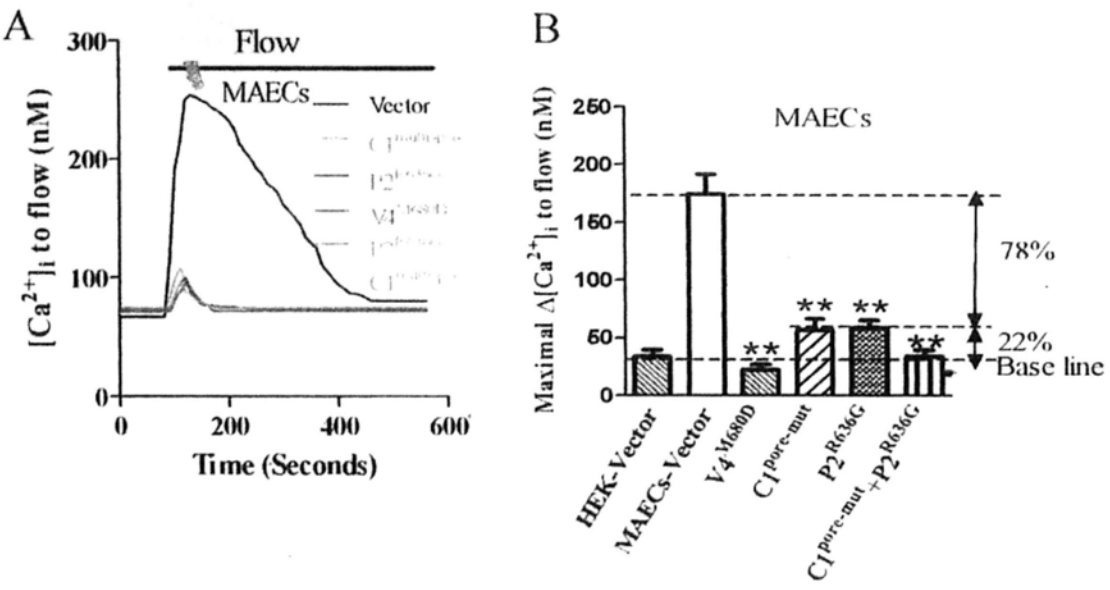

Figure 4- 14. Flow-induced $[Ca^{2+}]_i$ change in the primary cultured rat MAECs.

A. Representative traces illustrating the course of flow-induced $[Ca^{2+}]_i$ change. B. Summary showing the maximal amplitude of flow-induced $[Ca^{2+}]_i$ increase. Cells were transfected with empty vector (labeled as Vector), $TRPC1^{multi\text{-}pore}$ (labeled as $C1^{multi\text{-}pore}$), $TRPV4^{M680D}$ (labeled as $V4^{M680D}$), $TRPP2^{R636G}$ (labeled as $P2^{R636G}$), or $TRPC1^{multi\text{-}pore}$+$TRPP2^{R636G}$ (labeled as $C1^{multi\text{-}pore}$+$P2^{R636G}$). All cells were bathed in NPSS containing 1% BSA. The solid bar on top of the traces indicates the period when laminar flow was applied. Data are given as the mean ± SE (n = 8-10 experiments, 10 to 20 cells per experiment). $^{**}P< 0.01$ *vs* control (Vector).

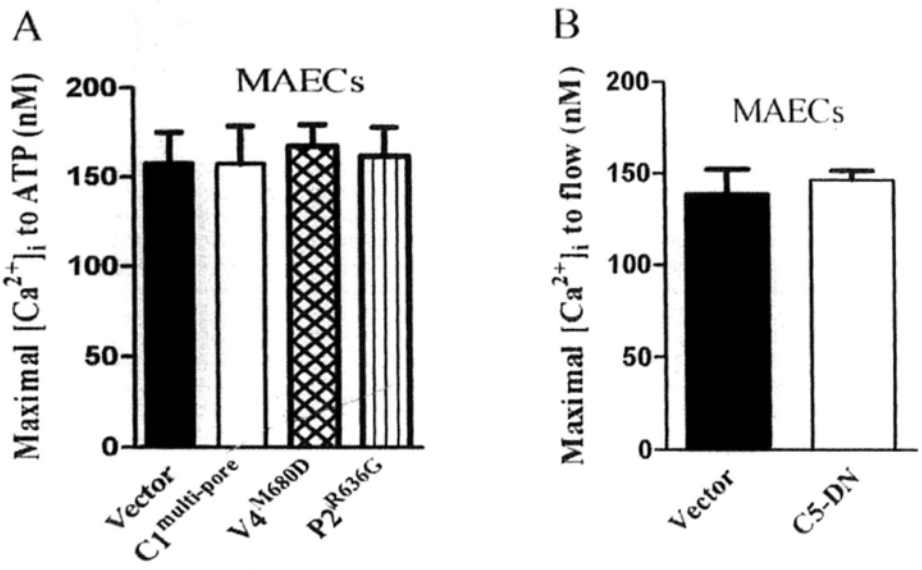

Figure 4- 15. Flow or ATP-induced $[Ca^{2+}]_i$ change in the primary cultured rat MAECs.

A, Summary showing the maximal amplitude of ATP-induced $[Ca^{2+}]_i$ increase, expressed as the maximal $\Delta[Ca^{2+}]_i$ to ATP (10μmol/L) B. Summary showing the maximal amplitude of flow-induced $[Ca^{2+}]_i$ increase, expressed as the maximal $\Delta[Ca^{2+}]_i$ to flow. All cells were bathed in NPSS containing 1% BSA. Cells were transfected with empty vector (labeled as Vector), $TRPC1^{multi-pore}$ (labeled as $C1^{multi-pore}$), $TRPV4^{M680D}$ (labeled as $V4^{M680D}$), $TRPP2^{R636G}$ (labeled as $P2^{R636G}$), TRPC5 dominant negative (labeled as C5-DN). Data are given as the mean±SE (n=6-8 experiments, 10 to 20 cells per experiment).

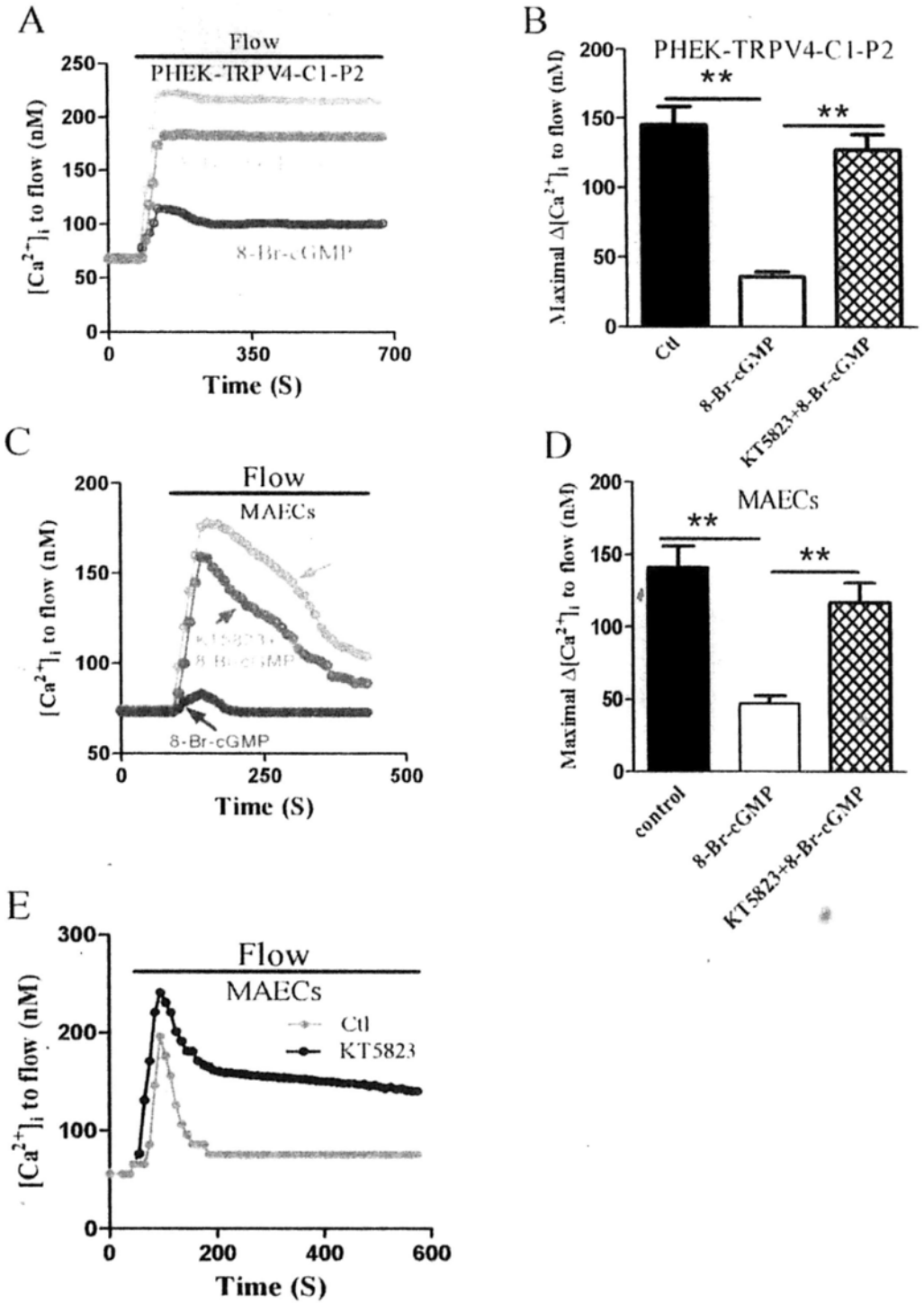
A
Flow
PHEK-TRPV4-C1-P2
8-Br-cGMP
$[Ca^{2+}]_i$ to flow (nM)
Time (S)
B
PHEK-TRPV4-C1-P2
Maximal $\Delta[Ca^{2+}]_i$ to flow (nM)
Ctl
8-Br-cGMP
KT5823+8-Br-cGMP
C
Flow
MAECs
8-Br-cGMP
$[Ca^{2+}]_i$ to flow (nM)
Time (S)
D
MAECs
Maximal $\Delta[Ca^{2+}]_i$ to flow (nM)
control
8-Br-cGMP
KT5823+8-Br-cGMP
E
Flow
MAECs
Ctl
KT5823
$[Ca^{2+}]_i$ to flow (nM)
Time (S)

Figure 4- 16 Flow-induced $[Ca^{2+}]_i$ change in PHEK cells coexpressed with TRPV4, -C1 and -P2 and primary cultured rat MAECs.

A, C, E. Representative traces illustrating the time course of flow-induced $[Ca^{2+}]_i$ change. B, D. Summary showing the maximal amplitude of flow-induced $[Ca^{2+}]_i$ increase. In A and B, HEK293 cells were stably transfected with PKG1α gene, labeled as PHEK; C and E, primary MAECs. All cells were bathed in NPSS containing 1% BSA. The solid bar on top of the traces indicates the period when laminar flow was applied. 8-Br-cGMP (2 mmol/L) or /and KT5823(1 μmol/L) were introduced 10 minutes before flow. Data are given as the mean±SE (n=6-8 experiments, 10 to 20 cells per experiment). $^{**}P<0.01$

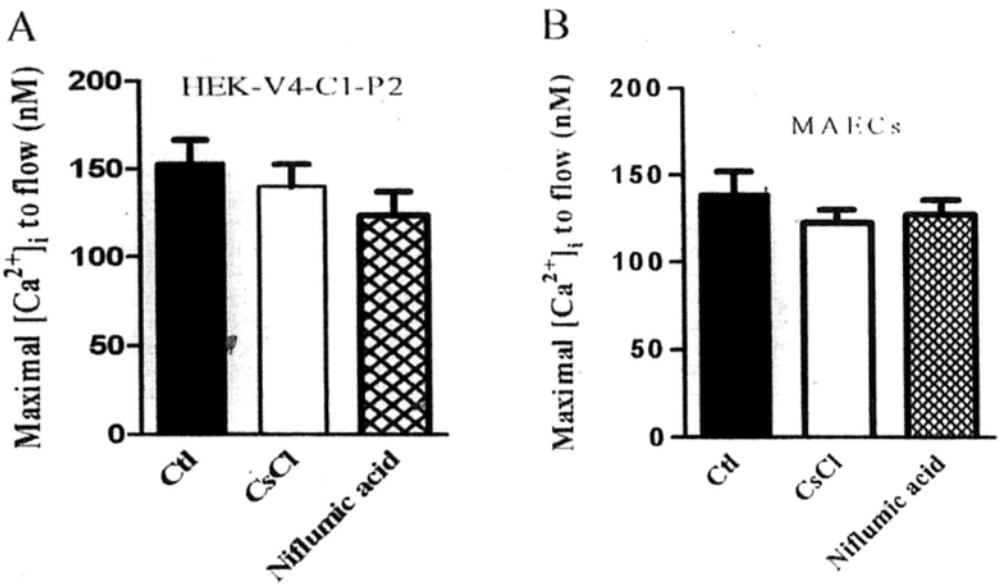

Figure 4- 17. Flow-induced $[Ca^{2+}]_i$ change in the primary cultured rat MAECs and HEK cells coexpressed with TRPV4, -C1 and -P2.

A, B. Summary showing the maximal amplitude of flow-induced $[Ca^{2+}]_i$ increase, expressed as the maximal $\Delta[Ca^{2+}]_i$ to flow. A, HEK cells coexpressed with TRPV4-C1-P2; B, the primary cultured rat MAECs. All cells were bathed in NPSS containing 1% BSA. CsCl (5 mmol/L) and Niflumic acid (40 μmol/L) were introduced 10 minutes before flow. Data are given as the mean±SE (n=6-8 experiments, 10 to 20 cells per experiment).

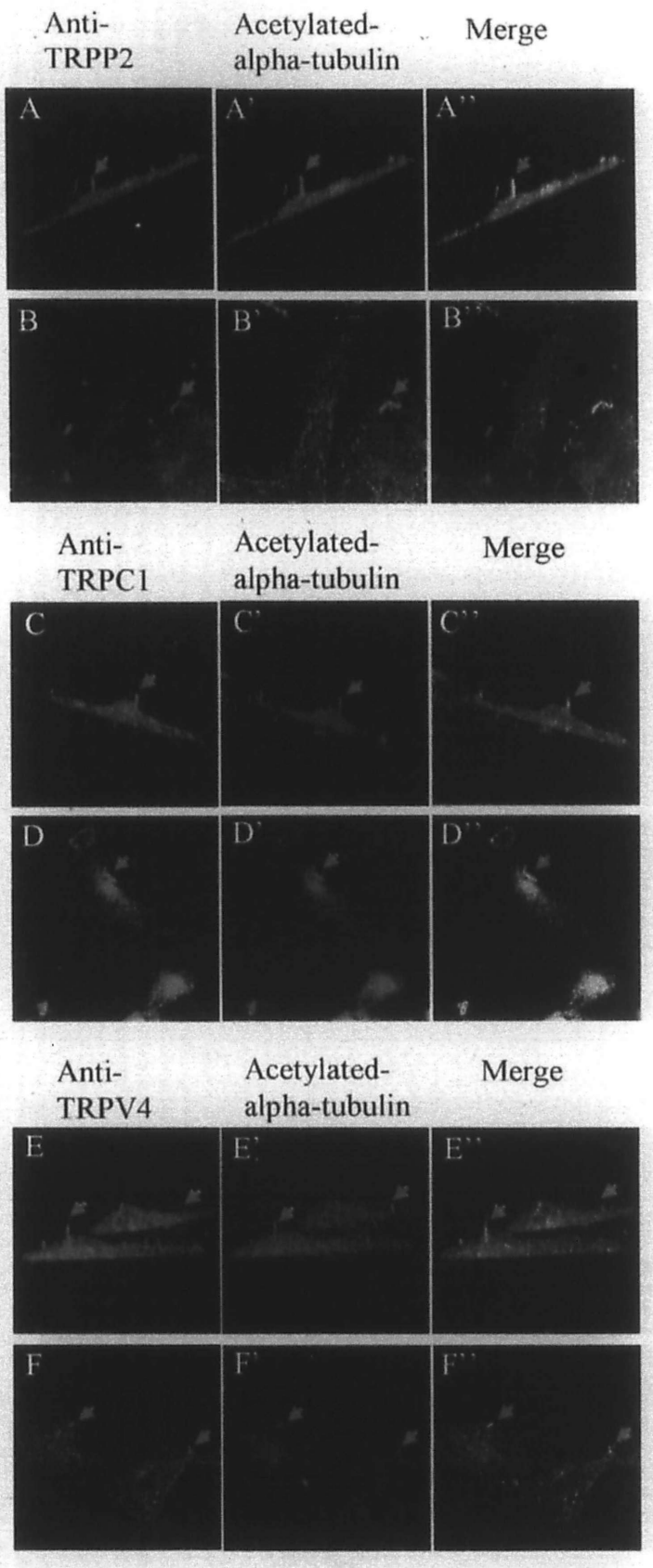

Figure 4- 18. TRPV4, TRPC1 and TRPP2 localize in primary cilia of primary cultured rat MAECs.

TRPV4 (A and B), TRPC1 (C and D), TRPP2 (E and F) and acetylated-alpha-tubulin (A' - F') colocalize in the primary cilium (A'' - F''; merge). A, C, E, confocal z sections show that the primary cilium emerges from the apical membrane. B, D, F, confocal images were acquired at the level of the apical membrane.

5. Chapter 5: Protein kinase G-sensitive TRPV4-TRPP2 channel complex mediates flow-induced Ca^{2+} influx in M1 CCD cell

5.1 Abstract

Several transient receptor potential (TRP) channels are sensitive to various forms of mechanical stress including fluid flow. Previously, it is known that TRPV4 and TRPP2 are expressed in renal epithelia, where they participate in the mechanosensory function of cilia and mediate Ca^{2+} entry in renal epithelia. In this chapter, co-IP experiments and double immunostaining experiments suggest that TRPV4 and TRPP2 physically interact with each other to form a heteromeric channel in M1 cortical collecting duct (CCD) cells and in HEK293 cells over-expressing TRPV4 and TRPP2. In HEK293 cells expressing TRPV4 alone, flow induced transient $[Ca^{2+}]_i$ rises and whole-cell currents. However, TRPP2 co-expression with TRPV4 markedly prolonged the $[Ca^{2+}]_i$ transients and whole-cell currents in response to flow. Activation of PKG by 8-Br-cGMP inhibited the flow-induced $[Ca^{2+}]_i$ rises and whole-cell currents in HEK293 cells co-expressing TRPV4 and TRPP2. The inhibitory effect of cGMP was abolished by PKG inhibitor KT5823. Furthermore, point mutations at two consensus PKG phosphorylation sites on TRPP2 markedly reduced the inhibitory effect of cGMP. In M1 CCD cells, flow-induced calcium influx was also inhibited by 8-Br-cGMP, the effect of which was reversed by KT5823. The cGMP inhibition was absent in M1 CCD cells pretreated with fusion peptides TAT-$TRPP2^{S827}$ + TAT-$TRPP2^{T719}$, which compete with endogenous PKG phosphorylation sites on TRPP2. In

conclusion, in this chapter I demonstrated that TRPV4 physically associated with TRPP2 in M1 CCD cells and HEK293 cells over-expression system. This association prolongs the flow-induced Ca^{2+} influx and enables this influx to be negatively regulated by PKG in M1 CCD cells and HEK293 cells over-expressing TRPV4 and -P2.

5.2 Introduction

The renal CCD is a flow-sensitive tissue where flow induces calcium influx and generates flow-sensitive calcium signaling in native collecting duct cells (Liu et al, 2003; Morimoto et al, 2006; Woda et al, 2002). Shear stress-induced by fluid flow provide the key signals that regulate glomerulotubular and ion transport in proximal tubule and distal nephron including CCD. Evidence from immunolocation showed the expression of TRPV4 at the cell membrane of M-1 cells and at the luminal membrane of mouse kidney CCD (Ling et al, 2007; Suzuki et al, 2003). Functionally, endogenous TRPV4 has been suggested to be a sensor for fluid flow in M1 CCD cells (Ling et al, 2007). It was found that, in mouse kidney M1 CCD cells and TRPV4-expressing HEK293 cells, hypotonicity- and flow-induced calcium influx could be largely abolished by using TRPV4-specific siRNA or a TRPV blocker ruthenium red (Caterina and Julius, 2001; Cebrian et al, 2004; Chen et al, 2001).

TRPP2, also named polycystin-2, PKD2, is another member of the transient receptor potential (TRP) family of ion channels that are expressed in both cilia and the plasma membrane of renal epithelia. TRPP2 is also suggested to participate in the mechanosensory function of cilia and mediates

Ca^{2+} signaling in renal epithelia (Ying et al, 2003; Nauli et al, 2003). One hypothesis suggested that TRPP2 may assemble with the PKD1 gene product polycystin-1, a large integral membrane protein with distant homology to TRP channels, to form a receptor–ion channel complex (Hanaoka et al, 2000; Köttgen, 2007). Evidence also suggests that TRPP2 could interact with two other members of TRP family, TRPC1 or TRPV4 (Bai et al, 2008; Kobori et al, 2009; Zhang et al, 2009; Köttgen et al, 2007; Stewart et al, 2010), contributing to other biological functions such as thermosensation.

In this chapter, I studied the physical and functional interaction of TRPV4 with TRPP2 in M1 CCD cells and HEK293 cell overexpression system. I also explored the regulation of TRPV4-P2 channels by protein kinase G (PKG).

5.3. Experimental Procedures

Detailed experimental procedures are described in Chapter 3.

5.4. Result

5.4.1 Physical association of TRPV4 with TRPP2 in heterologously expressed HEK293 cells and M1 CCD cells

It has been reported that TRPV4 and TRPP2 proteins form multimeric protein complex giving rise to biophysically and functionally discernible channel entities (Stewart et al, 2010; Köttgen et al, 2008). Thus we examined possible heteromerization between TRPV4 and TRPP2 in M1 CCD cells using co-IP and double immunostaining. Two antibodies for co-IP, anti-TRPV4 and anti-TRPP2, were previously reported to be highly specific (Yang et al, 2006, Bai

et al, 2008). In co-IP experiments, the anti-TRPP2 antibody could pull down TRPV4 in the protein lysates freshly prepared from M1 CCD cells and HEK293 cells co-expressing TRPV4 and P2 (Figure 5-1A, B left panel). Furthermore, an anti-TRPV4 antibody could reciprocally pull down TRPP2 (Figure 5-1A, B right panel). In control experiments, in which immunoprecipitation was performed with the IgG purified from preimmune serum, no band was observed (Figure 5-1A and B). These data indicate that TRPV4 physically associates with TRPP2 in M1 CCD cells and HEK293 cells co-expressing TRPV4 and TRPP2.

The selective interaction between TRPV4 and TRPP2 was verified by double immunostaining. Staining for TRPV4 and TRPP2 was observed in fixed M1 CCD cells, C57BL mouse kidney cross section, and fixed HEK293 cells co-expressing TRPV4 and P2 (Figure 5-1. C-E). Overlaying TRPV4 signal (green) with TRPP2 (red) showed clear co-localization (yellow) of TRPV4 and TRPP2 (Figure 5-1. C-E). Our studies also showed that TRPV4 and TRPP2 were co-localized in the cilia of M1 CCD cells (Figure 5-2. A-C) and HEK293 cells co-expressing TRPV4 and TRPP2 (Figure 5-2 D-F).

5.4.2 TRPP2 alters the kinetics of flow-induced $[Ca^{2+}]_i$ transient and whole-cell current in HEK293 Cells

Consistent with another report (Wu et al. 2007, Ma et al, 2010), fluid flow induced a $[Ca^{2+}]_i$ transient in HEK293 cells expressing TRPV4 (Figure 5-3A). Co-expression of TRPP2 with TRPV4 markedly prolonged the flow-induced $[Ca^{2+}]_i$ transient (Figure 5-3A). In fact, no apparent decay in $[Ca^{2+}]_i$ was observed within the duration of experiments of approximately 10 minutes (Figure 5-3A). In whole-cell patch clamp, flow also activated transient currents (Figure 5-4C). TRPP2 co-expression also markedly slowed down the

decay phase of this current transient (Figure 5-4C). In controls, both flow-induced $[Ca^{2+}]_i$ transient and whole-cell current transient were absent in wild-type HEK293 cells and those expressing TRPP2 (Figure 5- 3A,B and 4C,D). When any one of these two TRPs was replaced with their mutant counterpart (for example TRPV4 replaced with $TRPV4^{M680D}$), flow-induced $[Ca^{2+}]_i$ response became very small (Figure 3 B). A tiny residual fluorescence change, which could be observed in vector-transfected HEK293 cells as well as HEK293 cells over-expressing TRPP2, might be caused by slight cell movements during flow disturbance, not an indication of $[Ca^{2+}]_i$ change.

5.4.3. PKG modulation of flow-induced $[Ca^{2+}]_i$ rise in HEK cells co-expressing TRPV4 and TRPP2

Because the expression level of PKG1 proteins in wild-type HEK293 cells was low as determined by immunoblots, we first established a stably PKG1α-transfected HEK293 cell line and named it PKG-HEK293 (PHEK) cells. PHEK cells expressed a much higher level of PKG1α compared with that of wild-type HEK293 cells (Kwan et al, 2004). TRPV4 or TRPV4 plus TRPP2 genes were then transiently transfected into PHEK cells. In PHEK cells expressing TRPV4, pretreatment with a PKG activator, 8-Br-cGMP (2 mmol/L), had no effect on the flow-induced $[Ca^{2+}]_i$ increase (Figure 5- 5A, B). However, in cells co-expressing TRPV4 and TRPP2, 8-Br-cGMP markedly reduced the magnitude of the flow-induced $[Ca^{2+}]_i$ increase (Fig, 5C, D). KT5823 (1μmol/L), a potent and highly specific PKG inhibitor, abolished the inhibitory action of 8-Br-cGMP (Figure 5- 5C,D). Furthermore, we utilized mutant TRPP2 constructs $TRPP2^{T719A}$, $TRPP2^{S827A}$ and $TRPP2^{T719A\text{-}S827A}$, which have mutation at PKG phosphorylation sites Thr-719 or/and Ser-827. In cells co-expressed with TRPV4 and mutant TRPP2 that were mutated at

putative PKG phosphorylation sites ($TRPP2^{S827A}$ or $TRPP2^{T719A}$), the inhibitory action of 8-Br-cGMP was reduced if TRPP2 was replaced with $TRPP2^{T719A}$ or $TRPP2^{S827A}$, and the effect was abolished if TRPP2 was replaced with $TRPP2^{T719A\text{-}S827A}$ (Figure 5E). These data suggest that PKG does not act on TRPV4 itself. Instead, it inhibits the function of TRPV4-P2 complex by phosphorylating on serine 827 and threonine 719 of TRPP2.

5.4.4 Role of heteromeric TRPV4-P2 channels in flow-induced Ca^{2+} influx in M1 CCD cells

The expression of TRPV4 and TRPP2 in mouse M1 CCD cells have been reported elsewhere (Ling et al, 2007; Ying et al, 2003; Nauli et al, 2003), we also demonstrated the same here (Figure 5-1 and 2). In functional studies, we found that the expression of channel-dead mutants of TRPV4 and TRPP2 markedly reduced the flow-induced $[Ca^{2+}]_i$ transient in M1 CCD cells (Figure 5- 6A, B), supporting the key role of TRPV4 and TRPP2 in the flow response.

5.4.5 PKG modulation of $[Ca^{2+}]_i$ rise induced by flow in M1 CCD cells.

We next explored the role of PKG in flow response in M1 CCD cells. In M1 CCD cells, flow-induced Ca^{2+} influx was also inhibited by 8-Br-cGMP, the effect of which was reversed by KT5823 (2 μM) (Figure 5- 7A). We synthesized two fusion peptides by fusing PKG phosphorylation sites on TRPP2 to the membrane translocation signals from HIV-1 tat protein (TAT-$TRPC1^{S827}$, TAT-$TRPP2^{T719}$) (Schwarze et al, 1999). This allows efficient and abundant intracellular delivery of exogenous PKG substrate ($TRPP2^{S827}$ and $TRPP2^{T719}$) and thus suppresses the PKG phosphorylation on endogenous TRPP2 channels. The results show that treatment of M1 CCD cells with TAT-

TRPP2^{S827} + TAT-TRPP2^{T719} markedly reduced the 8-Br-cGMP inhibition on flow-induced $[Ca^{2+}]_i$ rises (Figure 5-7B.). Taken together, these data strongly suggest that cGMP and PKG act on TRPP2 to inhibit TRPV4-P2 channel complex, thereby suppressing flow-induced $[Ca^{2+}]_i$ rises.

5.5 Discussion

The major findings of this chapter are as follows: (1) Co-IP experiments and double immunostaining show that TRPV4 and TRPP2 physically interact with each other to form a heteromeric channel in the M1 CCD cells and HEK293 cells over-expressing TRPV4 and –P2. (2) Co-expression of TRPP2 with TRPV4 markedly slowed down the decay phase of flow-induced $[Ca^{2+}]_i$ transient and whole-cell currents. (3) Activation of PKG by cGMP inhibited the flow-induced calcium influx and whole-cell currents in HEK293 co-expressing TRPV4 and TRPP2. The inhibitory effect of 8-Br-cGMP was abolished by a PKG inhibitor KT5823. (4) Analysis of the primary amino acid sequence of TRPP2 revealed two potential phosphorylation sites for PKG (T719A and S827Q). Point mutations at these two consensus PKG phosphorylation sites of TRPP2 markedly reduced the inhibitory effect of cGMP. (5) In M1 CCD cells, flow-induced calcium influx was also inhibited by 8-Br-cGMP, the effect of which was reversed by KT5823. The cGMP inhibition was absent in M1 CCD cells that were pretreated with fusion peptides TAT-TRPP2^{S827} + TAT-TRPP2^{T719}, which compete with endogenous PKG phosphorylation sites on TRPP2. Taken together, my data suggest that TRPV4 and TRPP2 form heteromeric channels to mediate flow-induced Ca^{2+} influx in renal CCD cells, and that cGMP and PKG inhibited this Ca^{2+} influx via their action on TRPP2 subunit.

Previously, Köttgen et al (2008) have showed that TRPP2 and TRPV4 may interact to form a thermosensitive molecular sensor in the primary cilium of MDCK cells. Stewart et al (2010) used Atomic Force Microscopy to study the structure of the interaction of TRPP2 and TRPV4, and suggested a TRPP2:TRPV4 subunit stoichiometry of 2:2. The results from this chapter confirmed that TRPV4 and TRPP2 physically associated with each other to form a TRPV4-P2 channel complex. In HEK293 cells co-expressing TRPV4 and -P2 and in M1 CCD cells, I found that the antibody against TRPV4 could pull down TRPP2, and *vise versa*. Double immunostaining also found the colocalization of TRPV4 and TRPP2 in the primary cilia and plasma membrane of these cells. In the previous chapter, I have found that TRPV4 and TRPP2 can coassemble with TRPC1 to form heteromeric TRPV4-C1-P2 channels. However, TRPC1 only expressed in proximal tubule and thin descending, but not connecting tubule and CCD (Goel et al, 2006). Therefore, in M1 CCD cells, it is TRPV4-P2 not TRPV4-C1-P2 that mediates the flow response.

In M1 CCD cells and the HEK293 cells expressing TRPV4, flow-induced $[Ca^{2+}]_i$ rises were transient. In contrast, the flow-induced $[Ca^{2+}]_i$ rises in HEK293 cells expressing TRPV4 and -P2 displayed sustained time course. I attribute this transient nature of flow-induced $[Ca^{2+}]_i$ rises in M1 CCD cells to the cGMP-PKG inhibition on heteromeric TRPV4-P2 channels. HEK293 cells lack the components of nitric oxide-cGMP-protein kinase G signal cascades, and thus do not exhibit such an inhibition. In experiments, I found that flow-induced $[Ca^{2+}]_i$ rises could be inhibited by cGMP and PKG in M1 CCD cells. Furthermore, PKG inhibition on TRPV4-P2 was demonstrated in HEK293 cells that were stably overexpressed with protein kinase G (PHEK cells). The targeting site of cGMP and PKG was on TRPP2 subunit, because the cGMP inhibition was absent in PHEK293 cells that were transfected with

TRPV4 alone. Point mutation at two putative PKG phosphorylation sites on TRPP2 abolished the PKG inhibition on TRPV4-P2 complex. Furthermore, cGMP inhibition was absent in M1 CCD cells that were pretreated with TAT-TRPP2^{S827}+ TAT-TRPP2^{T719}, which compete with endogenous PKG phosphorylation sites on TRPP2. These data strongly suggest that NO-cGMP-PKG acts on the TRPP2 subunit in TRPV4-P2 channel complex to inhibit the flow-induced $[Ca^{2+}]_i$ rises in renal CCD epithelial cells. The negative regulation by PKG in flow-induced Ca^{2+} response of TRPV4-P2 complex has important significance for cell function. A prolonged Ca^{2+} influx would allow cells to produce more NO, enhancing dilation of renal tubule, renal epithelial ion transport (Liu et al, 2006; Kanai, 1995; Liu et al, 2003; Woda et al, 2002; Satlin et al, 2001; Taniguchi et al, 2007). However, excessive $[Ca^{2+}]_i$ and NO could lead to apoptosis and cell death (Choy et al, 2001). To protect from this, cells possess a negative feedback mechanism, in which flow-induced Ca^{2+} influx is inhibited by $[Ca^{2+}]_i$ via the Ca^{2+}-NO-cGMP-PKG pathway (Yao et al, 2000). In renal system, mechanical forces due to fluid flow and hydrodynamic pressure provide the key signals that regulate glomerulotubular balance in the proximal tubule (PT) and ion transport in the distal nephron including CCD. An increase in flow rate in the CCD micro-dissected *in vitro* produced a 20% increase in diameter and a threefold increase of $[Ca^{2+}]_i$ in principal and intercalated cells. In distal nephron segments, including the distal convoluted tubule, CNT and CCD, K^+ secretion is dependent in flow (Malnic G et al, 1989). In CCD, flow induced calcium influx-mediated by TRPV4 channel results in the activation of the maxi-K^+ channel and leads to the secretion of K^+ into the luminal fluid (Taniguchi et al, 2006). We believe that TRPV4-P2 channel complex may play a key role in modulating glomerulotubular balance and ion transport in kidney.

In conclusion, in this chapter I demonstrated that TRPV4 physically associated with TRPP2 in M1 CCD cells and HEK293 cells over-expression system. This association prolongs the flow-induced Ca^{2+} influx and enables this influx to be negatively regulated by PKG in M1 CCD cells.

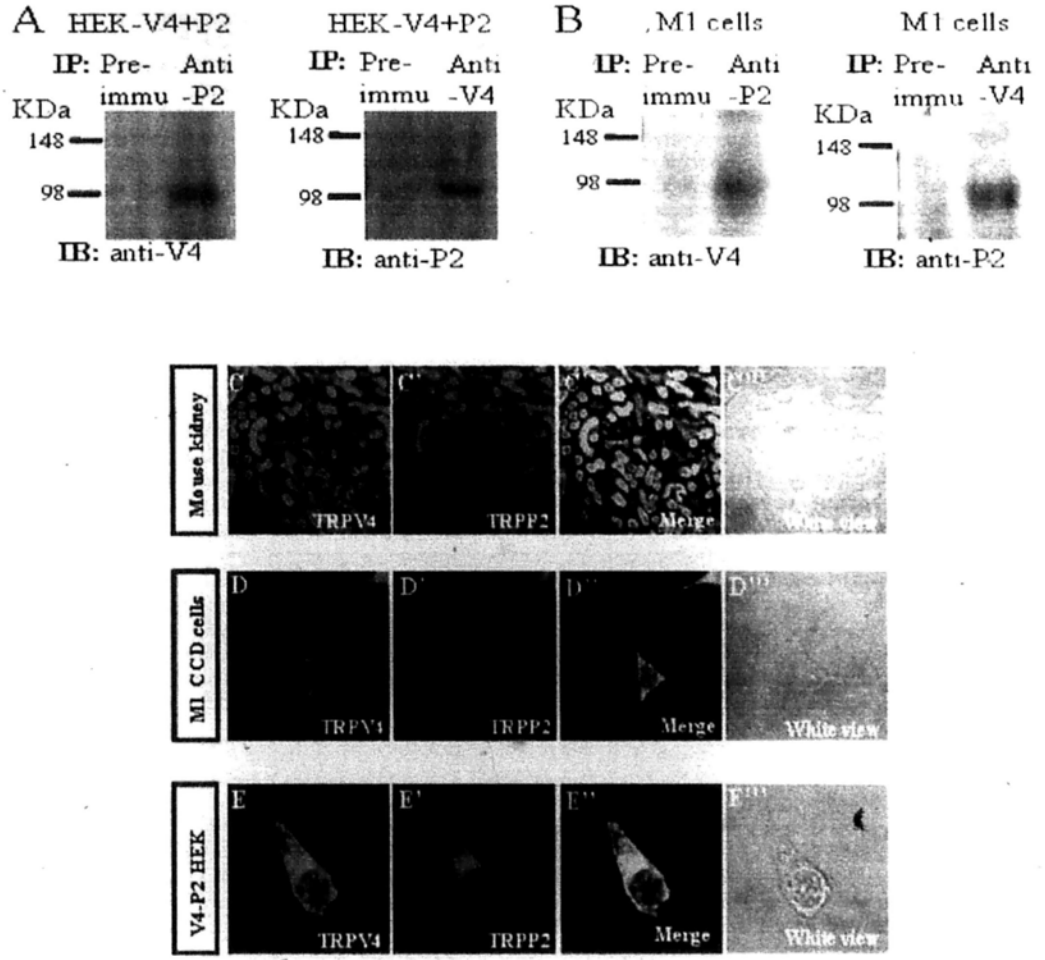

Figure 5- 1. Physical interaction of TRPV4 and TRPP2.

A, B. Co-IP. The pulling antibody and the blotting antibody were indicated. Control immunoprecipitation was performed using the preimmune IgG (labeled as preimmune). anti-P2 indicates anti-TRPP2; anti-V4, anti-TRPV4; IB, immunoblot; and IP, immunoprecipitation. n=3 experiments. C, D, E. double immunostainning. TRPV4 (C-E) and TRPP2 (C'-E') colocalize in the primary cilium (C''-E''). C'''-E''', is white view.

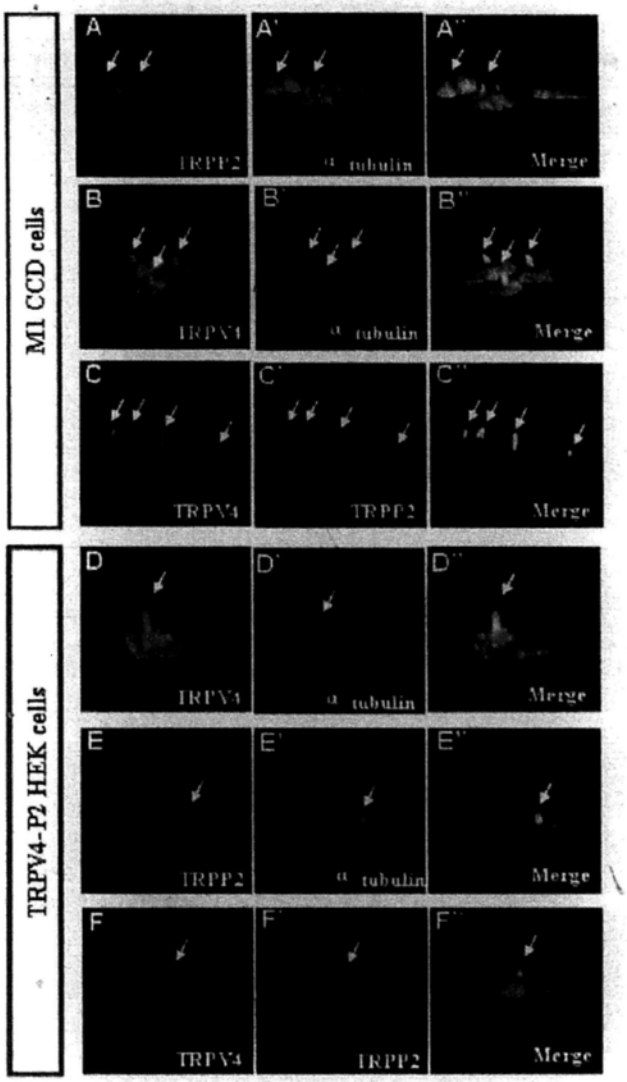

Figure 5- 2. TRPV4 and TRPP2 localize in the primary cilia of M1 CCD cells and HEK 293 cells co-expressing TRPV4 and -P2.

TRPP2 (A and E) or TRPV4 (B and D) and acetylated-alpha-tubulin (A'-B' and D'-E') colocalize in the primary cilium of M1 CCD cells and HEK293 cells co-expressing TRPV4 and -P2 (A''-B'' and D''-E''; merge). TRPV4 (C or F) or TRPP2 (C' and F') colocalize in the primary cilium of M1 CCD cells and HEK293 cells co-expressed with TRPV4-P2 (C'' and F''; merge). Confocal images represent stacks of z-series images that show the primary cilium emerging from the apical membrane.

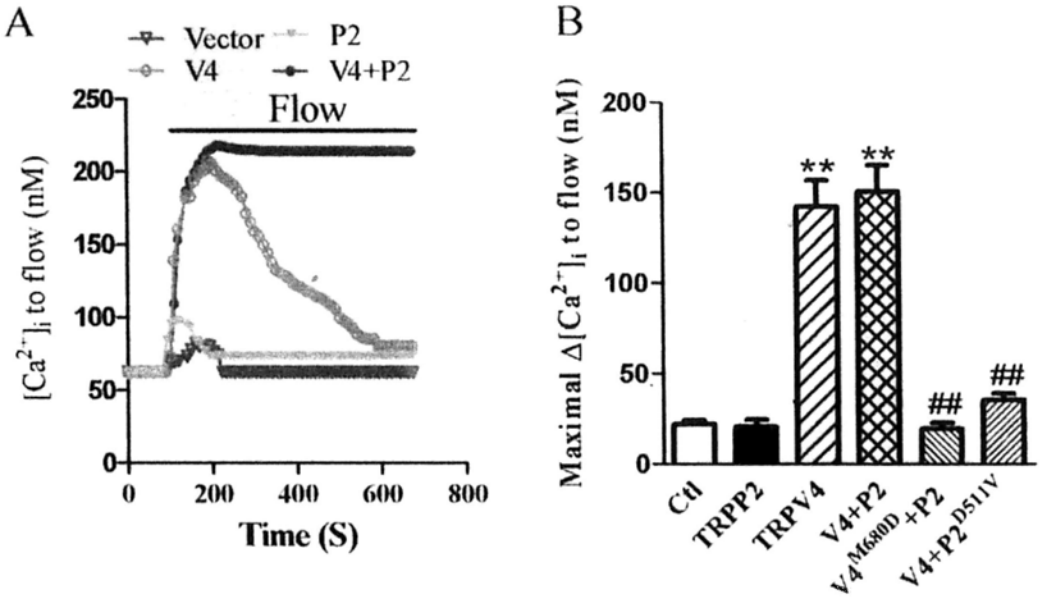

Figure 5- 3. Flow-induced $[Ca^{2+}]_i$ change in HEK293 cells expressing individual TRPV4, -P2 or co-expressing both isoforms.

A. Representative traces illustrating the time course of flow-induced $[Ca^{2+}]_i$ change. B. Summary showing the maximal amplitude of flow-induced $[Ca^{2+}]_i$ increase. All cells were bathed in NPSS containing 1% BSA. The solid bar on top of the traces indicates the period when laminar flow was applied. Data are given as the mean±SE (n=6 to 8 experiments, 8 to 20 cells per experiment). Cells were transfected with empty vector (labeled as Vector), TRPP2 (labeled as P2); TRPV4 (labeled as V4); or TRPV4+TRPP2 (labeled as V4+P2); $TRPV4^{M680D}$+TRPP2 (labeled as $V4^{M680D}$+P2); TRPV4+$TRPP2^{D511V}$ (labeled as V4+$P2^{D511V}$). **P<0.01 vs Vector.

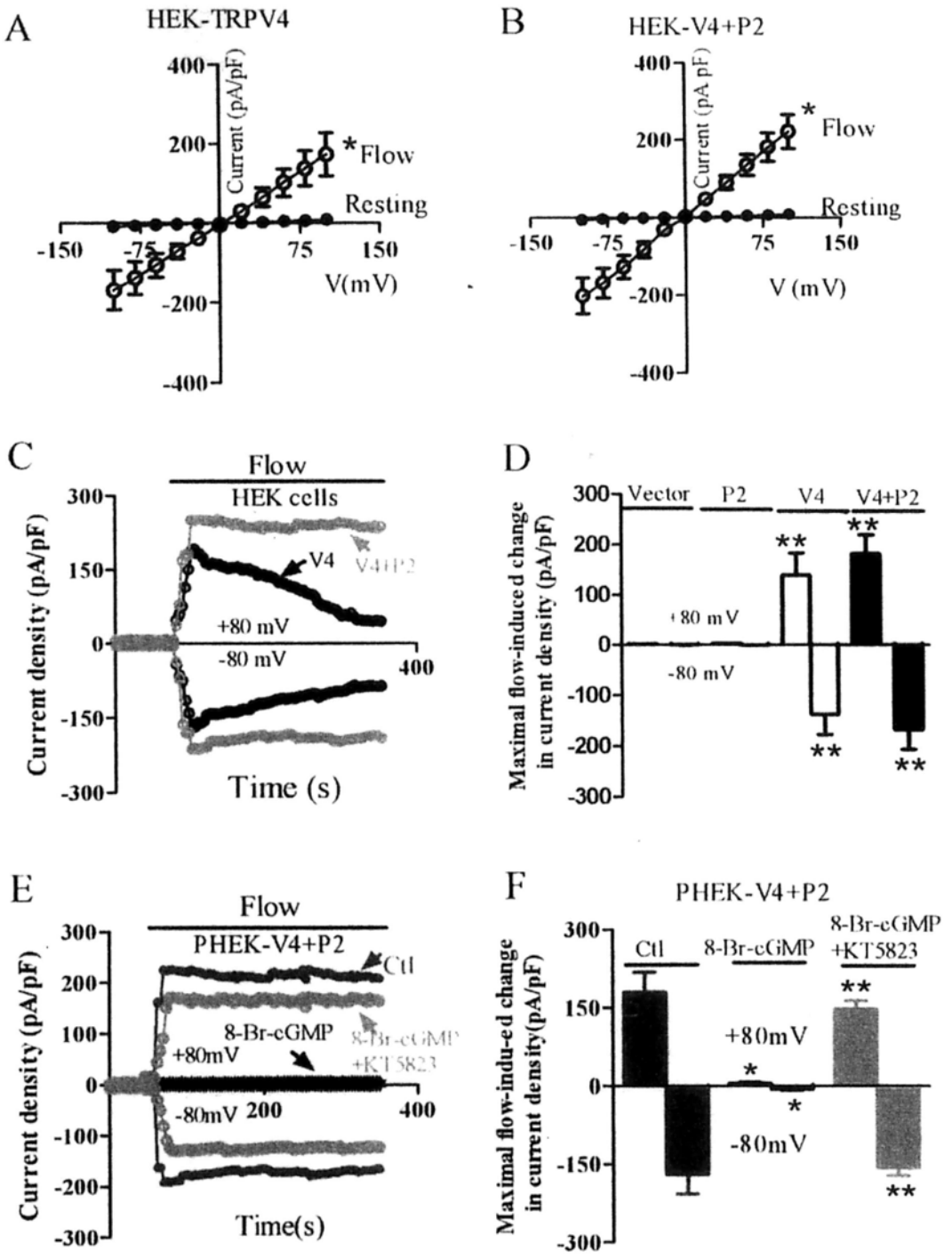
A
HEK-TRPV4
400
200
-200
-400
Current (pA/pF)
*Flow
Resting
-150
-75
75
150
V(mV)
B
HEK-V4+P2
400
200
-200
-400
Current (pA pF)
*
Flow
Resting
-150
-75
75
150
V (mV)
C
Flow
HEK cells
300
150
0
-150
-300
Current density (pA/pF)
V4
V4+P2
+80 mV
-80 mV
400
Time (s)
D
Vector
P2
V4
V4+P2
300
200
100
0
-100
-200
-300
Maximal flow-induced change in current density (pA/pF)
+80 mV
-80 mV
**
**
**
**
E
Flow
PHEK-V4+P2
300
200
100
0
-100
-200
-300
Current density (pA/pF)
Ctl
8-Br-cGMP
+80mV
-80mV
200
400
Time(s)
F
PHEK-V4+P2
Ctl
8-Br-cGMP
8-Br-cGMP
+KT5823
300
150
0
-150
-300
Maximal flow-indu-ed change in current density(pA/pF)
+80mV
-80mV
**
*
*
**

Figure 5- 4. Flow-induced change of whole-cell currents in HEK293 cells expressing different constructs.

A, D. I–V curves of TRPV4-expressing, or TRPV4 and TRPP2-coexpressing HEK293 cells before and after flow. C, E. Representative time course of flow-stimulated whole-cell currents at ±80 mV in HEK293 cells expressing TRPV4, or co-expressing TRPV4 plus -P2. D, F, Summary data of whole-cell currents before and after flow at ±80 mV. In E, F, HEK293 cells were stably transfected with PKG1α gene, labeled as PHEK cells. All cells were bathed in NPSS containing 1% BSA. The solid bar on top of the traces indicates the period when laminar flow was applied. 8-Br-cGMP (2 mmol/L) with or without KT5823 (1 μmol/L) was introduced 10 minutes before flow. Data are given as the mean±SE (n=6-8). Cells were transfected with empty vector (labeled as Vector), TRPP2 (labeled as P2); TRPV4 (labeled as V4); or TRPV4+TRPP2 (labeled as V4+P2). **P<0.01.

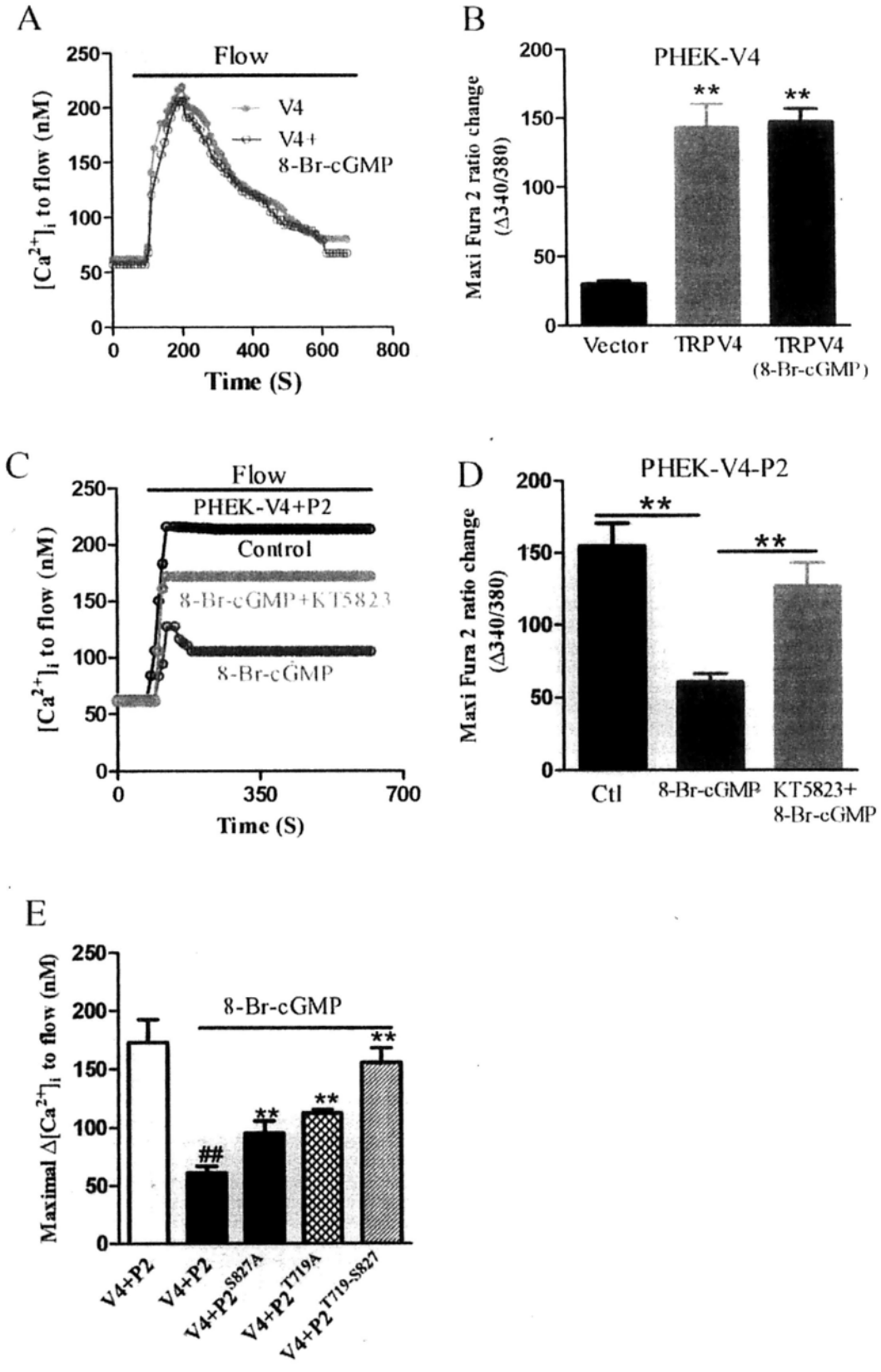
A
Flow
V4
V4+
8-Br-cGMP
[Ca2+]i to flow (nM)
Time (S)
B
PHEK-V4
Maxi Fura 2 ratio change (Δ340/380)
Vector
TRPV4
TRPV4 (8-Br-cGMP)
C
Flow
PHEK-V4+P2
Control
8-Br-cGMP+KT5823
8-Br-cGMP
[Ca2+]i to flow (nM)
Time (S)
D
PHEK-V4-P2
Maxi Fura 2 ratio change (Δ340/380)
Ctl
8-Br-cGMP
KT5823+ 8-Br-cGMP
E
8-Br-cGMP
Maximal Δ[Ca2+]i to flow (nM)
V4+P2
V4+P2S827A
V4+P2T719A
V4+P2T719-S827

Figure 5-5. Flow-induced $[Ca^{2+}]_i$ change in PHEK cells expressing individual TRPV4, TRPP2, or co-expressing both TRP isoforms.

A, C. Representative traces illustrating the time course of flow-induced $[Ca^{2+}]_i$ change. B, D, E. Summary showing the maximal amplitude of flow-induced $[Ca^{2+}]_i$ increase. HEK293 cells were stably transfected with PKG1α gene, labeled as PHEK293 cells. All cells were bathed in NPSS containing 1% BSA. The solid bar on top of the traces indicates the period when laminar flow was applied 8-Br-cGMP (2 mmol/L) with or without KT5823 (1 μmol/L) was introduced 10 minutes before flow. Data are given as the mean±SE (n=6 to 8 experiments, 8 to 20 cells per experiment). V4, indicates TRPV4; P2 indicates TRPP2; $P2^{S827A}$ and $P2^{T719A}$, point mutants of TRPP2. **P<0.01 compared to vector in B, to 8-Br-cGMP in D, and to V4+P2 with 8-Br-cGMP in E; ## P<0.01 compared to V4+P2 without 8-Br-cGMP.

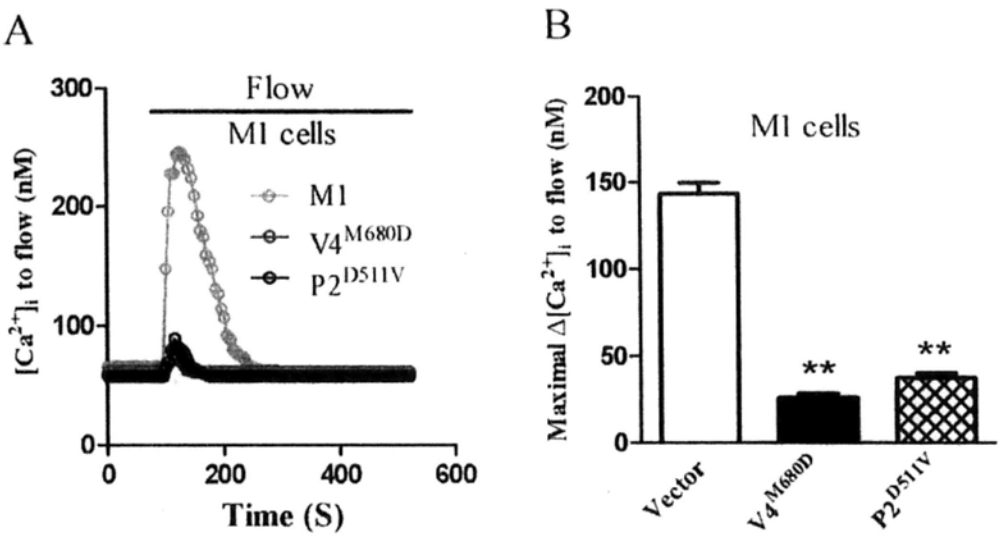

Figure 5- 6. Flow-induced $[Ca^{2+}]_i$ change in M1 CCD cells.

A. Representative traces illustrating the time course of flow-induced $[Ca^{2+}]_i$ change. B. Summary showing the maximal amplitude of flow-induced $[Ca^{2+}]_i$ increase. Cells were transfected with empty vector (labeled as Vector), $TRPV4^{M680D}$ (labeled as $V4^{M680D}$), or $TRPP2^{D511V}$ (labeled as $P2^{D511V}$). Data are given as the mean ± SE (n = 8-10 experiments, 10 to 20 cells per experiment). * $P< 0.01$ vs Vector.

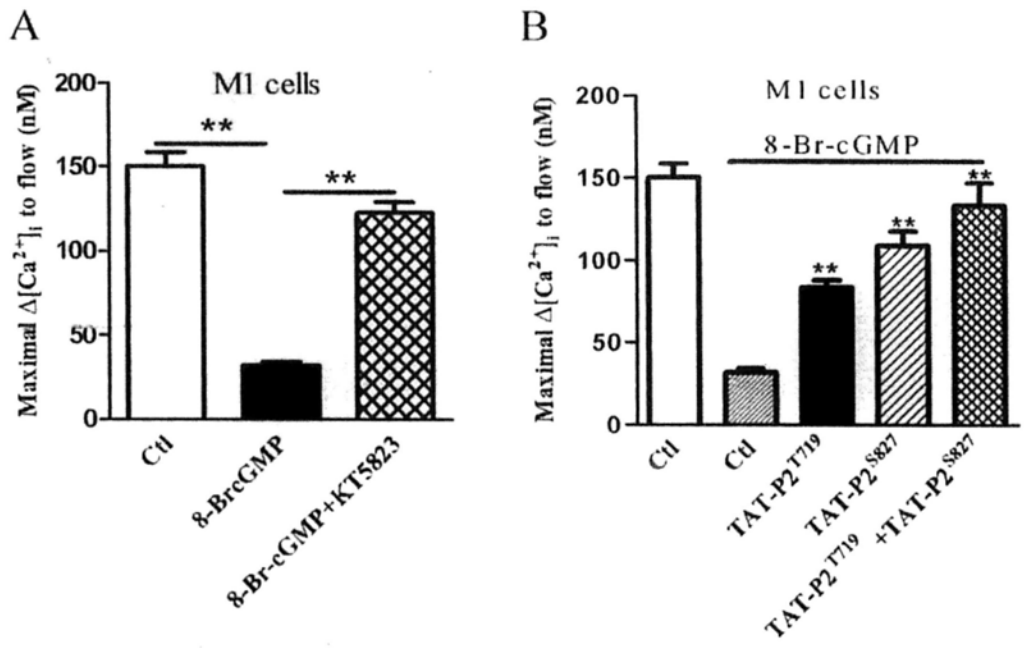

Figure 5- 7. PKG regulates flow-induced $[Ca^{2+}]_i$ change in M1 CCD cells.

Summary showing the maximal amplitude of flow-induced $[Ca^{2+}]_i$ increase. All cells were bathed in NPSS containing 1% BSA. 8-Br-cGMP (2 mmol/L) with or without KT5823 (1 μmol/L) or TAT-$P2^{T719A}$ and/or $TATP2^{S827A}$ were introduced 10 minutes before flow. Data are given as the mean±SE (n=6 to 8 experiments, 8 to 20 cells per experiment). **P<0.01

6. Chapter 6: General discussion and future direction

6.1 Major novel findings

6. 1.1 TRPV4-C1-P2 channels

It is well documented that functional TRP channels are composed of four TRP subunits. These four subunits could be identical (homomeric) or different (heteromeric) (Hofmann et al, 2002; Strübing et al, 2001). Heteromeric assembly usually occurs between the members within the same TRP subfamily (intra-subfamily) (Hofmann et al, 2002). Cross-subfamily assembly has only been reported between TRPV4 and -C1, TRPP2 and TRPC1, and TRPP2 and TRPV4 (Kobori, et al, 2009; Zhang, et al, 2009; Bai et al, 2008; Tsiokas et al, 1999; Stewart et al, 2010; Köttgen et al, 2008). Through three years of study, I was able to identify the first TRP channels that are composed of subunits across three different TRP subfamilies, i.e. TRPV4-TRPC1-TRPP2 channels. Furthermore, I demonstrated that TRPV4-C1-P2 is the main channel that mediates flow-induced Ca^{2+} influx and cation currents in native endothelial cells.

The main evidence was as follows:

a) I used three independent methods, which include two-step co-IP, chemical cross-linking and double immunostaining, to determine the physical interaction of three different TRP isoforms, TRPV4, -C1 and -P2. The results support that these three TRPs can physically associated with each other to form a complex. Such a complex was found in HEK293 cells co-expressing TRPV4, -C1 and -P2 and also in the primary cultured rat MAECs.

b) I used whole-cell patch clamp and fluorescent measurement of cytosolic Ca^{2+} to study the functional role of TRPV4-C1-P2 complex. The results showed that TRPV4-C1-P2 complex mediates flow-induced cation current and Ca^{2+} influx in HEK293 cells co-expressing these three TRP isoforms and also in the primary cultured rat MAECs.

I believe that my findings introduce a new concept that a functional TRP channel can be formed from subunits across three different subfamilies. I expect that such kind of heteromeric channels crossing three different TRP subfamilies can be activated by more diverse stimuli/agonists, thus allows diverse signals to converge on this TRP complex to initiate distinct cellular responses.

6. 1.2 TRPV4-P2 channels

In human body, vascular endothelial cells and renal tubular epithelial cells are two main types of cells that are exposed to fluid flow. Therefore, I also explored flow-sensitive TRP channels in renal cortical collecting duct M1 cell. I found that the main flow-responsive TRP channels in renal CCD M1 cells are TRPV4-P2 channels but not TRPV4-C1-P2 channels. This is mostly due to the fact that TRPC1 is not expressed in this segment of renal tubule. The main methods I used for this part of study are similar to those I used above.

The main evidence was as follows:

a) I used co-IP and double immunostaining to determine possible physical association of TRPV4 and TRPP2. I found the presence of TRPV4-P2

complex in HEK293 cells co-expressing TRPV4 and TRPP2, and also in renal CCD M1 cells.

b) I used fluorescent measurement of cytosolic Ca^{2+} to study the functional role of TRPV4-C1-P2 complex. The results showed that TRPV4-C1-P2 complex mediates flow-induced cation current and Ca^{2+} influx in HEK293 cells co-expressing these three TRP isoforms and also in M1 CCD cells.

c) I found that cGMP through its action on PKG-mediated phosphorylation on TRPP2 can inhibit TRPV4-P2 complex. Therefore, I identified two real PKG phosphorylation sites on TRPP2 proteins.

I believe that this part of the findings not only identifies the molecular identity of channels that mediate flow-induced Ca^{2+} influx in renal cortical collecting duct cells, but also uncovers a novel PKG-mediated regulation mechanism for Ca^{2+} influx, which is important for ion reabsorption/secretion in cortical collecting duct cells.

6.2 General Scheme

Based on the chapter 4 and 5, I conclude that TRPV4, -C1 and -P2 are capable of co-assembling to form heteromeric TRPV4-C1-P2 channels. The fourth subunit could be any of TRPV4, -C1, or -P2. In vascular endothelial cells, this heteromeric TRPV4-C1-P2 channels mediate flow-induced Ca^{2+} influx. I propose a schematic model for signal transduction following flow stimulation in figure 6-1. In this scheme, the channel is activated by flow stimulation. Subsequent Ca^{2+} entry activates nitric oxide synthase (NOS) to produce nitric oxide (NO), which elevates intracellular cGMP. As a feedback regulation, the elevated intracellular cGMP inhibits the Ca^{2+} entry through its action on TRPC1 or/and TRPP2. In M1 CCD cells, because of lack of TRPC1 expression, it is heteromeric TRPV4-P2 rather than TRPV4-C1-P2 that mediates flow-induced Ca^{2+} influx.

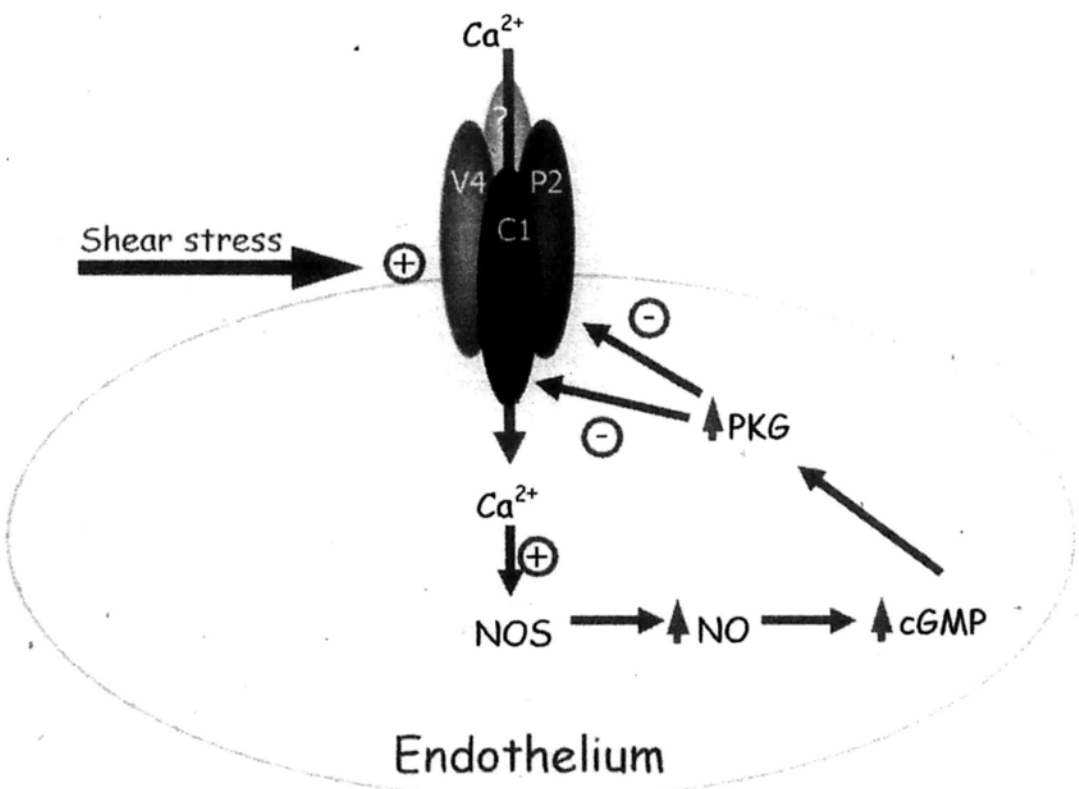

Figure 6-1. Model for signal transduction following flow stimulation.

6.3. Limitation and Future research direction

6.3.1 Subunit composition of flow-sensing TRP channels

In my study, I employed multiple independent including two-step co-IP, chemical cross-linking, and FRET detection to reveal physical interaction of TRPV4, -C1 and -P2. FRET results also suggested that the fourth subunit of this tetrameric channel can be any of those three TRPs, namely TRPV4, -C1, - or P2. There are some limitaions to immunoprecipitation and chemical cross-linking. Co-immunoprecipitation uses cell lysis as starting materials, the possibility of unspecific bindings could happen. Also immunoprecipitation does not provide quantitative data regarding the affinity or stoichiometry of an interaction. Some nonspecific chemical cross-linking could also happen, which may generate false positive signals. Among the three methods that were used to determine subunit assembly, FRET is most reliable. FRET data could provide most convincing evidence of subunit assembly. However, at the moment, FRET experiments were only carried out in the over-expressing HEK293 cells. In the future study, I will expend the FRET experiments in native vascular endothelial cells and renal epithelial cells. These experiments would give more convincing evidence on the subunit composition of flow-sensing TRP channels in native endothelial cells and renal epithelial cells.

6.3.2 Basic electrophysiological and pharmacological properties of heteromeric TRPV4-C1-P2 channels

Although I have used multiple biochemical, electrophysiological and mutagenesis methods to identify a new TRP channel, namely heteromeric TRPV4-C1-P2 channels. The detailed electrophysiological properties of the channels are not yet to be characterized. It is well documented that

heteromultimeric channels usually display properties that are distinct from those of homomeric channels. So we expect that TRPV4-C1-P2 would have electrophysiological properties different from those of homomeric TRPV4, TRPC1 or TRPP2. In future, I plan to examine the following properties of the channels:

a) Pharmacological profile of the newly-identified TRPV4-C1-P2 channel

It is expected that heteromeric TRPV4-C1-P2 channels should have their own characteristic pharmacological profile different from those of homomeric channels. In future study, I can use whole-cell patch clamp and Ca^{2+} measurement study to establish pharmacological properties of this channel. Several potential channel agonists/stimuli/antagonists will be used to modulate the channels. These include traditional TRPV4 agonist, 4α-PDD, EET, hypotonic stress, well-known TRPP2 agonists/antagonists citric acid, amiloride, TRPC1 inhibitor T1E3, etc. I will determine if these compounds/stimuli can affect the current amplitude and I-V relationship of this TRPV4-C1-P2 channel. These results would help to establish basic pharmacological properties of this newly-identified TRPV4-C1-P2 channel.

b) Single channel characteristics of heteromeric TRPV4-C1-P2 channel

I have already recorded the whole-cell current of heteromeric TRPV4-C1-P2, and found the I-V relationship of channels, being a relatively linear one. However, the single channel property of this channel is still unknown. In the future studies, I will examine the properties of these heteromeric TRPV4-C1-P2 channels at single channel level. I can use channel-specific

agoniste/antagonists generated from step a) above to modulate TRPV4-C1-P2 channels at single channel level, to obtain single channel slope conductance, and to determine which agonists/antagonists could affect the channel open probability (Po). The study could be performed in HEK293 cells over-expressing TRPV4-C1-P1 and also in native vascular endothelial cells.

c) Mono- and divalent cation permeability of TRPV4-C1-P2 heteromeric channel

An important property of ion channel is relative permeability/selectivity to different ions. In future, I plan to determine the relative permeability of TRPV4-C1-P2 and TRPP2-V4 channels to Na^+, Rb^+, K^+, Li^+ and Ca^{2+} based on reverse potential measurement. The methods have been well established and have been successfully used to character another TRP channels by my labmate (Ma et al, 2010). Briefly, after full activation of the current with 4α-PDD, extracellular solutions will be switched to the ones that contain different permeant cation species, for example from K^+-containing to Cs^+-containing bath solution. The relative permeability will be then calculated from the shifts in the reversal potential.

6.3.3 Other TRP assembly types in different tissues/organs

Our study identified the first TRP complex composed of member from three different subunits. But, it is also clear TRPV4-C1-P2 is not the only type of TRP assembly. In the renal epithelial cells, I have shown that the main flow-sensing TRP complex are TRPV4-P2 channels but not TRPV4-C1-P2

complex, presumably because the renal CCD epithelial cells do not express TRPC1.

Vascular trees are very complicated. Human vascular systems contain large-sized, medium-sized and small sized arteries. There are also tremendous heterogeneity of vascular systems in different vascular beds. Although my present study demonstrated TRPV4-C1-P2 channels as the main entity mediating flow-induced Ca^{2+} influx in small mesenteric arteries, it is unclear whether the same is true in other arteries and veins. Therefore, next I plan to perform similar studies to find out whether our scheme (TRPV4-C1-P2 channel) is universal for different-sized vessels and in different vascular bed, or whether other TRP assembly type exists in different vessels

Similarly, renal tubules contain many segments including proximal tubule, loop of Henle, convoluted tubules, cortical collecting duct and medullary collecting duct. My studies have only demonstrated the role of TRPV4-P2 channels in flow sensation in cortical collecting duct. In future, I plan to extend my study to determine whether TRPV4-P2 have similar functional role in other renal tubule segments or other TRP assembly play more important role in other renal tubular segments.

Furthermore, different tissues may have different TRP assembly pattern. In future, I will also explore other TRP assembly types in different tissues/organs.

6.3.4. Involvement of TRPV4-P2 and TRPV4-C1-P2 in renal, vascular and bone diseases

TRPV4-P2 and TRPV4-C1-P2 channels are main entities that mediate flow-induced Ca^{2+} influx in renal epithelial cells and vascular endothelial cells, respectively. It is well documented that mutation of TRPP2 results in polycystic kidney diseases, while mutation of TRPV4 is associated with neurogenerative disease Charcot-Marie-Tooth disease type 2C and skeletal disease spondylometaphyseal dysplasia. In the future, I will explore the possible role of TRPV4-P2, TRPV4-C1-P2 in these diseases. Because TRPV4, TRPP2 and TRPC1 are closely associated with each other, they may form functional complex. Mutation of any three genes could have similar consequences. In future, I will try to obtain some blood samples from patients with these diseases, then screen if mutations of TRPV4 and TRPC1 are also associated with polycystic kidney diseases, and to screen mutation of TRPP2 and TRPC1 could also result in neurogenerative diseases Charcot-Marie-Tooth disease type 2C and skeletal disease spondylometaphyseal dysplasia.

Reference

Aboualaiwi W A, Takahashi M, Mell BR, Jones TJ, Ratnam S, Kolb RJ, Nauli SM. Ciliary polycystin-2 is a mechanosensitive calcium channel involved in nitric oxide signaling cascades. Circ. Res. 2009, 104: 860–869.

Arniges M, Fernández-Fernández JM, Albrecht N, Schaefer M, Valverde MA. Human TRPV4 channel splice variants revealed a key role of ankyrin domains in multimerization and trafficking. J Biol Chem. 2006, 281(3):1580-1586.

Arniges M, Vázquez E, Fernández-Fernández JM, Valverde MA. Valverde, Swelling-activated Ca^{2+} entry via TRPV4 channel is defective in cystic fibrosis airway epithelia. J. Biol. Chem. 2004, 279, pp: 54062–54068.

Badano J L, Mitsuma N, Beales P L, Katsanis N. The ciliopathies: An emerging class of human genetic disorders. Annu. Rev. Genomics Hum. Genet. 2006, 7: 125–148.

Bai CX, Giamarchi A, Rodat-Despoix L, Padilla F, Downs T, Tsiokas L, Delmas P. Formation of a new receptor-operated channel by heteromeric assembly of TRPP2 and TRPC1 subunits. EMBO Rep. 2008, 9(5): 472-479.

Barakat AI, Leaver EV, Pappone PA, Davies PF. A flow-activated chloride-selective membrane current in vascular endothelial cells. Circ Res. 1999, 85: 820-828.

Bautista DM, Jordt SE, Nikai T, Tsuruda PR, Read AJ, Poblete J, Yamoah EN, Basbaum AI, Julius D. TRPA1 mediates the inflammatory actions of environmental irritants and proalgesic agents. Cell. 2006, 124:1269–1282.

Becker D, Bereiter-Hahn J, Jendrach M. Functional interaction of the cation channel transient receptor potential vanilloid 4 (TRPV4) and actin in volume regulation. Eur J Cell Biol. 2009, 88(3):141-52.

Becker D, Blase C, Bereiter-Hahn J, Jendrach M. TRPV4 exhibits a functional role in cell-volume regulation. J. Cell Sci. 2005, 118, pp: 2435–2440.

Bender FL, Mederos YSM, et al. The temperature-sensitive ion channel TRPV2 is endogenously expressed and functional in the primary sensory cell line F-11. Cell Physiol Biochem. 2005, 15: 183–194.

Bichet D, Peters D, Patel A, Delmas P, Honoré E. The cardiovascular polycystins: insights from autosomal dominant polycystic kidney disease and transgenic animal models. Trends Cardiovasc. Med. 2006, 16: 292–298.

Birder LA, Nakamura Y, Kiss S, Nealen ML, Barrick S,Kanai AJ, Wang E, Ruiz G, de Groat WC, Apodaca G, Watkins S, Caterina MJ. Altered urinary bladder function in mice lacking the vanilloid receptor TRPV1. Nat Neurosci. 2002, 5: 856–860.

Bode F, Sachs F, Franz MR. Tarantula peptide inhibits atrial fibrillation. Nature. 2001, 409: 35–36.

Brayden J E, Earley S, Nelson M T, Reading S. Transient receptor potential (TRP) channels, vascular tone and autoregulation of cerebral blood flow. Clin. Exp. Pharmacol. Physiol. 2008, 35: 1116–1120.

Bush EW, Hood DB, Papst PJ, Chapo JA, Minobe W, Bristow MR, Olson EN, McKinsey TA. Canonical transient receptor potential channels promote cardiomyocyte hypertrophy through activation of calcineurin signaling. J Biol Chem. 2006, 281: 33487–33496.

Busse R, Fleming I. Regulation of endothelium-derived vasoactive autacoid production by hemodynamic forces. Trends Pharmacol Sci. 2003, 24: 24–29.

Caterina M J, Rosen T A, Tominaga M, Brake A J, Julius D. A capsaicin-receptor homologue with a high threshold for noxious heat. Nature. 1999, 398: 436-441.

Caterina M J, Schumacher M A, Tominaga M, Rosen T A, Levine J D, Julius D. The capsaicin receptor: a heat-activated ionchannel in the pain pathway. Nature. 1997, 389: 816-824.

Caterina MJ, Julius D. The vanilloid receptor: a molecular gateway to the pain pathway. Annu Rev Neurosci. 2004, 24: 487–517.

Caterina MJ, Leffler A, Malmberg AB, Martin WJ, Trafton J, Petersen-Zeitz KR, Koltzenburg M, Basbaum AI, Julius, D. Impaired nociception and pain sen- sation in mice lacking the capsaicin receptor. Science. 2000, 288: 306–313.

Caterina MJ, Rosen TA, et al. A capsaicin-receptor homologue with a high threshold for noxious heat. Nature. 1999, 398(6726): 436–441.

Cebrian C, Borodo K, Charles N, Herzlinger DA. Morphometric index of the developing murine kidney. Dev Dyn. 2004, 231: 601–608.

Chang-Xi Bai, Sehyun Kim, Wei-Ping Li, Andrew J Streets, Albert C M Ong and Leonidas Tsiokas.Activation of TRPP2 through mDia1-dependent voltage gating. The EMBO Journal. 2008, 27: 1345-1356.

Chen J, Crossland RF, Noorani MM, Marrelli SP. Inhibition of TRPC1/TRPC3 by PKG contributes to NO-mediated vasorelaxation. Am J Physiol Heart Circ Physiol. 2009, 297(1): H417-424.

Chen XZ, Segal Y, Basora N, Guo L, Peng JB, Babakhanlou H, Vassilev PM, Brown EM, Hediger MA, Zhou J. Transport function of the naturally occurring pathogenic polycystin-2 mutant, R742X. Biochem Biophys Res Commun. 2001, 282: 1251–1256.

Choy JC, Granville DJ, Hunt DW, McManus BM. Endothelial cell apoptosis: biochemical characteristics and potential implications for atherosclerosis. J Mol Cell Cardiol. 2001, 33: 1673–1690.

Christoph T, Bahrenberg G, De Vry J, Englberger W, Erdmann VA, Frech M, Kögel B, Röhl T, Schiene K, Schröder W, Seibler J, Kurreck J. Investigation of TRPV1 loss-of-function phenotypes in transgenic shRNA expressing and knockout mice. Mol Cell Neurosci. 2008, 37: 579–589.

Chu X, Tong Q, Cheung JY, Wozney J, Conrad K, Mazack V, Zhang W, Stahl R, Barber DL, Miller BA.Interaction of TRPC2 and TRPC6 in erythropoietin modulation of calcium influx. J Biol Chem. 2004, 279(11): 10514-10522.

Chubanov V, Waldegger S, Mederos y Schnitzler M, Vitzthum H, Sassen MC, Seyberth HW, Konrad M, Gudermann T. Disruption of TRPM6/TRPM7 complex formation by a mutation in the TRPM6 gene causes hypomagnesemia with secondary hypocalcemia. Proc. Natl. Acad. Sci. U.S.A. 2004, 101: 2894–2899.

Ciura S and Bourque CW. Transient receptor potential vanilloid 1 is required for intrinsic osmoreception in organum vasculosum lamina terminalis neurons and for normalthirst responses to systemic hyperosmolality. J Neurosci. 2006, 26: 9069–9075.

Clapham DE. TRP channels as cellular sensors. Nature. 2003, 426: 517–524.

Corey DP, Garcia-Anoveros J, Holt JR, Kwan KY, Lin SY, Vollrath MA, Amalfitano A, Cheung EL, Derfler BH, Duggan A, Geleoc GS, Gray PA, Hoffman MP, Rehm HL, Tamasauskas D, Zhang DS. TRPA1 is a candidate for the mechanosensitive transduction channel of vertebrate hair cells. Nature. 2004, 432: 723–730.

Corey DP. What is the hair cell transduction channel? J Physiol. 2006, 576: 23–28.

Corey S, Clapham DE. The Stoichiometry of Gbeta gamma binding to G-protein-regulated inwardly rectifying K^+ channels (GIRKs). J Biol Chem. 2001, 276(14): 11409-11413.

Corey S, Krapivinsky G, Krapivinsky L, Clapham DE. Number and stoichiometry of subunits in the native atrial G-protein-gated K^+ channel, IKACh. J Biol Chem. 1998, 273(9): 5271-5218.

Cosens D, Manning A. Abnormal electroretinogram from a Drosophila mutant. Nature. 1969, 224: 285-287.

Damann N, Voets T, Nilius B. TRPs in our senses. Curr Biol. 2008, 18(18): R880-889.

Davies PF. Flow-mediated endothelial mechanotransduction. Physiol Rev. 1995, 75: 519–560.

Delmas P. Polycystins: from mechanosensation to gene regulation. Cell. 2004, 118: 145–148.

Delmas, P. Polycystins: polymodal receptor/ion-channel cellular sensors. Pflugers Arch. 2005, 451: 264–276.

Dietrich A, Chubanov V, Kalwa H, Rost BR & Gudermann T. Cation channels of the transient receptor potential superfamily: their role in physiological and pathophysiological processes of smooth muscle cells. Pharmacol Ther. 2006, 112: 744–760.

Dietrich A, Gudermann T. Trpc6. Handb Exp Pharmacol. 2007, 179: 125–141.

Dietrich A, Kalwa H, Storch U, Mederos YSM, Salanova B, Pinkenburg O, Dubrovska G, Essin K, Gollasch M, Birnbaumer L, Gudermann T. Pressure-induced and store-operated cation influx in vascular smooth muscle cells is independent of TRPC1. Pflugers Arch. 2007, 455: 465–477.

Dyachenko V, Husse B, Rueckschloss U, Isenberg G. Mechanical deformation of ventricular myocytes modulates both TRPC6 and Kir2.3 channels. Cell Calcium. 2009, 45: 38–54.

Earley S, Pauyo T, Drapp R, Tavares MJ, Liedtke W, Brayden JE. TRPV4-dependent dilation of peripheral resistance arteries influences arterial pressure. Am J Physiol Heart Circ Physiol. 2009, 297: H1096–H1102.

Earley S, Waldron BJ & Brayden JE. Critical role for transient receptor potential channel TRPM4 in myogenic constriction of cerebral arteries. Circ Res. 2004, 95: 922–929.

Ecder T, Schrier R W. Cardiovascular abnormalities in autosomal-dominant polycystic kidney disease. Nat. Rev. Nephrol. 2009, 5: 221–228.

Erler I, Hirnet D, Wissenbach U, Flockerzi V, Niemeyer BA. Ca2+-selective transient receptor potential V channel architecture and function require a specific ankyrin repeat. J Biol Chem. 2004, 279(33): 34456-34463.

Feng NH, Lee HH, Shiang JC, Ma MC.Transient receptor potential vanilloid type 1 channels act as mechanoreceptors and cause substance P release and sensory activation in rat kidneys. Am J Physiol Renal Physiol. 2008, 294(2): F316-325.

Fernandes J, Lorenzo IM, Andrade YN, Garcia-Elias A, Serra SA, Fernandez-Fernandez J, Valverde MA. IP3 sensitizes TRPV4 channel to the mechano- and osmotransducing messenger 5'-6'-epoxyeicosatrienoic acid. J Cell Biol. 2008, 181: 143–155.

Fleig A and Penner R. The TRPM ion channel subfamily: molecular, biophysical and functional features. Trends Pharmacol. Sci. 2004, 25: 633–639.

Fliegauf M, Benzing T, Omran H. When cilia go bad: cilia defects and ciliopathies. Nat. Rev. Mol. Cell Biol. 2007, 8: 880–893.

Fowler MA, Sidiropoulou K, Ozkan ED, Phillips CW & Cooper DC. Corticolimbic expression of TRPC4 and TRPC5 channels in the rodent brain. PLoS ONE. 2007, 2: e573.

Gao X, Wu L, O'Neil RG. Temperature-modulated diversity of TRPV4 channel gating: activation by physical stresses and phorbol ester derivatives through protein kinase C-dependent and -independent pathways. J Biol Chem. 2003, 278: 27129–27137.

García-Sanz N, Fernández-Carvajal A, Morenilla-Palao C, Planells-Cases R, Fajardo-Sánchez E, Fernández-Ballester G, Ferrer-Montiel A. Identification of

a tetramerization domain in the C terminus of the vanilloid receptor. J Neurosci. 2004, 24(23): 5307-5314.

Giamarchi, A. Padilla F, Coste B, Raoux M, Crest M, Honoré E, Delmas P.. The versatile nature of the calcium-permeable cation channel TRPP2. EMBO Rep. 2006, 7: 787-793.

Glazebrook PA, Schilling WP & Kunze DL. TRPC channels as signal transducers. Pflugers Arch. 2005, 451: 125–130.

Goel M, Sinkins WG, Schilling WP. Selective association of TRPC channel subunits in rat brain synaptosomes. J Biol Chem. 2002, 277(50): 48303-48310.

Goel M, Sinkins WG, Zuo CD, Estacion M, Schilling WP. Identification and localization of TRPC channels in the rat kidney. Am J Physiol Renal Physiol. 2006, 290(5): F1241-1252.

Gomis A, Soriano S, Belmonte C, Viana F. Hypoosmotic- and pressure-induced membrane stretch activate TRPC5 channels. J Physiol. 2008, 586(Pt 23): 5633-5649.

Gottlieb P, Folgering J, Maroto R, Raso A, Wood TG, Kurosky A, Bowman C, Bichet D, Patel A, Sachs F, Martinac B, Hamill OP, Honore E. Revisiting TRPC1 and TRPC6 mechanosensitivity. Pflugers Arch. 2008, 455(6): 1097-1103

Greka A, Navarro B, Oancea E, Duggan A & Clapham DE. TRPC5 is a regulator of hippocampal neurite length and growth cone morphology. Nat Neurosci. 2003, 6: 837–845.

Grimm C, Kraft R, Sauerbruch S, Schultz G, Harteneck C. Molecular and functional characterization of the melastatin-related cation channel TRPM3. J Biol Chem. 2003, 278: 21493–21501.

Hahn C, Schwartz M A. Mechanotransduction in vascular physiology and atherogenesis. Nat. Rev. Mol. Cell. Biol. 2009, 10: 53–62.

Hamill and Martinac, 2001 O.P. Hamill and B. Martinac, Molecular basis of mechanotransduction in living cells, Physiol Rev. 2001, 81 (2) pp. 685–740.

Harada J, Kokura K, Kanei-Ishii C, Nomura T, Khan MM, Kim Y, Ishii S. Requirement of the co-repressor homeodomain-interacting protein kinase 2 for ski-mediated inhibition of bone morphogenetic protein-induced transcriptional activation. J Biol Chem. 2003, 278(40): 38998-39005.

Harris P C and Torres V E. Polycystic kidney disease. Annu. Rev. Med. 2009, 60: 321–337.

Hartmannsgruber V, Heyken WT, Kacik M, Kaistha A, Grgic I, Harteneck C, Liedtke W, Hoyer J, Köhler R. Arterial response to shear stress critically depends on endothelial TRPV4 expression. PLoS ONE. 2007, 2: e827.

Hateboer N, v Dijk MA, Bogdanova N, Coto E, Saggar-Malik AK, San Millan JL, Torra R, Breuning M, Ravine D. Comparison of phenotypes of polycystic kidney disease types 1 and 2. European PKD1-PKD2 Study Group. Lancet. 1999, 353: 103-107.

Hateboer N, Veldhuisen B, Peters D, Breuning MH, San-Millan JL, Bogdanova N, Coto E, van Dijk MA, Afzal AR, Jeffery S, Saggar-Malik AK, Torra R, Dimitrakov D, Martinez I, de Castro SS, Krawczak M, Ravine D. Location of mutations within the PKD2 gene influences clinical outcome. Kidney Int. 2000; 57: 1444-1451.

He Y, Yao G, Savoia C, Touyz RM. Transient receptor potential melastatin 7 ion channels regulate magnesium homeostasis in vascular smooth muscle cells: role of angiotensin II. Circ Res. 2005, 96: 207–215.

Hellwig N, Albrecht N, Harteneck C, Schultz G, Schaefer M. Homo- and heteromeric assembly of TRPV channel subunits. J. Cell Sci. 2005, 118: 917-928.

Hildebrandt F & Otto E. Cilia and centrosomes: a unifying pathogenic concept for cystic kidney disease? Nat. Rev. Genet. 2005, 6: 928–940.

Hill K, Schaefer M. TRPA1 is differentially modulated by the amphipathic molecules trinitrophenol and chlorpromazine. J Biol Chem. 2007, 282: 7145–7153.

Hill M A, Davis M J, Meininger G A, Potocnik S J, Murphy T V. Arteriolar myogenic signalling mechanisms: Implications for local vascular function. Clin. Hemorheol. Microcirc. 2006, 34: 67–79.

Hoenderop JG, Nilius B, Bindels RJ. ECaC: the gatekeeper of transepithelial Ca2+ transport. Biochim Biophys Acta. 2002, 1600: 6–11.

Hoenderop JG, Vennekens R, Muller D, Prenen J, Droogmans G, Bindels RJ, Nilius B. Function and expression of the epithelial Ca^{2+} channel family: comparison of the mammalian epithelial Ca^{2+} channel 1 and 2. J. Physiol. 2001, 537: 747-761.

Hoenderop JG, Voets T, Hoefs S, Weidema F, Prenen J, Nilius B, Bindels RJ. Homo- and heterotetrameric architecture of the epithelial Ca^{2+} channels TRPV5 and TRPV6. EMBO J. 2003, 22(4): 776-785

Hofmann T, Chubanov V, Gudermann T, Montell C. TRPM5 is a voltage-modulated and Ca^{2+}-activated monovalent selective cation channel. Curr Biol. 2003, 13: 1153–1158.

Hofmann T, Obukhov AG, Schaefer M, Harteneck C, Gudermann T, Schultz G. Direct activation of human TRPC6 and TRPC3 channels by diacylglycerol. Nature. 1999, 397: 259–263.

Hofmann T, Schaefer M, Schultz G, et al. Subunits composition of mammalian transient receptor potential channels in living cell. Pro Natl Acad Sci USA. 2002, 99: 7461-7466.

Hofmann T, Schaefer M, Schultz G, Gudermann T. Subunit composition of mammalian transient receptor potential channels in living cells. Proc Natl Acad Sci USA. 2002, 99: 7461-7466.

Inoue R, Jensen LJ, Jian Z, Shi J, Hai L, Lurie AI, Henriksen FH, Salmonsson M, Morita H, Gottlieb P, Folgering J, Maroto R, Raso A, Wood TG, Kurosky A, Bowman C, Bichet D, Patel A, Sachs F, Martinac B, Hamill OP, Honore E. Revisiting TRPC1 and TRPC6 mechanosensitivity. Pflugers Arch. 2007, 455: 529–540.

Inoue R, Jensen LJ, Shi J, Morita H, Nishida M, Honda A & Ito Y. Transient receptor potential channels in cardiovascular function and disease. Circ Res. 2006, 99: 119–131.

Iwata Y, Katanosaka Y, et al. A novel mechanism of myocyte degeneration involving the Ca^{2+}-permeable growth factor-regulated channel. J Cell Biol. 2003, 161(5): 957–967.

Jenke M, Sanchez A, Monje F, Stuhmer W, Weseloh RM, Pardo LA. C-terminal domains implicated in the functional surface expression of potassium channels. EMBO J. 2003, 22: 395–403.

Kanai AJ, Strauss HC, Truskey GA, Crews AL, Grunfeld S, Malinski T. Shear stress induces ATP-independent transient nitric oxide release from vascular endothelial cells, measured directly with a porphyrinic microsensor. Circ Res. 1995, 77: 284–293.

Kanzaki M, Zhang YQ, et al. Translocation of a calcium-permeable cation channel induced by insulin-like growth factor-I. Nat Cell Biol. 1999, 1(3): 165–170.

Kawarabayashi Y, Mori M, Mori Y, Ito Y. Synergistic activation of vascular TRPC6 channel by receptor and mechanical stimulation via phospholipase C/diacylglycerol and phospholipase A2/{omega}-hydroxylase/20-HETE pathways. Circ Res. 2009, 104: 1399–1409.

Kobori T, Smith GD, Sandford R, Edwardson JM.The transient receptor potential channels TRPP2 and TRPC1 form a heterotetramer with a 2:2 stoichiometry and an alternating subunit arrangement. Biol Chem. 2009, 284(51): 35507-35513.

Köhler R, Heyken WT, Heinau P, Schubert R, Si H, Kacik M, Busch C, Grgic I, Maier T, Hoyer J. Evidence for a functional role of endothelial transient receptor potential V4 in shear stress-induced vasodilatation. Arterioscler Thromb Vasc Biol. 2006, 26: 1495–1502.

Köttgen M, Buchholz B, Garcia-Gonzalez MA, Kotsis F, Fu X, Doerken M, Boehlke C, Steffl D, Tauber R, Wegierski T, Nitschke R, Suzuki M, Kramer-Zucker A, Germino GG, Watnick T, Prenen J, Nilius B, Kuehn EW, Walz G. TRPP2 and TRPV4 form a polymodal sensory channel complex. J Cell Biol. 2008, 182(3): 437–447.

Kraft R, Harteneck C. The mammalian melastatin-related transient receptor potential cation channels: an overview. Pflugers Arch 2005, 451: 204–211.

Kwan HY, Huang Y, Yao X. Store-operated calcium entry in vascular endothelial cells is inhibited by cGMP via a protein kinase G-dependent mechanism. J Biol Chem. 2000, 275(10): 6758-6763.

Kwan HY, Huang Y, Yao X. Regulation of canonical transient receptor potential isoform 3 (TRPC3) channel by protein kinase G. Proc Natl Acad Sci U S A. 2004, 101(8): 2625-2630.

Kwan KY, Allchorne AJ, Vollrath MA, Christensen AP, Zhang DS, Woolf CJ, Corey DP. TRPA1 contributes to cold, mechanical, and chemical nociception but is not essential for hair-cell transduction. Neuron. 2006, 50: 277–289.

Launay P, Fleig A, Perraud AL, Scharenberg AM, Penner R, Kinet JP. TRPM4 is a Ca^{2+}-activated nonselective cation channel mediating cell membrane depolarization. Cell. 2002, 109: 397–407.

Lee N, Chen J, Sun L, Wu S, Gray KR, Rich A, Huang M, Lin JH, Feder JN, Janovitz EB, Levesque PC, Blanar MA. Expression and characterization of human transient receptor potential melastatin 3 (hTRPM3). J. Biol. Chem. 2003, 278: 20890–20897.

Leitner A, Walzthoeni T, Kahraman A, Herzog F, Rinner O, Beck M, Aebersold R. Probing native protein structures by chemical cross-linking, mass spectrometry, and bioinformatics. Mol Cell Proteom. 2010, 9: 1634–1649.

Lepage PK, Boulay G. Molecular determinants of TRP channel assembly. Biochem Soc Trans. 2007, 35: 81-83.

Lepage PK, Lussier MP, Barajas-Martinez H, Bousquet SM, Blanchard AP, Francoeur N, Dumaine R, Boulay G. Identification of two domains involved in the assembly of transient receptor potential canonical channels. J Biol Chem. 2006, 281(41): 30356-30364.

Li M, Jiang J, Yue L. Functional characterization of homo- and heteromeric channel kinases TRPM6 and TRPM7. J. Gen. Physiol. 2006, 127: 525–537.

Liedtke W and Friedman JM. Abnormal osmotic regulation in trpv4-/- mice. Proc Natl Acad Sci USA. 2003, 100: 13698–13703.

Liedtke W, Choe Y, Martí-Renom MA, Bell AM, Denis CS, Sali A, Hudspeth AJ, Friedman JM, Heller S. Vanilloid receptor-related osmotically activated channel (VR-OAC), a candidate vertebrate osmoreceptor. Cell. 2000, 103: 525–535.

Lintschinger B, Balzer-Geldsetzer M, Baskaran T, Graier WF, Romanin C, Zhu MX, Groschner K. Coassembly of Trp1 and Trp3 proteins generates diacylglycerol- and Ca^{2+}-sensitive cation channels.J Biol Chem. 2000, 275(36): 27799-27805.

Liu C, Ngai CY, Huang Y, Ko WH, Wu M, He GW, Garland CJ, Dora KA, Yao X. Depletion of intracellular Ca^{2+} stores enhances flow-induced vascular dilatation in rat small mesenteric artery. Br J Pharmacol. 2006, 147: 506–515.

Liu CL, Huang Y, Ngai CY, Leung YK, Yao XQ. TRPC3 is involved in flow- and bradykinin-induced vasodilation in rat small mesenteric arteries. Acta Pharmacol Sin. 2006, 27(8): 981-990.

Liu D, Liman ER. Intracellular Ca^{2+} and the phospholipid PIP2 regulate the taste transduction ion channel TRPM5. Proc Natl Acad Sci USA. 2003, 100: 15160–15165.

Liu W, Xu S, Woda C, Kim P, Weinbaum S, Satlin LM. Effect of flow and stretch on the $[Ca^{2+}]_i$ response of principal and intercalated cells in cortical collecting duct. Am J Physiol Renal Physiol. 2003, 285(5): F998-F1012.

Liu X, Bandyopadhyay BC, Singh BB, Groschner K, Ambudkar IS. Molecular analysis of a store-operated and 2-acetyl-sn-glycerol-sensitive non-selective cation channel. Heteromeric assembly of TRPC1-TRPC3. J Biol Chem. 2005, 280(22): 21600-21606.

Liu X, Singh BB, Ambudkar IS. TRPC1 is required for functional store-operated Ca^{2+} channels. Role of acidic amino acid residues in the S5-S6 region. J Biol Chem. 2003, 278: 11337-11343.

Loot AE, Popp R, Fisslthaler B, Vriens J, Nilius B, Fleming I. Role of cytochrome P450-dependent transient receptor potential V4 activation in flow-induced vasodilatation. Cardiovasc Res. 2008, 80: 445–452.

Lupas AN, Gruber M. The structure of alpha-helical coiled coils. Adv. Protein Chem. 2005, 70: 37–78.

Ma R, Li WP, Rundle D, Kong J, Akbarali HI, Tsiokas L. PKD2 functions as an epidermal growth factor-activated plasma membrane channel. Mol Cell Biol. 2005, 25(18): 8285-8298.

Ma X, Cao J, Luo J, Nilius B, Huang Y, Ambudkar IS, Yao X.Depletion of intracellular Ca^{2+} stores stimulates the translocation of vanilloid transient receptor potential 4-c1 heteromeric channels to the plasma membrane. Arterioscler Thromb Vasc Biol. 2010(b), 30(11): 2249-2255.

Ma X, Qiu S, Luo J, Ma Y, Ngai CY, Shen B, Wong CO, Huang Y, Yao X. Functional role of vanilloid transient receptor potential 4-canonical transient

receptor potential 1 complex in flow-induced Ca^{2+} influx. Arterioscler Thromb Vasc Biol. 2010(a), 30(4): 851-858.

Malnic G, Berliner RW, Giebisch G. Flow dependence of K_ secretion in cortical distal tubules of the rat. Am J Physiol Renal Fluid Electrolyte Physiol. 1989, 256: F932–F941.

Maroto R, Raso A, Wood TG, Kurosky A, Martinac B, Hamill OP. TRPC1 forms the stretch-activated cation channel in vertebrate cells. Nat Cell Biol. 2005, 7: 179–185.

Marrelli SP, O'Neil RG, Brown RC, Bryan RM, Jr. PLA2 and TRPV4 channels regulate endothelial calcium in cerebral arteries. Am J Physiol Heart Circ Physiol. 2007, 292: H1390–H1397.

Maruyama Y, Nakanishi Y, Walsh EJ, Wilson DP, Welsh DG, Cole WC. Heteromultimeric TRPC6-TRPC7 channels contribute to arginine vasopressin-induced cation current of A7r5 vascular smooth muscle cells. Circ Res. 2006, 98(12): 1520-1527.

McKemy DD, Neuhausser WM, Julius D. Identification of a cold receptor reveals a general role for TRP channels in thermosensation. Nature. 2002, 416: 52–58.

Mederos Y, Schnitzler M, Storch U, Meibers S, Nurwakagari P, Breit A, Essin K, Gollasch M, Gudermann T. Gq-coupled receptors as mechanosensors mediating myogenic vasoconstriction. EMBO J. 2008, 27: 3092–3103

Mendoza SA, Fang J, Gutterman DD, Wilcox DA, Bubolz AH, Li R, Suzuki M, Zhang DX. TRPV4-mediated endothelial Ca^{2+} influx and vasodilation in response to shear stress. Am J Physiol Heart Circ Physiol. 2010, 298(2): H466-476.

Mishra SK and Hoon MA. Ablation of TRPV1 neurons reveals their selective role in thermal pain sensation. Mol Cell Neurosci. 2010, 43: 157–163.

Montell C. The TRP superfamily of cation channels. Sci STKE. 2005, 22; 2005(272): re3.

Mori Y, Takada N, Okada T, Wakamori M, Imoto K, Wanifuchi H, Oka H, Oba A, Ikenaka K and Kurosaki T. Differential distribution of TRP Ca^{2+} channel isoforms in mouse brain. Neuroreport. 1998, 9, pp: 507-515.

Morimoto T, Liu W, Woda C, Carattino MD, Wei Y, Hughey RP, Apodaca G, Satlin LM, Kleyman TR. Mechanism underlying flow stimulation of sodium absorption in the mammalian collecting duct. Am J Physiol Renal Physiol. 2006, 291: F663-F669.

Morita H, Honda A, Inoue R, Ito Y, Abe K, Nelson MT, Brayden JE. Membrane stretch-induced activation of a TRPM4-like nonselective cation channel in cerebral artery myocytes. J Pharmacol Sci. 2007, 103: 417–426.

Müller D, Hoenderop JG, Meij IC, van den Heuvel LP, Knoers NV, den Hollander AI, Eggert P, García-Nieto V, Claverie-Martín F, Bindels RJ. Molecular cloning, tissue distribution and chromosomal mapping of the human epithelial Ca^{2+} channel (ECAC1). Genomics. 2000, 67: 48-53.

Muraki K, Iwata Y, Katanosaka Y, Ito T, Ohya S, Shigekawa M, Imaizumi Y. TRPV2 is a component of osmotically sensitive cation channels in murine aortic myocytes. Circ Res. 2003, 93(9): 829-838.

Nadler MJ, Hermosura MC, Inabe K, Perraud AL, Zhu Q, Stokes AJ, Kurosaki T, Kinet JP, Penner R, Scharenberg AM, Fleig A. LTRPC7 is a Mg.ATP-regulated divalent cation channel required for cell viability. Nature. 2001, 411: 590–595.

Naeini RS, Witty MF, Seguela P, Bourque CW. An N-terminal variant of Trpv1 channel is required for osmosensory transduction. Nat Neurosci. 2006, 9: 93–98.

Nakayama H, Wilkin BJ, Bodi I, Molkentin JD. Calcineurin-dependent cardiomyopathy is activated by TRPC in the adult mouse heart. FASEB J. 2006, 20:1660–1670.

Nauli S M, Kawanabe Y, Kaminski JJ, Pearce WJ, Ingber DE, Zhou J. Endothelial cilia are fluid shear sensors that regulate calcium signaling and nitric oxide production through polycystin-1. Circulation. 2008, 117: 1161–1171.

Nauli SM, Alenghat FJ, Luo Y, Williams E, Vassilev P, Li X, Elia AE, Lu W, Brown EM, Quinn SJ, Ingber DE, Zhou J. Polycystins 1 and 2 mediate mechanosensation in the primary cilium of kidney cells. Nature Genetics. 2003, 33: 129–137.

Nauli SM, Kawanabe Y, Kaminski JJ, Pearce WJ, Ingber DE, Zhou J.Endothelial cilia are fluid shear sensors that regulate calcium signaling and nitric oxide production through polycystin-1, Circulation. 2008, 117: pp. 1161–1171.

Nauli SM, Zhou J. Polycystins and mechanosensation in renal and nodal cilia, Bioessays 2004, 26: pp. 844–856.

Nijenhuis T, Hoenderop JG, van der Kemp AW, Bindels RJ. Localization and regulation of the epithelial Ca2+ channel TRPV6 in the kidney. J Am Soc Nephrol. 2003, 14: 2731–2740.

Nilius B, Prenen J, Droogmans G, Voets T, Vennekens R, Freichel M, Wissenbach U, Flockerzi V. Voltage dependence of the Ca2+-activated cation channel TRPM4. J Biol Chem. 2003, 278: 30813–30820

Nilius B, Vennekens R. From cardiac cation channels to the molecular dissection of the transient receptor potential channel TRPM4. Pflugers Arch. 2006, 453: 313–321.

Numata T, Shimizu T, Okada Y. Direct mechano-stress sensitivity of TRPM7 channel. Cell Physiol Biochem. 2007a, 19: 1–8.

Numata T, Shimizu T, Okada Y. TRPM7 is a stretch- and swelling-activated cation channel involved in volume regulation in human epithelial cells. Am J Physiol Cell Physiol. 2007b, 292: C460–467.

Oancea E, Wolfe JT, Clapham DE. Functional TRPM7 channels accumulate at the plasma membrane in response to fluid flow. Circ Res. 2006, 98:245–253.

Ohba T, Watanabe H, Murakami M, Takahashi Y, Iino K, Kuromitsu S, Mori Y, Ono K, Iijima T, Ito H. Upregulation of TRPC1 in the development of cardiac hypertrophy. J Mol Cell Cardiol. 2007, 42:498–507.

Olesen S, Clapham DE, Davies PF. Haemodynamic shear stress activates a K+ current in vascular endothelial cells. Nature. 1988, 331: 168-170.

Onohara N, Nishida M, Inoue R, Kobayashi H, Sumimoto H, Sato Y, Mori Y, Nagao T, Kurose H. TRPC3 and TRPC6 are essential for angiotensin II-induced cardiac hypertrophy. EMBO J. 2006, 25:5305–5316.

Park KS, Kim Y, Lee YH, Earm YE, Ho WK. Mechanosensitive cation channels in arterial smooth muscle cells are activated by diacylglycerol and inhibited by phospholipase C inhibitor. Circ Res. 2003, 93: 557–564.

Park SP, Kim BM, Koo JY, Cho H, Lee CH, Kim M, Na HS, Oh U. A tarantula spider toxin, GsMTx4, reduces mechanical and neuropathic pain. Pain. 2008, 137: 208–217.

Pedersen SA, Nilius B. Transient receptor potential channels in mechanosensing and cell volume regulation. Methods Enzymol. 2007, 428:183–207.

Peier AM, Moqrich A, Hergarden AC, Reeve AJ, Andersson DA, Story GM, Earley TJ, Dragoni I, McIntyre P, Bevan S, Patapoutian A. A TRP channel that senses cold stimuli and menthol. Cell. 2002, 108: 705–715.

Peng JB, Chen X Z, Berger U V, Weremowicz S, Morton CC, Vassilev P M, Brown EM and Hediger MA. Human calcium transport protein CaT1. Biochem. Biophys. Res. Commun. 2000, 278: 326-332

Pérez CA, Huang L, Rong M, Kozak JA, Preuss AK, Zhang H, Max M, Margolskee RF. A transient receptor potential channel expressed in taste receptor cells. Nat. Neurosci. 2002, 5: 1169–1176.

Perraud A, Fleig A, Dunn CA, Bagley LA, Launay P, Schmitz C, Stokes AJ, Xhu Q, Bessman MJ, Penner R, Kinet JP, Scharenberg AM. ADP-ribose gating of the calcium-permeable LTRPC2 channel revealed by Nudix motif homology. Nature. 2001, 411: 595–599.

Philipp S, Hambrecht J, Braslavski L, Schroth G, Freichel M, Murakami M, Cavalie A, Flockerzi V. A novel capacitative calcium entry channel expressed in excitable cells. EMBO J. 1 1998, 7: 4274–4282.

Poteser M, Graziani A, Rosker C, Eder P, Derler I, Kahr H, Zhu MX, Romanin C, Groschner K. TRPC3 and TRPC4 associate to form a redox-sensitive cation channel. Evidence for expression of native TRPC3-TRPC4 heteromeric channels in endothelial cells. J Biol Chem. 2006, 281(19): 13588-13595.

Praetorius H A, Spring K R. A physiological view of the primary cilium. Annu. Rev. Physiol. 2005, 67: 515–529.

Praetorius H A, Spring K R. Bending the MDCK cell primary cilium increases intracellular calcium. J. Membr. Biol. 2001, 184: 71–79.

Praetorius H A & Spring K R. Removal of the MDCK cell primary cilium abolishes flow sensing. J. Membr. Biol. 2003, 191: 69–76.

Prawitt D, Monteilh-Zoller MK, Brixel L, Spangenberg C, Zabel B, Fleig A, Penner R. TRPM5 is a transient Ca^{2+}-activated cation channel responding to rapid changes in $[Ca^{2+}]_i$. Proc Natl Acad Sci USA. 2003, 100: 15166–15171.

Putney JW Jr. The enigmatic TRPCs: multifunctional cation channels. Trends Cell Biol. 2004, 14: 282–286.

Reynolds DM. Aberrant splicing in the PKD2 gene as a cause of polycystic kidney disease. J Am Soc Nephrol. 1999, 10: 2342-2351.

Riccio A, Medhurst AD, Mattei C, Kelsell RE, Calver AR, Randall AD, Benham CD, Pangalos MN. mRNA distribution analysis of human TRPC family in CNS and peripheral tissues. Brain Res Mol Brain Res. 2002, 109 : 95–104.

Runnels LW, Yue L, Clapham DE. TRP-PLIK, a bifunctional protein with kinase and ion channel activities. Science. 2001, 291: 1043–1047.

Rutter AR, Ma QP, Leveridge M, Bonnert TP. Heteromerization and colocalization of TrpV1 and TrpV2 in mammalian cell lines and rat dorsal root ganglia. Neuroreport. 2005, 16(16):1735-1739.

Saliez J, Bouzin C, Rath G, Ghisdal P, Desjardins F, Rezzani R, Rodella LF, Vriens J, Nilius B, Feron O, Balligand JL, Dessy C. Role of caveolar compartmentation in endothelium-derived hyperpolarizing factor-mediated relaxation: Ca2+ signals and gap junction function are regulated by caveolin in endothelial cells. Circulation. 2008, 117: 1065–1074.

Satlin LM, Sheng S, Woda CB, Kleyman TR. Epithelial Na^+ channels are regulated by flow. Am J Physiol Renal Physiol. 2001, 280(6): F1010-F1018.

Schaefer M, Plant TD, Obukhov AG, Hofmann T, Gudermann T & Schultz G. Receptor-mediated regulation of the nonselective cation channels TRPC4 and TRPC5. J Biol Chem. 2000, 275: 17517–17526.

Schilling WP, Goel M. Mammalian TRPC channel subunit assembly.Novartis Found Symp. 2004, 258: 18-30.

Schlingmann KP, Weber S, Peters M, Niemann Nejsum L, Vitzthum H, Klingel K, Kratz M, Haddad E, Ristoff E, Dinour D, Syrrou M, Nielsen S, Sassen M, Waldegger S, Seyberth HW, Konrad M. Hypomagnesemia with secondary hypocalcemia is caused by mutations in TRPM6, a new member of the TRPM gene family. Nat Genet. 2002, 31: 166–170.

Schwarze SR, Ho A, Vocero-Akbani A, Dowdy SF. In vivo protein transduction: Delivery of a biologically active protein into the mouse. Science. 1999, 285(5433): 1569-1572.

Seth M, Zhang ZS, Mao L, Graham V, Burch J, Stiber J, Tsiokas L, Winn M, Abramowitz J, Rockman HA, Birnbaumer L, Rosenberg P. TRPC1 channels are critical for hypertrophic signaling in the heart. Circ Res. 2009, 105: 1023–1030.

Sharif Naeini R, Folgering JH, Bichet D, Duprat F, Lauritzen I, Arhatte M, Jodar M, Dedman A, Chatelain FC, Schulte U, Retailleau K, Loufrani L, Patel A, Sachs F, Delmas P, Peters DJ, Honoré E. Polycystin-1 and -2 dosage regulates pressure sensing. Cell. 2009, 139: 587–596.

Smith G D, Gunthorpe M J, Kelsell R E, Hayes P D, Reilly P, Facer P, Wright J E, Jerman J C, Walhin J P, Ooi L. TRPV3 is a temperature-sensitive vanilloid receptor-like protein. Nature. 2002. 418: 186-190.

Spassova MA, Hewavitharana T, Xu W, Soboloff J, Gill DL. A common mechanism underlies stretch activation and receptor activation of TRPC6 channels. Proc Natl Acad Sci USA. 2006, 103: 16586–16591.

Staruschenko A, Jeske NA, Akopian AN. Contribution of TRPV1-TRPA1 interaction to the single channel properties of the TRPA1 channel. J Biol Chem. 2010, 285(20):15167-15177.

Stewart AP, Smith GD, Sandford RN, Edwardson JM. Atomic force microscopy reveals the alternating subunit arrangement of the TRPP2-TRPV4 heterotetramer. Biophys J. 2010, 99(3): 790-797.

Stoos BA, Naray-Fejes-Toth A, Carretero OA, Ito S, Fejes-Toth G. Characterization of a mouse cortical collecting duct cell line. Kidney Int. 1991, 39: 1168-1175.

Strotmann R, Harteneck C, Nunnenmacher K, Schultz G, Plant T. OTRPC4, a nonselective cation channel that confers sensitivity to extracellular osmolarity. Nat Cell Biol. 2000, 2: 695–702.

Strübing C, Krapivinsky G, Krapivinsky L, Clapham DE. TRPC1 and TRPC5 form a novel cation channel in mammalian brain. Neuron. 2001, 29: 645-655.

Strübing C, Krapivinsky G, Krapivinsky L, Clapham DE. Formation of novel TRPC channels by complex subunit interactions in embryonic brain, Journal of Biological Chemistry. 2003, 278: 39014–39019.

Strübing C, Krapivinsky G, Krapivinsky L, Clapham DE. TRPC1 and TRPC5 form a novel cation channel in mammalian brain. Neuron. 2001, 29(3): 645-655.

Suchyna TM, Johnson JH, Hamer K, Leykam JF, Gage DA, Clemo HF, Baumgarten CM, Sachs F. Identification of a peptide toxin from Grammostola spatulata spider venom that blocks cation-selective stretch-activated channels. J Gen Physiol. 2000, 115: 583–598.

Suchyna TM, Tape SE, Koeppe RE 2nd, Andersen OS, Sachs F, Gottlieb PA. Bilayer-dependent inhibition of mechanosensitive channels by neuroactive peptide enantiomers. Nature. 2004, 430: 235–240.

Suzuki M, Hirao A, Mizuno A. Microtubule-associated protein 7 increases the membrane expression of transient receptor potential vanilloid 4 (TRPV4). J Biol Chem. 2003, 278: 51448-51453.

Suzuki M, Mizuno A, Kodaira K, Imai M. Impaired pressure sensation in mice lacking TRPV4. J Biol Chem. 2003, 278: 22664–22668.

Szücs G, Heinke S, Droogmans G, Nilius B. Activation of the volume-sensitive chloride current in vascular endothelial cells requires a permissive intracellular Ca^{2+} concentration. Pflugers Arch. 1996, 431: 467-469.

Taniguchi J, Tsuruoka S, Mizuno A, Sato J, Fujimura A, Suzuki M. TRPV4 as a flow sensor in flow-dependent K^+ secretion from the cortical collecting duct. Am J Physiol Renal Physiol. 2007, 292(2): F667-673.

Teilmann SC, Byskov AG, Pedersen PA, Wheatley DN, Pazour GJ, Christensen ST. Localization of transient receptor potential ion channels in primary and motile cilia of the female murine reproductive organs. Mol Reproduction and Development. 2005, 71: 444-452.

Theun de Groot1, René J M Bindels1, Joost G J Hoenderop. TRPV5: an ingeniously controlled calcium channel. Kidney International. 2008, 74: 1241–1246.

Thodeti CK, Matthews B, Ravi A, Mammoto A, Ghosh K, Bracha AL, Ingber DE. TRPV4 channels mediate cyclic strain-induced endothelial cell reorientation through integrin-to-integrin signaling. Circ Res. 2009, 104(9): 1123-1130.

Tian W, Salanova M, Xu H, Lindsley JN, Oyama TT, Anderson S, Bachmann S, Cohen DM. Renal expression of osmotically responsive cation channel TRPV4 is restricted to water-impermeant nephron segments. Am J Physiol Renal Physiol. 2004, 287(1): F17-24.

Tsiokas L, Arnould T, Zhu C, Kim E, Walz G, Sukhatme VP. Specific association of the gene product of PKD2 with the TRPC1 channel.Proc Natl Acad Sci U S A. 1999, 96(7): 3934-3939.

Tsuruda PR, Julius D, Minor DL Jr. Coiled coils direct assembly of a cold-activated TRP channel. Neuron. 2006, 51(2): 201-212.

Van Abel M, Huybers S, Hoenderop JG, van der Kemp AW, van Leeuwen JP, Bindels RJ. Age-dependent alterations in Ca2+ homeostasis: role of TRPV5 and TRPV6. Am J Physiol Renal Physiol. 2006, 291(6): F1177-1183.

Van de Graaf SF, Bindels RJ, Hoenderop JG. Physiology of epithelial Ca^{2+} and Mg^{2+} transport. Rev Physiol Biochem Pharmacol. 2007, 158: 77–160.

Vennekens R, Hoenderop JG, Prenen J, Stuiver M, Willems PH, Droogmans G, Nilius B, Bindels RJ. Permeation and gating properties of the novel epithelial Ca^{2+} channel. J Biol Chem. 2000, 275: 3963–3969.

Vennekens R, Nilius B. Insights into TRPM4 function, regulation and physiological role. Handb Exp Pharmacol. 2007, 179: 269–285.

Voets T, Nilius B, Hoefs S, van der Kemp AW, Droogmans G, Bindels RJ, Hoenderop JG. TRPM6 forms the Mg^{2+} influx channel involved in intestinal and renal Mg^{2+} absorption. J. Biol. Chem. 2004, 279: 19–25.

Voets T, Prenen J, Vriens J, Watanabe H, Janssens A, Wissenbach U, Bodding M, Droogmans G, Nilius B. Molecular determinants of permeation through the cation channel TRPV4. J Biol Chem. 2002, 277: 33704-33710.

Watanabe H, Vriens J, Suh S H, Benham C D, Droogmans G, Nilius B. Heat-evoked activation of TRPV4 channels in a HEK293 cell expression system and in native mouse aorta endothelial cells. J. Biol.Chem. 2002, 277: 47044-47051.

Welsh DG, Morielli AD, Nelson MT, Brayden JE. Transient receptor potential channels regulate myogenic tone of resistance arteries. Circ Res. 2002, 90: 248-250.

Wes P D, Chevesich J, Jeromin A, Rosenberg C, Stetten G, Montell C. TRPC1, a human homolog of a Drosophila store-operated channel. Proc. Natl. Acad. Sci. U. S. A. 1995, 92: 9652–9656.

Willette RN, Bao W, Nerurkar S, Yue TL, Doe CP, Stankus G, Turner GH, Ju H, Thomas H, Fishman CE, Sulpizio A, Behm DJ, Hoffman S, Lin Z, Lozinskaya I, Casillas LN, Lin M, Trout RE, Votta BJ, Thorneloe K, Lashinger ES, Figueroa DJ, Marquis R, Xu X. Systemic activation of the transient receptor potential vanilloid subtype 4 channel causes endothelial failure and circulatory collapse: part 2. J Pharmacol Exp Ther. 2008, 326: 443-452.

Wilson P D. Polycystic kidney disease. N. Engl. J. Med. 2004, 350: 151-164.

Woda CB, Leite M Jr, Rohatgi R, Satlin LM. Effects of luminal flow and nucleotides on $[Ca^{2+}]_i$ in rabbit cortical collecting duct. Am J Physiol Renal Physiol. 2002, 283: F437-F446.

Woda CB, Leite M Jr, Rohatgi R, Satlin LM. Effects of luminal flow and nucleotides on $[Ca^{2+}]_i$ in rabbit cortical collecting duct. Am J Physiol Renal Physiol. 2002, 283(3): F437-F446.

Woolfson DN. The design of coiled-coil structures and assemblies. Adv. Protein Chem. 2005, 70, 79-112.

Wu L, Gao X, Brown RC, Heller S, O'Neil RG. Dual role of the TRPV4 channel as a sensor of flow and osmolality in renal epithelial cells. Am J Physiol Renal Physiol. 2007, 293: F1699-F1713.

Xu XZ, Chien F, Butler A, Salkoff L, Montell C. TRPgamma, a drosophila TRP-related subunit, forms a regulated cation channel with TRPL. Neuron. 2000, 26(3): 647-657.

Xu XZ, Li HS, Guggino WB, Montell C. Coassembly of TRP and TRPL produces a distinct store-operated conductance. Cell. 1997, 89(7): 1155-1164.

Xu XZ, Moebius F, Gill DL, Montell C. Regulation of melastatin, a TRP-related protein, through interaction with a cytoplasmic isoform. Proc. Natl. Acad. Sci. U.S.A. 2001, 98: 10692-10697.

Yang XR, Lin MJ, McIntosh LS, Sham JS. Functional expression of transient receptor potential melastatin- and vanilloid-related channels in pulmonary arterial and aortic smooth muscle. Am J Physiol Lung Cell Mol Physiol. 2006, 290: L1267-L1276.

Yao X, Garland CJ. Recent developments in vascular endothelial cell transient receptor potential channels. Circ Res. 2005, 97: 853–863.

Yao X, Kwan HY, Chan FL, Chan NW, Huang Y. A protein kinase G-sensitive channel mediates flow-induced Ca^{2+} entry into vascular endothelial cells. FASEB J. 2000, 14: 932-938.

Ying Luo, Peter M. Vassilev, Xiaogang Li, Yoshifumi Kawanabe, and Jing Zhou. Native Polycystin 2 Functions as a Plasma Membrane Ca^{2+}-Permeable Cation Channel in Renal Epithelia. Mol Cell Biol. 2003, 23(7): 2600-2607.

Yu Y, Ulbrich MH, Li MH, Buraei Z, Chen XZ, Ong AC, Tong L, Isacoff EY, Yang J. Structural and molecular basis of the assembly of the TRPP2/PKD1 complex. Proc Natl Acad Sci U S A. 2009, 106(28): 11558-11563.

Zhang DX, Mendoza SA, Bubolz AH, Mizuno A, Ge ZD, Li R, Warltier DC, Suzuki M, Gutterman DD. Transient receptor potential vanilloid type 4-deficient mice exhibit impaired endothelium-dependent relaxation induced by acetylcholine in vitro and in vivo. Hypertension. 2009, 53: 532–538.

Zhang P, Luo Y, Chasan B, González-Perrett S, Montalbetti N, Timpanaro GA, Cantero Mdel R, Ramos AJ, Goldmann WH, Zhou J, Cantiello HF. The multimeric structure of polycystin-2 (TRPP2): structural-functional correlates of homo- and hetero-multimers with TRPC1. Hum Mol Genet. 2009, 18: 1238-1251.

Zheng J, Trudeau MC, Zagotta WN. Rod cyclic nucleotide-gated channels have a stoichiometry of three CNGA1 subunits and one CNGB1 subunit. Neuron. 2002, 36: 891-896.

Zhou J. Polycystins and primary cilia: primers for cell cycle progression. Annu. Rev. Physiol. 2009, 71: 83–113.